HELEN MOISE

ENERGY DISPERSIVE X-RAY FLUORESCENCE SPECTROMETRY AND KINETIC MODELING OF ELEMENTAL STRONTIUM IN HUMAN BONE

By HELEN MOISE, B.SC., M.SC.

A Thesis Submitted to the School of Graduate Studies in Partial Fulfilment of the

Requirements for the Degree Doctor of Philosophy

DOCTOR OF PHILOSOPHY (2014) McMaster University

(Medical Physics) Hamilton, Ontario

TITLE: Energy Dispersive X-ray Fluorescence Spectrometry and Kinetic Modeling of Elemental Strontium in Human Bone.

AUTHOR: Helen Moise, B.Sc. (Université Concordia), M.Sc (Ryerson University)

SUPERVISORS: Dr. David Chettle and Dr. Ana Pejović- Milić

NUMBER OF PAGES: xxiii, 185

ABSTRACT

For the first time in the available literature, this work presents data based on long term *in-vivo* human bone strontium measurements performed with an in-house custom developed I-125 based X-ray fluorescence system (IVXRF). Its negligible radiation risk and non-invasive nature allowed for frequent measurements at the ankle and finger sites, obtaining information about trabecular and cortical bone, respectively. While the phantom standards used to calibrate the system cannot be used to extract absolute bone strontium concentration, analysis of phantom consistency indicated excellent reproducibility, reporting a mean normalized strontium signal ± SD of 1.1198 ± 0.02171. This work comprises two important contributions besides system analysis; (i) the continued measurements of osteoporotic individuals self-administering with strontium supplements in order to acquire long term data and (ii) kinetic modeling.

A total of 21 individuals (18 females, 3 males) were measured throughout the study, 10 are baseline individuals (no prior history of strontium intake and for whom natural bone strontium readings were acquired). Although similar patterns of strontium uptake were observed for all individuals, a wide variation of the strontium signal between individuals was observed, raising the question of physiological influences. Power and exponential functions were tested on 8 baseline individuals based on one and two compartmental configurations. Parameters represented the mean baseline strontium signal,

half-life and strontium uptake. Ankle and finger values showed correlation of 0.804, which is significant at the 95% level. Half-lives (300 ± 163) days and (2200 ± 1661) days ($p=0.000711$ and $p=0.0147$) for the ankle and finger, respectively, indicated statistically significant different times, suggesting one compartment has a quicker turnover than the other. However, while the exponential model best describes the data set, the models were inconclusive which points to the need for a more controlled study, eliminating variable factors between individuals such as dosage, health and dietary consumption.

ACKNOWLEDGEMENTS

Since this thesis involves the subject of bones, I thought it would be appropriate to include one of my favorite quotes by Reba McEntire: “To succeed in life, you need three things: a wishbone, a backbone and a funny bone”. While I would like to think I have a funny bone and a strong backbone, my wish and goal to obtain my PhD could not have happened without the support and guidance of my supervisors, my family, friends and colleagues.

It was an honor to have worked with two wonderful supervisors: Dr. David Chettle and Dr. Ana Pejović-Milić, who was also my supervisor at Ryerson University. Both are experts in the field of medical physics and I am grateful for their support, encouragement and guidance throughout my graduate studies. Their doors were always open and they were always available to help you whether it was with research, academics or personal matters. Their commitments not just to their students but to numerous projects are amazing. My sentiments are clearly shared by my fellow colleagues, given that both of them have won teaching awards and awards from the academic community. Thank you!

I also wish to express my thanks to Dr. Gregory Wohl, my supervisory committee member, for his valuable feedback and time. Acknowledgments also goes to Dr. Karen Beattie and the late Dr. Colin Webber; their discussions as part of my supervisory committee helped challenge the way I looked at my work. Gratitude also goes to Mike Inskip, visiting scientist at McMaster University, for sharing his knowledge, enthusiasm and interest in the strontium study.

I also thank my colleagues of the OENMRG research group, the faculty, administrative staff and graduate students of the medical physics department. There are so many talented individuals!

Special thanks go to the volunteers who devoted their time to the study. Their commitment to the study has made this work possible for which I am grateful and it was a pleasure to know them. Particular thanks go to Marjorie Filice and Charla Murray for their contagious smiles and continued friendship. They're awesome!

But last and foremost, I wish to dedicate this thesis to my late mother, Ana, who passed away as I approached my final year. She was my inspiration and best friend. Losing her was very difficult but it's a blessing to have my wonderful father and brother. Their continued encouragement and support helped me to persevere. Reflecting back, I not only feel that I have completed my doctoral studies gaining new academic insight but gained a lifetime of memories.

TABLE OF CONTENTS

LIST OF FIGURES

Chapter 1

Chapter 2

Chapter 3

Chapter 4

Chapter 5

Attached Paper (Moise et al., 2012)

Chapter 6

Chapter 7

Appendix

LIST OF TABLES

Chapter 1

Chapter 2

Chapter 3

Chapter 4

Chapter 5

Attached Paper (Moise et al., 2012)

Attached Paper (Moise et al., 2014)

Chapter 6

LIST OF ABBREVIATIONS AND SYMBOLS

A
ADC: analogue digital converter
Ag: silver

B
BMD: bone mineral density

C
Ca: calcium
CaHA- calcium hydroxyapatite
COX-2: cylcooxygenase
CT: computerized tomography
CV: coefficient of variance

D
DXA: dual-energy X-ray absorptiometry
DPA: dual photon absorptiometry

E
EDXRF: energy dispersive X-ray fluorescence
ERK: extracellular signal-regulated kinase

F
FWHM: full width height maximum
Fl-fluorine
Fe: iron

G
Ge : germanium
Ge(Li) :germanium- lithium

H
HA: hydroxyapatite
HR-pQCT: high resolution peripheral quantitative computed tomography
HV: high voltage

I
I: iodine
ICP-MS: inductively coupled plasma-mass spectrometry

ICRP: International Commission on Radiological Protection
IP3: inositol phosphate 3
IVNAA- *In-vivo* neutron activation analysis
IVXRF: *In-vivo* X-ray Fluorescence Spectrometry

K
K_{α}: K-alpha
K_{β}: K-beta
KES: K-edge subtraction imaging

L
LA-ICP-MS: laser- ablation- inductively coupled mass spectrometry

M
MDL: minimum detection limit
MRI: magnetic resonance imaging

N
Na: sodium

P
Pb: lead
PIXE: proton-induced X-ray emission
poP: plaster of Paris
ppm: parts per million

R
Rb: rubidium
REB: research ethics board

S
SD: standard deviation
Si(Li): silicon-lithium
SOTI: Spinal Osteoporosis Therapeutic Intervention
Sr: strontium
SRμXRF: synchrotron radiation micro X-ray fluorescence

T
Te: tellurium
TROPOS: Treatment of Peripheral Osteoporosis Study

U
UD: ultra distal
US: ultrasound

W
WDXRF: wavelength dispersive X-ray fluorescence
WHO: World Health Organization

X
XRF: X-ray fluorescence spectrometry

Y
Y: yttrium

Z
Zr: zirconium

DECLARATION OF ACADEMIC ACHIEVEMENT

This thesis presents research work involving not only system analysis but the measurements of individuals suffering from osteoporosis and/or osteopenia based on the technique of *in-vivo* X-ray fluorescence spectrometry (IVXRF) as well. The Ryerson and McMaster University bone in strontium study was initiated as collaboration between Ryerson University (REB#2007-212-1) and McMaster University (REB #07-402). An initial baseline volunteer was recruited to join the study in December 2008 and based on the observations obtained from the initial subject; further volunteers were recruited in early 2010. The continuation of the study was necessary in order to obtain long term data successfully. This work differentiates from previous work in the respect that new knowledge and data were acquired as a result of the long term measurements. Kinetic modeling was also performed in this work.

The results obtained in this thesis work over a period of four years are unique in the sense that for the first time, bone strontium measurements as performed on the osteoporotic volunteers with the IVXRF system are made available in the literature. In the literature, bone strontium measurements in humans and animals have consisted primarily of *ex-vivo* studies based on bone biopsies, chemical analysis on excised bone and in the case of *in-vivo* studies, dual photon absorptiometry and dual energy X-ray analysis, so this work presented with a unique data set. Two papers on the long-term human bone strontium measurements have been published in the Journal of Bone (Moise et al., 2012 and Moise et al., 2014). Dr. Ana Pejović-Milić, my co-supervisor, is the

corresponding author on both of these papers and helped in implementing the recruitment of individuals.

In addition to continued measurements and modeling of the data, analysis of the fitting routine and elements thought to overlap with the strontium peaks were investigated. Dr. David Chettle, who is my supervisor at McMaster University, contributed to the fitting analysis by revising the FORTRAN program code to analyze rubidium peaks. He also contributed to the interpretation of the fitting analysis in chapter six by investigating the significance of the parameter related to bone strontium uptake.

Both of my supervisors have been instrumental in providing research funding and support throughout the work reported in this thesis.

CHAPTER 1: BONE AND THE ELEMENT STRONTIUM

1.1 Elements in the Human Body

The human body consists of a range of elements, from major constituents such as oxygen, carbon, hydrogen and nitrogen, through to trace elements, all of which are found in organs, tissues and bones. The elements can be further classified as essential or non-essential. Mertz (1981) defined essential elements as those elements considered important for life sustaining processes whereas nonessential elements are not thought to provide for any specific biological role in the human body. Some of the essential and non-essential elements are shown in figure 1.1 below.

1 H																2 He
3 Li	4 Be											5 B	6 C	7 N	8 O	9 F	10 Ne
11 Na	12 Mg											13 Al	14 Si	15 P	16 S	17 Cl	18 Ar
19 K	20 Ca	21 Sc	22 Ti	23 V	24 Cr	25 Mn	26 Fe	27 Co	28 Ni	29 Cu	30 Zn	31 Ga	32 Ge	33 As	34 Se	35 Br	36 Kr
37 Rb	38 Sr	39 Y	40 Zr	41 Nb	42 Mo	43 Tc	44 Ru	45 Rh	46 Pd	47 Ag	48 Cd?	49 In	50 Sn?	51 Sb	52 Te	53 I	54 Xe

Figure 1.1: Periodic table showing essential elements (shaded) and non-essential elements (non shaded) (Mertz, 1981).

While the roles of essential elements are well known, non-essential elements are also of interest as they are present in trace amounts in the human body and may share similar chemical behavior and properties. For example, bone seeker elements such as lead (Pb) and strontium (Sr), which is the element of interest in this work, are examples of non-

essential elements similar to calcium (Ca) in the sense they accumulate and are stored in bone. However, as shown by the question marks in figure 1.1, for cadmium (Cd) and tin (Sn), there is some uncertainty about the classification of which elements are truly essential.

While Mertz (1981) provided for a simple definition of what makes an element essential, a more precise definition includes the following criteria (Reilly, 2008):

i. it is present in healthy tissue
ii. it is present between different organisms at a relatively constant concentration
iii. its deficiency causes specific biochemical changes
iv. such biochemical changes are associated with equivalent abnormalities among different species
v. supplementation with the element corrects the abnormalities

Thus, taking into account the expanded definition of essentiality, while Sn is now considered as an essential element for life (Underwood, 2012), the roles of other elements in the non-essential category, such as boron (B), rubidium (Rb), lithium (Li) and strontium (Sr) among others, still remain debatable. The uncertainty about the true number of essential elements arises not only due to the analytical difficulties of measuring concentrations at very low levels but also due to the differing concepts of essentiality among different investigators (Reilly, 2008). At the present time, although further studies may have expanded our knowledge and classification of essential elements, figure 1.1 still remains valid.

As shown in figure 1.1, nearly all essential elements occur in all chemical groups of the periodic table, except for groups 3, 4 and 18 (Reilly, 2008). The masses of elements present in the human body are shown in Table 1.1.

Element	Mass	Element	Mass
Oxygen	43 kg	Barium	22 mg
Carbon	16 kg	Iodine	20 mg
Hydrogen	7 kg	Tin	20 mg
Nitrogen	1.8 kg	Titanium	20 mg
Calcium	1.0 kg	Boron	18 mg
Phosphorus	780 g	Nickel	15 mg
Potassium	140 g	Selenium	15 mg
Sulphur	140 g	Chromium	14 mg
Sodium	100 g	Manganese	12 mg
Chlorine	95 g	Arsenic	7 mg
Iron	4.2 g	Lithium	7 mg
Fluorine	2.6 g	Cesium	6 mg
Zinc	2.3 g	Mercury	6 mg
Silicon	1.0 g	Germanium	5 mg
Rubidium*	0.68 g	Molybdenum	5 mg
Strontium	0.32 g	Cobalt	3 mg
Bromine	0.26 g	Antimony	2 mg
Lead*	0.12 g	Silver	2 mg
Copper	72 mg	Niobium	1.5 mg
Aluminum*	60 mg	Zirconium	1.0 mg
Cadmium*	50 mg	Lanthanam	0.8 mg
Cerium	40 mg	Gallium	0.7 mg

Table 1.1 Masses of elements present in the human body in reference man (70 kg) (Helmenstine, 2014). *Note that smaller values may be reported in other literature.

1.2 Bone Anatomy

The human skeleton comprises 213 bones, excluding the sesamoid bones (Clarke 2008). It has numerous functions. For example, the skeleton provides structural support, allows for movement, protects internal organs, acts as a mineral reservoir, helps maintain acid-base balance and plays a role in hematopoiesis (Peel, 2008). The composition of bone is such that it is approximately 60% inorganic, 30% organic, and 10% water (Keaveny et al. 2004). The inorganic phase of bone, also known as the mineral composition, consists of hydroxyapatite (HA), whose chemical formula is:

$Ca_{10}(PO_4)_6(OH)_2$ (McCloskey and Furnival, 2013). However, this composition is not purely HA which has a Ca:P ratio of 5:3 or 1.67 (McCloskey and Furnival, 2013), but rather it contains minor constituents such as potassium (K), magnesium (Mg), strontium, sodium (Na), carbonate and chloride or fluoride (Keaveny et al., 2004) and hence its Ca:P ratio ranges from 1.37 to 1.87 (McCloskey and Furnival, 2013). The organic phase, by contrast consists primarily of collagen, of which 90% is type I, and noncollagenous proteins such as osteocalcin, osteonectin, and bone sialoprotein (Keaveny et al., 2004).

Bone consists of two types of tissues; namely compact and spongy bone, also known as cortical and trabecular bone, respectively (Keaveny et al, 2004, Peel 2008). Cortical bone makes up 80% of the skeletal mass and can be found in the shaft of long bones and on the outer shell around trabecular bone at the end of joints and vertebrae. On the outer shell, cortical thicknesses can vary depending on the bone site and values can range between 0.2-4 mm (Karjalainen et al., 2008, Treece et al., 2010). By contrast, trabecular bone makes up 20% of the skeletal mass and can be found at the end of long bones, in vertebrae, making up the majority of vertebral bodies and in flat bones (Hollister, 2014, McCloskey and Furnival, 2013). Within a skeletal site, the ratio of cortical and trabecular bone differs throughout, such that the vertebra is composed of a cortical to trabecular ratio of 25:75, the femoral head of 50:50 and the radial diaphysis 95:5 (Clarke 2008). Their further properties are listed in Table 1.2.

	Cortical Bone	Trabecular Bone
Porosity	5-10%	50-90%
Volume fraction	0.90 (0.85-0.95)	0.20 (0.05-0.60)
Total surface area (body)	3.5×10^6 mm^2	7.0×10^6 mm^2
Surface/Bone volume (mm^2/mm^3)	2.5	20
Metabolism	Slow turnover rate	Fast turnover rate
Apparent density[1]	1.85 g/ cm^3	Varies, according to site spine: 0.10 g/ cm^3 tibia: 0.30 g/ cm^3 femur(proximal, load bearing): 0.60 g/ cm^3

Table 1.2: Some properties of cortical and trabecular bone (Hollister,2013, 2004, [1]Keaveny et al., 2004).

Bone is continuously undergoing remodeling, consisting of the renewal and repair of bone, in which under normal conditions, there is no net change in bone mass (Hodgson et al., 2007). In other words, the amount of bone removed is replaced by an equal amount. (Hodgson et al.,2007). Completion of a remodeling cycle takes place over three to six months (Hodgson et al., 2007, Marie, 2001) and consists of four principal stages which includes activation, resorption, reversal and formation by a number of bone cells involving osteoclasts, osteoblasts, osteocytes and lining cells (Hodgson et al., 2007). Bone remodeling is predominant in trabecular bone due to the greater surface area compared to cortical bone, such that the turnover rate is approximately ten times greater (Hodgson et al., 2007, Peel, 2008). Nevertheless, an imbalance in the bone remodeling cycle may occur as a result of ageing and other factors such as previous glucocorticoid therapy (Peel, 2008). Such an imbalance likely leads to bone disorders such as osteopenia and osteoporosis (Marie, 2010).

1.3 Bone Disorders

Osteopenia and osteoporosis are defined as skeletal diseases that are characterized by low bone mass, reduced bone strength and increased risk of bone fractures (Peel, 2008). Osteopenia and osteoporosis are diagnosed based on bone mineral density scores (BMD) and T-scores, as shown in Table 1.3 below. While bone mineral density values are typically expressed as g per cm^3, T-scores are numerically expressed, such that they describe a person's BMD value expressed as a standard deviation score in comparison to a healthy, young, reference population having the same ethnicity background and gender (Peel, 2008). According to the World Health Organization (2007), also known as WHO, the young adult mean is typically based on Caucasian women within the age of 20-29. BMD measurements commonly include measurements taken at the hip, forearm and spine (Peel, 2008) using dual-energy X-ray absorptiometry (DXA) (Peel, 2008). However, as stated by WHO (2007), T-scores should be reserved for persons aged 50 years and above, otherwise the Z-score should be considered. The Z-score is defined as the number of standard deviations the measurement is above or below the age matched mean bone mineral density (Laya, 2014). Although, the Z-score is less commonly used, it is useful in identifying individuals who should undergo evaluation for secondary causes of osteoporosis (Laya, 2014).

BMD T-score	Diagnosis
>-1	Normal
<-1 to >-2.5	Osteopenia
<-2.5	Osteoporosis
<-2.5 including fragility fracture	Severe osteoporosis

Table 1.3: Diagnosis of osteopenia and osteoporosis based on BMD values (Peel, 2008).

Treatment for osteoporosis includes anti-resorptive drugs such as bisphosphonates, anabolic drugs such as parathyroid hormone (PTH) 1-34 and lifestyle changes. However, an alternative therapy to the above named drugs includes stable strontium. Research has shown strontium to be an effective and promising treatment (Dahl et al., 2001, Marie, 2001, Boivin et al.,2010, Neuprez et al., 2008). In Europe, stable strontium is sold in a drug form, under the brand name Protelos© (Les Laboratoires Servier), also known as strontium ranelate, as shown in figure 1.2.

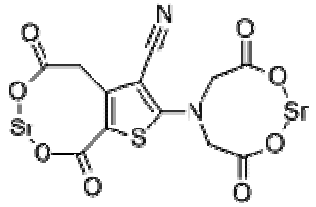

Figure 1.2: Structure of strontium ranelate, Protelos© (Blake and Fogelman, 2006).

However, in North America, while strontium ranelate is not available for purchase, other forms of stable strontium in the form of strontium salts such as strontium citrate and strontium carbonate are available for purchase through health food stores.

1.4 Strontium

Strontium, an alkaline earth metal, was first discovered in 1790 in a mine near the Scottish village, Strontian and was isolated in 1808 (Pors, 2004). Belonging to the group II elements of the Periodic table, it has an atomic number of 38, atomic mass of 87.62 g mol^{-1} and ionic and Vanderwaals radii of 0.113nm and 0.215 nm, respectively making it just slightly larger than calcium whose ionic and Vanderwaals radii are 0.099nm and

0.197nm, respectively (Lenntech, 2014). It is an interesting element, with naturally occurring strontium being a mixture of four stable isotopes: Sr-84 (0.56%), Sr-86 (9.86%), Sr-87(7.02%) and Sr-88 (82.56%) (Pors, 2004). Although, strontium is not found freely in nature due to its reactive and oxidizing properties (Pors, 2004), it is a ubiquitous element that is found both in our natural environment, in manmade sources and in the human body.

1.5 Natural Sources of Strontium

Natural sources of strontium include soil, rocks and water. Strontium makes up 0.036% of the Earth's crust (Turekian, 1961) and its concentration in soil and drinking water ranges in the values between 0.001 and 39 mg/l (Pors, 2004). It is mostly found in the form of the sulfate mineral celestite ($SrSO_4$) and the carbonate strontianite ($SrCO_3$) with the former occurring frequently in sedimentary deposits (Lenntech, 2014). Its size makes it attractive for mining and leading countries in world production of strontium minerals include China, Spain, Mexico, Argentina, Morocco and Turkey (Brown et al., 2010). It is thought that the geographical differences of strontium present in the environment are reflective of the amount of strontium in living organisms (Schoeninger and Peebles, 1981).

The amount of strontium in living organisms, such as humans, depends on the amount ingested. Dietary strontium rich foods include dairy, grains and leafy green vegetables, such as cabbage (45ppm) and lettuce (74 ppm), onions (50 ppm) to low strontium rich foods such as corn (0.4 ppm) and oranges (0.5 ppm) (Lenntech, 2014). In plants, the concentration of strontium is reflective of the amount of strontium present in the soil

(Pors, 2004). Other strontium rich foods may include seafood such as mollusks due to the high strontium content in sea water. In general, a normal diet intake of strontium amounts to 2-4 mg per day (Pors, 2004).

1.6 Strontium in the Human Body

Of the strontium that is orally ingested, more than 99% of the body burden is found in teeth and bones (Pors, 2004, Zhaoyang et al, 2011) and it is estimated that strontium is present in 0.32g in man giving an assumed mass of 70 kg (Helmenstine, 2014) or in terms of ppm, approximately 4.6 ppm (Health Effects, 2013), making it a trace element. As defined by Science Encyclopedia (2014), trace elements are those elements present in amounts smaller than 0.001% of the dry weight (less than 10 ppm).

Compared to other elements, strontium behaves chemically similar to calcium, such that the protein binding of strontium in serum or plasma is of the same order of magnitude as calcium (Pors, 2004). Like calcium and magnesium, it forms divalent cations in biological fluids (Pors, 2004) but only makes up 0.00046% of the body mass as shown in Table 1.4.

Element	Atomic Number	Amount (g)	% of Body Mass
Mg	12	19	0.027
Ca	20	1000	1.4
Sr	38	0.32	0.00046

Table 1.4 Group II elements and their respective properties in reference man (Pors, 2004).

While its essentiality is debatable in the literature, it has been shown to have a dual paradoxical nature providing both detrimental effects and beneficial effects.

1.7 Toxicological and Systemic effects

1.7.1 Inhalation Exposure

Stable strontium is mostly acquired in humans through dietary intake. However, while literature has suggested stable strontium to be of low toxicity in humans, deaths in humans have been reported in relation to stable strontium in the form of strontium chromate (Health Effects, 2013). In this occupational exposure case, the deaths were due to lung cancer resulting from the inhalation of strontium chromate. While stable strontium itself contributes to the solubility of strontium chromate, it was the chromate agent that enters the lung cells where it is metabolized into a genotoxic agent (ATSDR, 2004).

1.7.2 Oral ingestion

Long term consumption of water with high strontium concentration has been shown to cause enamel mottling in humans (Curzon and Spector, 1977). Similar enamel defects on the anterior teeth were seen in young rats fed with strontium carbonate after three weeks of consumption (Storey 1962). Furthermore, there have been several animal and human studies showing that at high doses strontium causes bone deformities and abnormalities such as rickets and osteomalacia (Marie and Holt 1986, Özgur et al. 1996).

As cited by Storey (1962), skeletal defects due to strontium were first demonstrated by Lehnerdt (1910) with later studies showing rachitic effects in young rats (Storey 1962). Storey (1962) showed that young rats (weighing 50 to75 grams) fed with a diet (% mass) of 1.5% calcium (Ca), 0.9% phosphorus (P) and 1.8% strontium in the form of strontium carbonate, developed a rachitic gait at three weeks of dietary intake. Some rats also

showed spinal kyphosis and bent tibiae. It was also observed that the most obvious changes occurred in the distal end of the femur and proximal end of the tibia, with progressive widening growth of the cartilage (Storey, 1962). Widening of the bone occurs when more compact bone has been deposited on the periphery of bone (Tamarkin, 2011). Similar bone abnormalities and defects have been observed in further studies involving animals (Johnson et al. 1968, Reinholt et al. 1984, Marie and Holt 1986, Neufeld and Boskey 1994). Furthermore as cited by ATSDR (2004), high levels of strontium also reduce absorption of glucose, histidine and alanine by the duodenum to levels typical of rachitic chickens. However, whether animal studies may be relevant to humans remains debatable due to the nature of experimental conditions which include differences in metabolism, duration of study and amounts of strontium dosages administered. Adult rats are not a suitable model to study bone effects in adult humans because of the absence of a Haversian bone remodeling system in the rat and the persistence of the epiphyseal cartilage into adulthood. This causes the long bones to continue to lengthen into adulthood, and therefore the rate of strontium incorporation will be proportionally higher (ATSDR, 2004, Leininger and Riley, 1990).

In the epidemiological study by Özgur et al. (1996) which was carried out in the Ulas Health Region of Sivas, Turkey, a high prevalence rate of 32% of rickets was found in children, compared to the national average of 4.4% among children up to 60 months of age (ATSDR, 2004). As cited by ATSDR (2004), the study's objective was to determine whether the soil in the region may have been a contributing factor. The study looked at the strontium concentration in soil from 55 surrounding villages, and 2140 children

between the ages of 6-60 months from these regions who were examined for rickets symptoms such as craniotabes (thinning of the cranium), rachitic rosary (beadlike growths at the end of the ribs), bulging in the wrist, bone deformities of the legs and delayed closure of the fontatelles (ATSDR 2004).

It was found that the prevalence of rickets was highest among children exposed to soils containing the greatest strontium concentration (>350 ppm). Furthermore, interestingly, the study also pointed out that the prevalence of rickets between groups of children exposed to low and high concentration of soil strontium (>350 ppm versus <350 ppm) did not differ for children who were breast fed for 24 months or longer. This suggested that breast feeding provided a protective effect against strontium toxicity in nursing infants by supplying both calcium and protein, which in turn reduces strontium absorption into bone (ATSDR 2004). However, based on the detrimental effects of strontium in these studies, one of the questions that arise is at what concentration is strontium toxic to humans since low doses of strontium have been shown to be beneficial for the treatment of osteoporosis (Neuprez et al., 2008).

One of the earliest studies showing the beneficial effects of strontium in bone was by Shorr and Carter (1947) who suggested that strontium exerted a beneficial effect in bone in post-menopausal women suffering from osteoporosis (Storey 1962). More recent studies, during the early 2000's, confirm this suggestion (Dahl et al. 2001, Neuprez et al. 2008, Boivin et al. 2010, Doublier et al. 2011). The beneficial action of strontium has been suggested to act by increasing bone strength (Bain et al. 2008), and as cited by Neuprez et al. (2008), reducing bone resorption and promoting bone formation. In

addition to osteoporosis, a recent study by Reginster and colleagues (2013) has shown that strontium ranelate may also have an indirect beneficial action for other disorders such as osteoarthritis. Different from osteoporosis, osteoarthritis is a disease characterized by joint degeneration (Reginster et al.,2013). The overall beneficial effects such as reduced vertebral and nonvertebral factures, increased bone mineral density and reduced progression of spinal osteoarthritis are due to the antiresorptive properties of strontium ranelate.

However, with regards to strontium ranelate, it should be noted here, that as of 2014, an advisory against strontium ranelate was put into effect, due to reports of adverse side effects, which included serious cardiac events such as those reported in the "Assessment report for Protelos and Osseor", by the European Medicines Agency (2012). Nevertheless, of debate is whether the side effects are related to the drug itself, the predisposed health risks of the individuals or rather to the elemental strontium. Regardless, knowing the amount of strontium in bone is of interest, especially since there are no published data available on dose response and toxicity levels in humans and the understanding of the mechanism of strontium action in bone.

1.8 Mechanism of Strontium in Bone

There have been several theories proposed relating to the mechanism of action of strontium in human bone. Figure 1.3 illustrates the reducing bone resorption and bone formation effects of strontium ranelate and as indicated by Marie (2006), suggested mechanisms include:

- Strontium acts on the calcium sensing receptor found in bone cells thereby activating inositol phosphate 3 (IP3) production and mitogen-activated protein kinase (MAPK) signaling.

- Strontium exerts its action on osteoblasts, inducing cylcooxygenase (COX)-2 expression and prostaglandin E_2 (PGE_2) production by activating the extracellular signal-regulated kinase (ERK) signaling pathway.

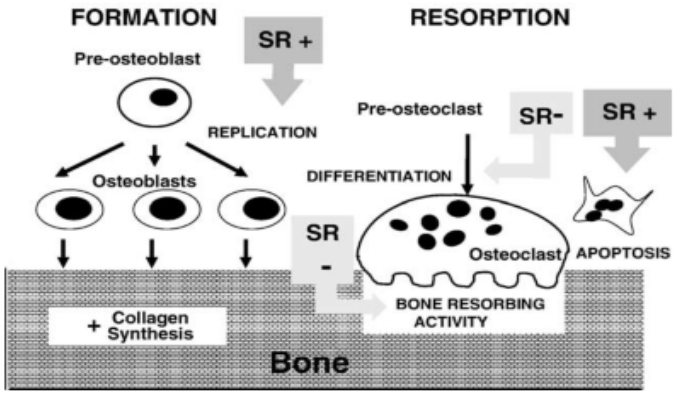

Figure 1.3: Bone formation and anti bone resorption effects of strontium ranelate (Marie 2006).

1.9 Strontium Absorption and Elimination

While 99% of the body burden of strontium is stored in bone mineral with very low amounts in soft tissues (Peebles and Schoeninger 1981), dietary strontium is absorbed mostly through the gastrointestinal tract (GI), mainly from the jejunum (Pors, 2004). The active transport mechanism involves a calcium binding protein (Dahl et al. 2001). In this manner, as cited by ATSDR (2004), studies have estimated that 11 to 28% of the oral strontium ingested is absorbed from the gastrointestinal tract (GI).

However, while strontium binds to proteins in human serum, the characterization of these proteins to which strontium binds to have not yet been identified (ATSDR 2004). The biochemically similar nature of strontium with calcium, suggests that strontium binds

to similar calcium binding proteins, but due to the smaller size of the calcium atom, strontium is bound to a lesser degree. Thus, for strontium to be absorbed preferentially, it should be ingested separately from calcium (Schrooten et al.1998, Pors, 2004). Interestingly, as strontium is incorporated into bone through ionic exchange with calcium, as described below, studies involving monkeys treated with strontium ranelate over a period of 13 and 52 weeks, showed that a maximum of one calcium ion out of every ten in the bone matrix was replaced by strontium in monkeys (Doublier et al., 2011, Oliveira et al., 2012) and a maximum of 0.5 ion in osteoporotic women (Doublier et al., 2011). The larger radius of strontium (0.113 nm or 1.13Å) compared to that of calcium (0.099 nm or 0.99Å) also may induce changes in the mineral properties of bone, such as lattice parameters, crystallite size and crystallinity (Oliveira et al., 2012).

Likewise, strontium is also thought to form complexes with various inorganic anions such as carbonate and phosphate, as well as carboxylic acids such as citrate and lactate (ATSDR 2004). Lactose along with other carbohydrates can promote both strontium and calcium intestinal absorption (Pors, 2004). As stated previously, the absorption of dietary strontium into the GI tract is an active transport process, however, the transfer of strontium from the GI tract (mucosal side) to blood (serosal side) is entirely passive (Pors, 2004). This is in contrast to calcium, in which the transport of calcium from the GI tract into blood could be an active transport process (Pors, 2004). Nevertheless, the amount of strontium compared to calcium in the body skeleton is low, such that strontium is typically 0.032% of the calcium content (Pors, 2004). Although strontium is absorbed mainly via the GI tract, transported into serum and incorporated almost exclusively into

bone, it is also absorbed to a smaller degree by the lungs and skin. The kidney excretes the majority of absorbed strontium while it is also excreted to a much lesser extent by feces and sweat (Cohen-Solal, 2002). In reference man, assuming a body weight of 70 kg, and daily dietary intake of strontium is approximately 2 mg, the loss of strontium in terms of mg per day is 0.34 mg through urine, 1.5 through feces, 0.02 through sweat and 0.2 $x10^{-3}$ in hair (Nielsen, 2004).

As cited by Dahl et al. (2001), strontium uptake and incorporation into bone was suggested to occur by two mechanisms:

(i) Ionic exchange. An initial rapid mode which depends on osteoblastic activity, whereby Sr^{2+} is taken up by ionic exchange with bone Ca^{2+}, bound to preosteoid proteins or a combination of these.

(ii) Absorption and exchange at the crystal surface. This is a slower mechanism by which Sr^{2+} is incorporated into the crystal lattice of the bone mineral.

Within the bone tissue itself, as stated by Frankaer et al., (2014), strontium is postulated to incorporate in different locations as shown in figure 1.4.

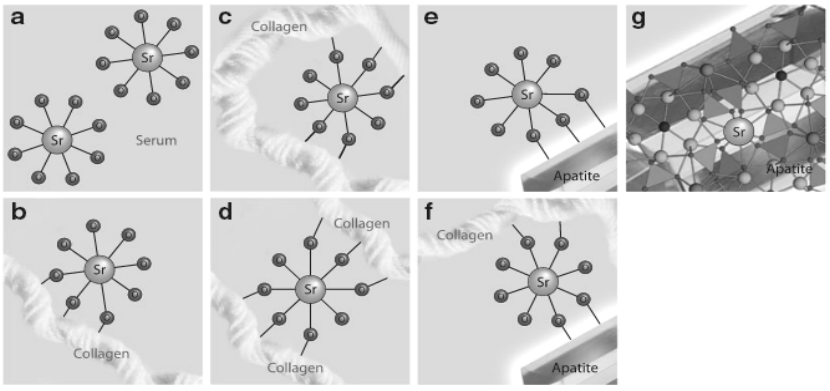

Figure 1.4: Possible locations of strontium incorporated within the bone tissue. These locations include: (a) in serum, (b) adsorbed to the surface of collagen, (c) intrafibrillar cross-linking of a collagen polymer, (d) interfibrillar cross-linking of collagen polymers, (e) adsorbed to the surface of hydroxyapatite (HA) nanocrystals through binding of the hydrated layer, (f) ionic coupling of collagen polymer to HA surface and (g) full incorporation into the bone apatite. (Frankaer et al., 2014).

Interestingly, Boivin et al.(1996) found that new and old bone incorporated strontium in slightly different ways, such that the second mechanism of absorption and exchange was the dominant process in old bone whereas a mixture of the two mechanisms was seen in newly formed bone. This is in agreement with Dahl et al. (2001) who stated that "there is a relatively rapid uptake into new bone and long-term exchange processes in old bone". In a study by Frankaer et al., (2014), involving administration of up to 1000 mg strontium malonate per kg body weight to dogs over a period of 52 weeks, it was observed that 35-45% of the strontium present was incorporated into the calcium hydroxyapatite (CaHA) by ionic substitution with the remaining strontium present either on the surface of HA crystals or absorbed in collagen. It has also been suggested that strontium is incorporated in a dose dependent manner in both cortical and trabecular bone such that it mainly occurred in new bone and in trabecular bone (Pors, 2004). This is most likely explained by the increased porosity and blood surface area of trabecular bone compared to cortical bone. Furthermore, the incorporation of strontium into bone likely depends on a variety of biological factors. Dahl et al (2001) lists five of these factors which include: dosage, gender, plasma levels, skeletal site and duration of strontium intake. However, the extent to which these factors influence human bone strontium levels is not yet clear as Dahl et al (2001) based their five factors on animal studies.

While strontium incorporation is thought to occur by the two mechanisms described previously, strontium elimination from bone has been suggested to occur via a combination of three processes (Dahl et al., 2001):

i) clearance from exchangeable pools of bone

ii) displacement of strontium from sites within the apatite crystal via long term processes

iii) removal from the mineral phase and matrix via osteoclastic resorption

It has also been suggested that the elimination of strontium in bone depends on the bone remodeling activity and how deep the level of incorporation is (Dahl et al. 2001). Furthermore, the terminal half-life of strontium is suggested to be very long, with a suggested time of 3 years for humans, estimated with a nonlinear model and 200-300 days, estimated with a three exponential model (Dahl et al. 2001). However, an unanswered question is whether there is a difference in the half-life estimates between normal bone and diseased bone such as in the case of osteoporosis or osteopenia.

1.10 Tests to Assess Bone Strontium

There are several techniques reported in the literature to assess bone strontium levels and its distribution in humans and animals. These techniques include invasive and non-invasive methods, as well as analysis *in-vivo, ex-vivo* and *in-vitro*. A brief summary of some methods used in the literature are shown in Table 1.5 on the next page.

Group	Method	Type	Subjects
Bärenholdt et al., (2009)	Dual photon absorptiometry (DPA) Dual X-ray absorptiometry (DXA) Bone mineral density (BMD)	non-invasive *in-vivo*	humans
Nielsen et al., (2004)	DPA	non-invasive *in-vivo*	animals, humans
Boivin et al., (2010)	Bone biopsy	invasive *ex-vivo*	humans
Doublier et al.,(2011)	Bone biopsy Focal X-ray microanalysis Quantitative microradiography X-ray cartography	invasive *ex-vivo*	humans
Li et al.,(2011)	Micro CT on lumbar vertebrae Serum analysis (Sr and Ca)	invasive *ex-vivo*	animals
Hwang et al., (2008)	Bone turnover markers (alkaline phosphatase)	invasive *ex-vivo*	humans
Bayhan et al., (2009)	Serum analysis (plasma homocysteine)	invasive *ex-vivo*	humans
Rizzoli et al.,(2012)	High resolution peripheral quantitative computed tomography (HR-pQCT)	non invasive *in-vivo*	humans
Cattani-Lorente et al., (2013)	Micro computed tomography based finite elemental analysis on excised lumbar vertebrae	invasive, *in-vitro*	animals
Cooper et al., (2012)	Synchrotron radiation dual energy K-edge subtraction imaging (KES) on vertebral samples	invasive, *ex-vivo*	animals
Bellis et al., (2009)	Monochromatic microbeam X-ray fluorescence on excised tibia	invasive, *ex- vivo*	animals
Zaichick et al., (1999)	Energy dispersive X-ray fluorescence (EDXRF)	non-invasive *in-vivo*	humans
Oliveira et al., (2012)	Synchrotron radiation micro X-ray fluorescence (SRμXRF) on excised teeth and bones	invasive, *ex-vivo*	animals
Moise et al., (2012)	EDXRF	non invasive, *in-vivo*	humans

Table 1.5: Some methods reported in the literature to assess strontium distribution and uptake in bone.

In addition to some of the common techniques employed in the literature as shown in Table 1.5, other methods to assess strontium influence in bone include proton-induced X-ray emission (PIXE) and laser- ablation- inductively coupled mass spectrometry (LA-ICP-MS), which may also allow for assessing strontium distribution in bone (Bellis et al., 2008). However, most of the techniques used to assess bone strontium levels come with the significant disadvantages of being invasive, limited in sensitivity, limited in sample size and limited to the amount of information gained (i.e. information related to short term exposure). Although, non-invasive methods such as BMD, DXA and DPA methods have recently been employed over the last few years, such methods also present with limitations and concern. For example, BMD measurements taken with DXA, in individuals taking strontium present with the concern of artefactual increases in BMD values, due to the fact that strontium atoms attenuate X-rays much more strongly than calcium atoms do (Blake and Fogelman, 2007). Table 1.6 summarizes some of the limitations and disadvantages of these techniques.

Method	Limitation/Disadvantage
Dual photon absorptiometry (DPA)	cannot be used to monitor changes in % strontium in the patient[1] not sensitive to measure natural bone strontium levels[1]
Dual x-ray absorptiometry (DXA) Bone mineral density (BMD)	Artefactual increases due to strontium lead to overestimation of BMD[2]
Laser-ablation inductively coupled plasma mass spectrometry (LA-ICPMS)	instability issues and element fractionation[3]
Bone biopsy	painful, cannot be done more than twice [4]
Bone turnover markers	affected by food and time of day[5]
Serum analysis	information related to short term exposure
Focal X-ray microanalysis Quantitative microradiography X-ray cartography	*ex-vivo* requires excised bone samples
High resolution peripheral quantitative computed tomography (HR-pQCT)	movement by the patient during scans introduces artefacts and affect quality of scan, influence of edge detection artefacts affecting parameters and overestimating cortical thickness by ~2%[6]
Synchrotron radiation micro X-ray fluorescence (SRμXRF)	*ex-vivo*
X-ray fluorescence spectrometry (XRF)	time (in the case of IVXRF measurements, 30 minutes for each measurement site)

Table 1.6: Main disadvantage of some methods used to assess bone strontium levels. [1]Bärenholdt et al., (2009), [2]Neilsen et al., (2004),[3]Bellis et al (2009), [4]ATSDR (2004), [5]Kendler et al.,(2009), [6]Rizzoli et al.,(2012).

Furthermore, while Bärenholdt et al., (2009) claim that they present for the first time in literature, results of patient studies with long term, non-invasive measurements of bone strontium content using the method of DPA, such method is limited by the inability to measure natural bone strontium levels, as reported by the previous group, Nielsen et al. (2004). With respect to XRF bone strontium measurements performed in humans, there have also been experimental limitations reported in early studies. For example, Wielopolski et al. (1983) measured strontium in the tibial shaft but did not measure

overlying soft tissue thickness and thus could not correct for attenuation of the strontium signal. Hence, the development and optimization of the bone strontium IVXRF system by our research group (Pejović-Milić, 2004, Zamburlini, 2008) presented with the significant advantage to measure bone strontium levels non-invasively and with the sensitivity to measure natural bone strontium levels.

1.11 Contents of this Thesis

As mentioned above, this thesis uses the IVXRF system for bone strontium measurements. The objective of this work was to collect long-term data of bone strontium in human subjects who self-administered with strontium supplements and who were suffering from osteoporosis and/or osteopenia. Furthermore, these data should provide a suitable data set to conduct the modeling of strontium uptake in human diseased bone. This work is significant, considering that there do not appear to exist any long-term studies using the method of IVXRF in human subjects taking strontium supplements nor are there sufficient data relating to the modeling of strontium in long-term osteoporotic and/or osteopenic individuals.

Chapter one is devoted to an introduction to strontium, its importance, bone anatomy and a brief overview of tests used to assess bone strontium levels. Chapter two introduces the IVXRF system and describes the general physics behind it. It also includes an overview of system development and the IVXRF technique. Chapter three follows with examination of spectral fitting and discusses the issue of fitting spectra showing high bone strontium content. Additional elements, such as rubidium (Rb), yttrium (Y) and

zirconium (Zr) are also discussed as these elements could be observed in bone measurements. Chapter four looks at the reproducibility and consistency of the ultrasound measurements and the calibration phantoms used in this work. Chapter five introduces previous work performed with this system and the new work involving long-term measurements over the last four years. It also introduces the publication of results that were published in 2012 and 2014 in the journal Bone (Moise et al., 2012, 2014). Continuing with these measurements, chapter six presents the modeling work performed and introduces key parameters such as half-life and an uptake coefficient. The thesis then concludes with chapter seven which includes bone strontium measurements of individuals from different parts of the world, recommendations for future work and concludes with highlights of important observations.

CHAPTER 2: ENERGY DISPERSIVE X-RAY FLUORESCENCE SPECTROMETRY

2.1 X-ray Fluorescence Spectrometry

XRF is a useful technique that allows for elements to be measured and identified in samples, including in the human body through non-destructive analysis due to the fact that each element emits its own unique set of characteristic X-rays. Elemental analysis may include *in-vivo* studies such as in this work, or *ex-vivo* and *in-vitro* methods. While *in-vivo* methods are direct measurements within an intact human subject/organism, *ex-vivo* and *in-vitro* analysis involves the extraction and isolation of an organ or tissue from the body. The difference between the latter two is that while *ex-vivo* studies are carried in an external environment (e.g. excised bone), *in-vitro* (meaning within glass) studies involves analysis within a test tube or dish and may also include analysis of isolated cells.

As cited by Mattsson and Börjesson (2008), several elements subject to IVXRF measurements have been studied in the literature. Although not comprehensive, Table 2.1 lists some of these elements.

Element (Z)	Application	*In-Vivo* Measurement Site	K absorption edge (keV)	K_α X-ray energies (keV)
Iron (26)	medical	eye, skin	7.11	6.39, 6.40
Copper (29)	medical	eye, skin	8.98	8.03, 8.05
Zinc (30)	medical	eye, skin	9.66	8.62, 8.64
Arsenic (33)	environmental	skin	11.87	10.51, 10.54
Strontium (38)	natural	bone	16.11	14.10, 14.17
Silver (47)	occupational, medical	skin	25.51	21.99, 22.16
Cadmium (48)	occupational, environmental	kidneys, liver	26.71	22.98, 23.17
Iodine (53)	natural, medical	thyroid, blood	33.17	28.32, 28.62
Xenon (54)	medical	brain	34.56	29.46, 29.78
Barium (56)	medical	lungs	37.44	31.82, 32.19
Platinum (78)	medical	kidneys, liver, tumors	78.40	65.12, 66.83
Gold (79)	medical	kidneys, liver, bone joints	80.73	66.99, 68.81
Mercury (80)	occupational, environmental	kidney, liver, thyroid, bone	83.10	68.89, 70.82
Lead (82)	occupational, environmental	bone, kidney	88.00	72.80, 74.97
Bismuth (83)	medical	stomach, intestines, brain tumor	90.53	74.81, 77.11
Thorium (90)	medical	liver, spleen	109.65	89.96, 93.35
Uranium (92)	nuclear weapon industry	bone, lung	115.61	94.66, 98.44

Table 2.1: Elements measured based on *in-vivo* XRF (Mattsson and Börjesson, 2008).

2.2 General Physics Principle behind X-ray Fluorescence

The principle of XRF is based on exposing matter such as bone in this case, to an external source of photons that may interact with the atom. Various photon excitation sources have been used in the literature, and some examples include radioisotopes such as I-125 and Cd-109 and X-ray sources. Although there are a number of ways in which

gamma rays and X-rays interact in matter, such as photoelectric absorption, Compton scattering, Rayleigh scattering and pair production, in which the photon disappears or scatters (Knoll, 2000), of significance in this work are the first three processes.

2.2.1 Photoelectric Absorption

The photoelectric effect is a type of interaction between a photon and an atom in which an orbital electron is ejected from the atom and the photon disappears, transferring all of its energy, *hv* to the atomic electron (Khan, 1994) as shown in figure 2.1. It is also the dominant process for low energy incident photons and is enhanced by absorber materials (also the material of interest) having high atomic number, Z (Knoll, 2000). The probability of photoelectric absorption in terms of atomic number and energy may be approximated by equation 2.1 as (Khan, 1994):

(Equation 2.1) $$\frac{\tau}{\rho} \cong \frac{Z^3}{E^3}$$

Where τ/ρ is the mass photoelectric attenuation coefficient

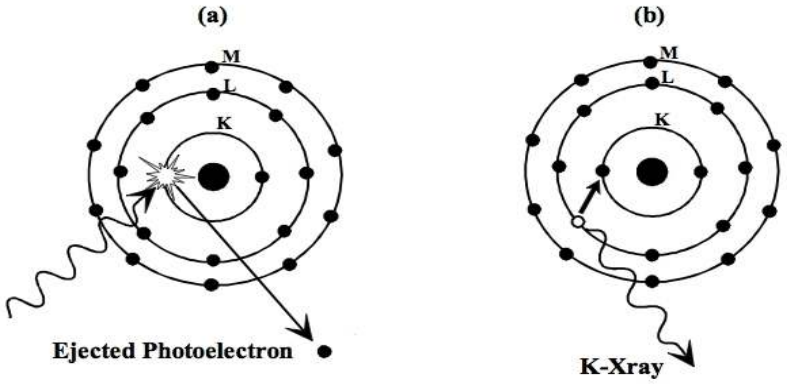

Figure 2.1 The photoelectric effect; (a) photon absorption and ejection of an orbital electron and (b) characteristic K X-ray emitted (Kieranmaher, 2001)

The resulting kinetic energy of the photoelectron (the ejected electron) can be expressed by equation 2.2 (Khan, 1994):

(Equation 2.2) $$KE = h\nu - E_B$$

Where E_B is the binding energy of the electron.

Such interactions may take place with any bound electron but is most probable with the K, L, M or N shells. When the orbital electron has been ejected from its shell, a vacancy is created and the atom is left in an excited state. In order to regain stability and go back to its lowest energy state or ground state, higher-level, outer orbital electrons may fill this vacancy. The energy that is liberated in this transition from an excited state to a ground state takes the form of a characteristic X-ray photon. However, in addition to the binding energy liberated in the form of a characteristic X-ray, it may also be emitted in the form of an Auger electron (Knoll, 2000).

The energy of the characteristic X-ray photon $h\nu$, is given by the difference between the initial and final states. For instance, as described by Knoll (2000), if the vacancy is created in the K shell of an atom, then when that vacancy is filled, a characteristic K X-ray is emitted, and if the transition involved an electron from the outer L shell descending to the K shell, then the energy of the photon may be described by Equation 2.2 as:

(Equation 2.3) $$h\nu = E_K - E_L$$

Where E_k and E_L are the electron binding energies of the K and L shells, respectively (Khan, 1994).

The photon produced in this case, may be termed a K-alpha or K_α photon. Likewise, as shown in figure 2.2, if the filling electron originated in the higher, M shell, a K-beta or K_β photon is produced, having a slightly larger energy, and so on (Knoll, 2000).

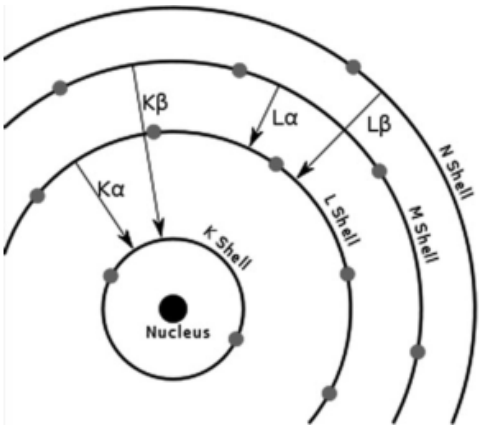

Figure 2.2: Schematic diagram showing orbital transitions (Shackley, 2011)

In this way, vacancies that are created in the outer shells by the filling of a K shell vacancy are then subsequently filled with the emission of L, M, N,…series characteristic X-rays (Knoll, 2000). Furthermore, since the K-series X-rays have the greatest energy compared to the L-series, they are generally of most significance and as described by Knoll (2000), their energy increases regularly with the element's atomic number. Hence, because each element has its own unique energy of the characteristic X-ray emitted, it provides for the foundation for XRF and elemental analysis (NRCan, 2013, Knoll, 2000).

There are two types of XRF, namely wavelength dispersive X-ray fluorescence (WDXRF) and as used in this work, energy dispersive X-ray fluorescence (EDXRF). The difference between the two is that the former uses various crystals to separate the emitted

X-rays based on their wavelengths while the latter uses detectors (i.e. semi-conductor detectors such as Si(Li) to separate and distinguish the emitted X-rays based on their energies.

In this work, the primary element of interest is strontium measured with an energy dispersive X-ray fluorescence system, whose K-absorption edge energy is at 16.105 keV, and whose characteristic K X-ray energies and relative intensities, are shown in Table 2.2 below. Thus considering Table 2.2, the reference to the strontium K-alpha includes the combination of both the K-lines at alpha 1 and alpha 2 whereas the strontium K-beta includes the combination of both the K lines at beta 1 and beta 3.

Line	Energy (keV)	Relative Intensity (%) (per 100 K-shell vacancies)
$K_{\alpha 2}$	14.098	20.3
$K_{\alpha 1}$	14.165	39.1
$K_{\beta 1}$	15.836	5.63
$K_{\beta 2}$	16.085	1.00
$K_{\beta 3}$	15.825	2.91
$K_{\beta 5}$	15.970	0.0215

Table 2.2 Strontium characteristic K X-ray energies and relative intensities (Lawrence Berkley National, 2001, Zamburlini, 2008c).

While radioisotopes are the simplest choice for excitation sources a suitable isotope source in XRF measurements would emit X-rays that are closest to and slightly higher than the absorption edge energy of the element of interest (Shackley, 2011); the closer the energy is to the K-edge, the greater the photoelectric cross section will be, contributing to the strontium X-ray signal (Pejović-Milić et al., 2004).

The second type of interaction of significance is Compton scattering. Also known as incoherent scattering or inelastic scattering, the photon is scattered at an angle, rather than disappearing as in the case above.

2.2.2 Compton Scattering

While in photoelectric absorption, the photon interacts with a tightly bound electron, in Compton scattering the photon interacts with a loosely bound, outer electron, such that it transfers some of its energy to the electron and is scattered at an angle, θ. (Khan, 1994). Figure 2.2 below illustrates the interaction of a photon with an M shell electron.

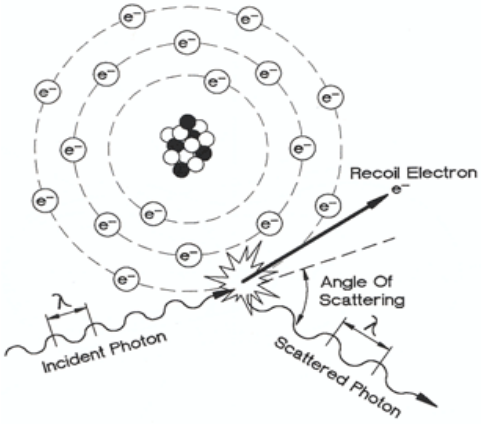

Figure 2.3: Compton scattering (Busse, 2014)

The energy of the scattered photon, termed *hv'* with respect to the scattering angle, θ, may be expressed as (Khan, 1994):

(Equation 2.4)

$$hv' = hv \frac{1}{1 + (\frac{hv}{m_0 c^2})(1 - \cos\theta)}$$

or simplified to $$hv' = \frac{hv}{1+\alpha(1-\cos\theta)}$$

where the rest mass energy of the electron is given by $m_o c^2$ and is calculated to be 0.511 MeV, given that the mass of an electron is 9.11x 10^{-31} kg (Knoll, 2000).

Likewise, the energy of the recoil electron may be expressed as (Khan, 1994):

(Equation 2.6) $$E = hv\frac{\alpha(1-\cos\theta)}{1+\alpha(1-\cos\theta)}$$

where as above, $\alpha = hv/m_0 c^2$

Hence the maximum energy that can be transferred to an electron is when the collision occurs head on, such that the photon makes a direct hit with the electron. In this case, the photon is scattered at an angle of 180 degrees ($\theta=\pi$). However, although the maximum energy is transferred to the electron, the photon will always retain some of the original energy. From equation 2.4, this can be expressed as (Khan, 1994):

(Equation 2.7) $$hv'_{\min} = \frac{hv}{1+2(\frac{hv}{m_0 c^2})} \quad \textbf{or} \quad hv'_{\min} = \frac{hv}{1+2\alpha}$$

And the electron's maximum energy expressed as (Khan, 1994):

(Equation 2.8) $$E_{\max} = hv\frac{2\alpha}{1+2\alpha}$$

In addition to the above scenario in which the electron receives the maximum energy from the photon, a case may occur when the photon makes a grazing hit with the electron, such that the electron is emitted at a right angle and the photon is scattered in the forward

direction ($\theta \cong 0^0$) (Khan, 1994). Hence, the electron will have very little energy and the scattered photon will have almost the same energy as the incident one (Knoll, 2000).

The probability that Compton scattering will occur depends on the number of electrons available for interaction and therefore it increases linearly with increasing atomic number, Z (Knoll, 2000). The Klein-Nishina formula, as given in equation 2.9, predicts the angular distribution of scattered gamma rays (Knoll, 2000):

(Equation 2.9):

$$\frac{d\sigma}{d\Omega} = Zr_0^2\left(\frac{1}{1+\alpha(1-\cos\theta)}\right)^2\left(\frac{1+\cos^2\theta}{2}\right)\left(1+\frac{\alpha^2(1-\cos\theta)^2}{(1+\cos^2\theta)[1+\alpha(1-\cos\theta)]}\right)$$

where, $d\sigma/d\Omega$ is the differential scattering cross section, r_o is the classical electron radius and as previously described, $\alpha = h\nu/m_0 c^2$.

However, while two special situations have been described above where the photon either interacts with the electron head on or just grazes it, in normal circumstances, a continuum of energies can be transferred to the electron ranging from zero up to the maximum, since all scattering angles can occur in the sample (Knoll, 2000).

In terms of Compton scattering with respect to the human body, because the human body has variable thicknesses and is composed of elements with the low atomic number, the magnitude of the background in the characteristic X-ray region originates predominately from Compton scattering (Pejović-Milić et al., 2004). Therefore it should be considered that strontium excitation would not only be excited by primary photons but by photons that undergo Compton scattering in the body as well (Pejović-Milić et al., 2004). The minimum energy arising from the photon excitation source of I-125

(described later on) as used in this work is the silver (Ag) K-alpha at 22.1 keV. The minimum energy of the Compton scattered silver X-ray is 20.3 keV which is still considerably in excess of the K-shell binding energy of strontium. Hence, the presence of silver in the I-125 source makes it a suitable source to excite strontium in bone. For interest, the energy of the main Compton peak is shown in Table 2.4. The third important interaction considered is Rayleigh scattering, which is discussed next.

2.2.3 Rayleigh Scattering

Further to Compton scattering as discussed above, another important type of scattering is Rayleigh scattering, also known as elastic scattering. Unlike photoelectric absorption or Compton scattering discussed previously, in Rayleigh scattering there is virtually no energy transfer since the scattered X-rays have the same wavelength as the incident beam; the gamma-ray photon retains its original energy after the scattering event (Khan, 1994, Knoll, 2000).

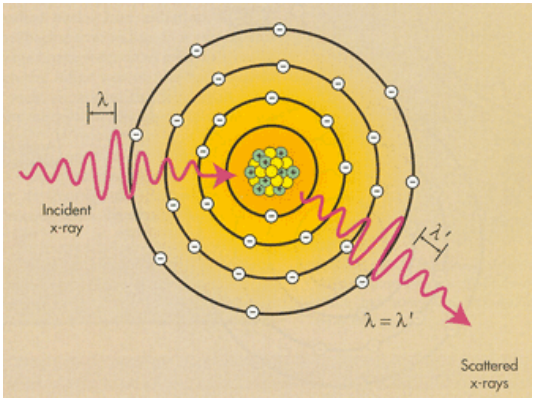

Figure 2.4: Rayleigh (coherent) scattering (Busse, 2014).

In this type of event, the gamma-ray photon interacts coherently with all the electrons of an absorber atom and the atom is neither excited nor ionized. However the direction of the photon is changed such that the average deflection angle decreases with increasing energy; hence, the probability of Rayleigh scattering is significant for low energy photons and is most prominent in high- Z absorbers (Knoll, 2000). One of the important source peaks in the strontium analysis of this work arises from the elastic scattering of the 35.5 keV gamma-ray from the I-125 photon excitation source.

In the case of bone IVXRF measurements, the feasibility and advantages of using coherent normalization have been investigated and used in the literature for bone lead measurements (Somervaille et al, 1985) to correct for factors such as bone size. However, in the case of strontium measurements, the range of photon energies is much lower; 14.1 keV (strontium K-alpha) to the 35.5 keV gamma ray (from I-125 source) in comparison to the lead measurements which can be 4 times higher in photon energy range (Zamburlini et al, 2008a). The feasibility of coherent normalization of bone strontium measurements to either the silver coherent peak at 22.1 keV or to the 35.5 keV photons has been investigated previously by Zamburlini and colleagues (2008a) and is further discussed in section 2.4.

Thus, in conclusion, while photons travel a certain distance before undergoing interactions, the chances of interactions can be characterized by a fixed probability of occurrence per unit path length in the absorber (Knoll, 2000).

2.3 Attenuation

The sum of the probabilities of the three main interactions discussed may be expressed as:

(Equation 2.11) $$\mu = \tau(photoelectric) + \sigma(Compton) + \sigma(Rayleigh)$$

where μ is the linear attenuation coefficient.

However, the usage of the linear attenuation coefficient is limited by the fact that it varies with the absorber's density, even though the material may be the same and hence the mass attenuation coefficient may be more useful (Knoll, 2000). The mass attenuation coefficient is defined as the linear coefficient divided by the absorber density, as shown in equation 2.12 (Knoll, 2000):

(Equation 2.12) $$mass\ attenuation\ coefficient = \frac{\mu}{\rho}$$

In turn, the number of transmitted photons, *I*, may be expressed either in terms of the linear or mass attenuation coefficients such that (Knoll, 2000):

(Equation 2.13) $$I = I_o e^{-\mu x} \quad \text{or} \quad I = I_o e^{-\left(\mu/\rho\right)\rho x}$$

where *x* is the thickness of the absorber and the product ρx is also known as the absorber's mass thickness.

Photon energies having low energies in the range of 20 keV or less will have low penetrating ability and the body will attenuate most of the X-rays. In the case of bone strontium IVXRF measurements, in which measurements are performed in human living

subjects, it is expected that photon attenuation due to soft tissue overlying the bone measurement site will contribute significantly to photon attenuation.

Taking into account the difference between the strontium K-alpha and strontium K-beta energies, the information gathered with the IVXRF system only allows for measurement within a few mm of bone. As stated by Pejović-Milić (2001), when the attenuation of both the incoming and outgoing radiation is taken into account, the strontium K-alpha signal originates from 1.71 mm and the strontium K-beta signal from 2.33 mm thickness of cortical bone. Therefore, the strontium signal obtained from the IVXRF system which is proportional to the bone strontium levels, relates to information at the bone surface only and not deeper within the bone volume.

As cited by Zamburlini (2008c) and Heirwegh (2008), Table 2.3 below lists the values of linear attenuation coefficients (μ) and mean free paths (λ) for the strontium K-alpha and K-beta X-rays. Knoll (2000) defines the mean free path "as the average distance traveled in the absorber before an interaction takes place."

	Skin		Cortical Bone	
	K-alpha	K-beta	K-alpha	K-beta
μ	0.215 mm^{-1}	0.158 mm^{-1}	1.98 mm^{-1}	1.48 mm^{-1}
λ	4.6 mm	6.3 mm	0.51 mm	0.70 mm

Table 2.3: Linear attenuation coefficients and mean free paths for the strontium K X-rays used in this work.

Based on soft-tissue photon attenuation and the total linear attenuation coefficients, equation 2.13 can be written in terms of the strontium K-alpha and K-beta X-rays as:

(Equation 2.14) $$K_{\alpha}: \ln\left(\frac{I}{I_o}\right) = (-3.58 \pm 0.04)x + (0.156 \pm 0.006)$$

(Equation 2.15) $$K_{\beta:} \ln\left(\frac{I}{I_o}\right) = (-2.86 \pm 0.04)x + (0.162 \pm 0.006)$$

where x is the soft tissue thickness, I and I_o are the initial intensity of the strontium X-rays after passage through the soft tissue and the intensity of the strontium X-rays emitted from the bone surface, respectively.

The above equations report the negative total linear attenuation coefficients in units of cm^{-1} and the associated uncertainties are based on the work from Zamburlini et al., (2008a) in which the bone strontium measurements were modeled using Monte Carlo simulation (EGS5).

Thus, the strontium signal observed in the measurements must be corrected for these considerations and other experimental factors. Hence, in this work a two step correction method as indicated by Zamburlini (2008c) was applied to the strontium measurements.

2.4 Two Step Correction Method

To correct for photon attenuation as they pass through overlying soft-tissue, ultrasound soft tissue measurements using a portable 10 MHz ultrasound system (TeleMed Echoblaster 128 EXT-1Z) were performed at each measurement bone site in order to determine the corresponding soft tissue thickness. Images were taken in sagittal and transverse transducer planes and the average of the thicknesses was used in the correction. The consistency of the ultrasound measurements and correlation with body mass is further discussed in chapter four. However, in addition to soft tissue photon attenuation, other factors that may affect the observed strontium signal include:

experimental conditions such as anatomical factors (bone volume, shape, and size), source strength and positioning and reproducibility. For this reason, normalization of the strontium X-rays to the coherent X-ray at 35.5 keV is used as the second step in the correction of the strontium signal. The choice and use of the coherent peak to correct effectively for these factors were investigated by Zamburlini and colleagues (2008a).

2.5 Detector and Measurement Set-Up

In this work, a lithium drifted silicon detector (Si(Li)) was used for the bone strontium measurements. The geometry relative to the measurement site, choice of radioisotope, bone measurement sites and system minimum detection limit (MDL) were previously studied by Pejović-Milić et al., (2002, 2004) and Zamburlini et al.,(2006, 2007a).
The initial set-up of the IVXRF system included Cd-109 as the photon excitation source in a 90 degree geometry, relative to the sample site. Using this set-up, Pejović-Milić and colleagues (2004) successfully measured natural bone strontium levels in ten healthy individuals. The minimum detection limit was 0.250 mg strontium per g calcium and the effective dose was 80 nanosieverts (nSv) for a thirty minute measurement. The system was then later refined to investigate the use of an alternate source, I-125 and 180 degree geometry by Zamburlini and colleagues (2006). This led to an improvement in the MDL to 0.0446 mg strontium per g calcium and an effective whole body dose of 49 and 87 nSv for the finger and ankle, respectively (with respect to a 30 MBq source and thirty minute measurement).

The MDL associated with these measurements may be determined as:

(Equation 2.16) $$MDL = \frac{2\sigma}{\text{slope}}$$

where σ the uncertainty in the zero calibration phantom and the slope refers to the slope in the system calibration line (phantoms used to calibrate the system).

Currently, the combined MDL (MDL of K-alpha and MDL of K-beta) of the *in-vivo* bone strontium XRF system is calculated to be approximately 21-23 μg strontium per g of calcium. Using this set-up, another pilot study (Zamburlini et al., 2007a) was performed involving twenty two subjects. As a result of this pilot study, several questions were brought up relating to strontium levels, including the unexpected result why a smaller value than the theoretical 4-5, was being obtained for the expected K-alpha to K-beta ratio. The reason behind this ratio is discussed in chapter three. Thus, with these questions in tow, the follow-up work looked at different imaging modalities to correct for overlying soft-tissue thickness (Heirwegh, 2008) and further bone strontium measurements in a wider cohort of individuals suffering from bone diseases (Moise et al., 2012).

2.5.1 In-vivo X-ray Fluorescence System

The IVXRF system includes an EG & G Ametek-AMT Si(Li) detector (Ortec©, USA) having a 16mm active diameter with 5.65 mm of sensitive crystal thickness. The detector is protected by a Beryllium window which also absorbs some of the soft X-rays. The energy resolution is 230 eV at 5.9 keV and at 14.1 keV the energy resolution (FWHM) is 272 eV. The photon excitation source used with this detector is I-125 in the form of loose,

sealed brachytherapy seeds (IsoAid©, USA). The I-125 seed (model IAI-125A) excitation source, manufactured by IsoAid© is shown in figure 2.5 below.

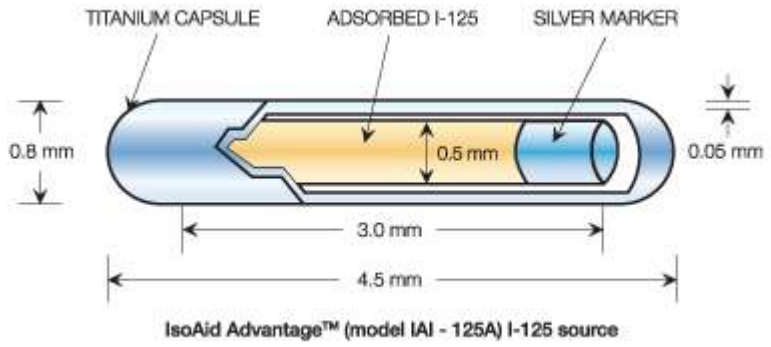

Figure 2.5: Radioisotope source; I-125 seed used (IsoAid©, USA).

As shown in figure 2.5, the 3.0 mm long silver marker (0.5 mm diameter) contains adsorbed I-125 (from a 1 μm thick layer of silver iodide) encased within a titanium capsule of 0.05 mm thickness and outside diameter of 0.8 mm (Carleton 2013, IsoAid©). The entire seed has a length of 4.5 mm and the typical activity (at the time of manufacture) in this work was 23.6 MBq per seed. As a result of the silver marker and interaction, silver X-rays are emitted. This presents with the advantage of increasing the fluorescence yield of strontium since as shown in Table 2.4, the photoelectric cross section for strontium at 22.16 keV is 47.8 cm^2/g. However, in addition to the emission of the silver X-rays, tellurium X-rays are also emitted because of the decay of I-125 to stable tellurium through electron capture and internal conversion of the 35.5 keV gamma rays, as shown in figure 2.6.

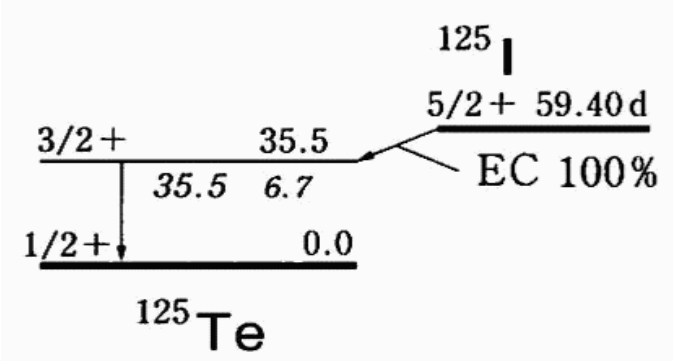

Figure 2.6: Decay of I-125 into Te-125 (Atpages, 2010).

As illustrated in the above figure, I-125 decays by electron capture to the first excited state of Te-125, which then undergoes internal conversion ~93% of the time and emits 35.5 keV gamma rays ~7% of the time.

The energy of the photons emitted by the source is shown in Table 2.4 along with the relative probability for a photon of each energy to be emitted by the source.

	Energy (keV) (relative intensity)	Photoelectric $(\mu/\rho)_{abs}$ for strontium (cm^2/g)
I-125	35.49 (3.91%)	13.2
Tellurium (Te) X-rays	27.20 and 27.47 (58.18%) 30.94 and 30.99 (11.63%) 31.70 (2.56%)	28.2 19.3 18.1
Silver (Ag) X-rays	21.99 and 22.16 (18.47%) 24.91 and 24.94 (4.40%) 25.46 (0.87%)	47.8 35.1 32.9

Table 2.4: I-125 source; emission energies and photoelectric interaction cross section (Zamburlini et al., 2007a).

The I-125 source is placed in a custom made central source holder, which itself is held in place by three plastic arm struts, as shown in figure 2.7.

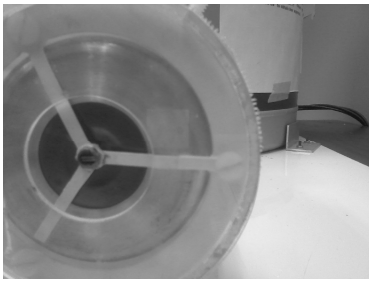

Figure 2.7: Source holder and collimator

Using the I-125 source, as shown in figure 2.8, bone strontium measurements were taken at two different sites for thirty minutes each:

(i) Finger bone; dorsal side of the index finger in the center of the middle phalanx.

and

(ii) Ankle bone; joint at the most prominent part of the medial malleolus of the tibia.

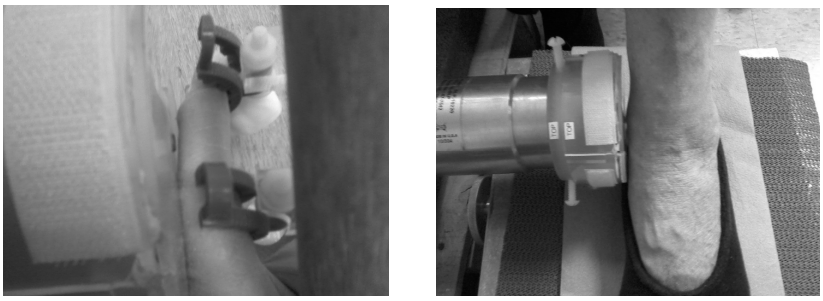

(a) **(b)**

Figure 2.8: Bone strontium measurements in (a) finger and (b) ankle, representing primarily cortical and trabecular bone, respectively.

The above two bone sites were chosen based on these sites having the smallest overlying soft-tissue thickness (Pejović-Milić et al., 2002) and represent primarily cortical bone (finger) and trabecular bone (ankle). In this work the IVXRF system was used to monitor osteoporotic and/or osteopenic individuals self administering with strontium supplements in order to obtain long term data to be used for modeling and gain further insight into

strontium kinetics. This was possible to do with the IVXRF system since the main advantages are that it poses negligible radiation risk and is non-invasive, meaning that measurements could be performed without the restrictions imposed by other methods used in the literature such as bone biopsies and the dual photon absorptiometry technique.

Along with the I-125 source and Si(Li) detector as described earlier, the pulse processing and count sorting was performed using the Ortec® DSPEC Plus digital gamma ray spectrometer and Maestro™ software, respectively. The system optimization parameters were previously investigated by Zamburlini and colleagues (2008b) and remained constant throughout this work. Table 2.5 gives the optimized peak shaping parameters, dead time and technical properties used.

Parameter		Value
HV		-1000 V
DSPP Properties	Effective gain Amplifier gain	2.79 0.5570
ADC	Conversion gain (channels)	2048
Peak Shaping	Rise Time Cusp Width Tail	10 μs 0 0.80 0
Dead Time	Human Measurements Phantoms	30-50% 15-30 %
Measurement Time (humans and phantoms)		1800 seconds (real time)

Table 2.5: Parameters and technical information used in detector settings.

Subsequently, the spectra for each measurement were then analyzed using a modified in-house, non linear least squares Marquardt based fitting routine.

2.6 Sample Spectra

A typical sample spectrum obtained with this system before fitting (figure 2.9) and after fitting (figure 2.10) is shown below, with the peaks of interest highlighted. The counts as shown in the spectrum below and in further spectra in this thesis refer to the number of counts per channel.

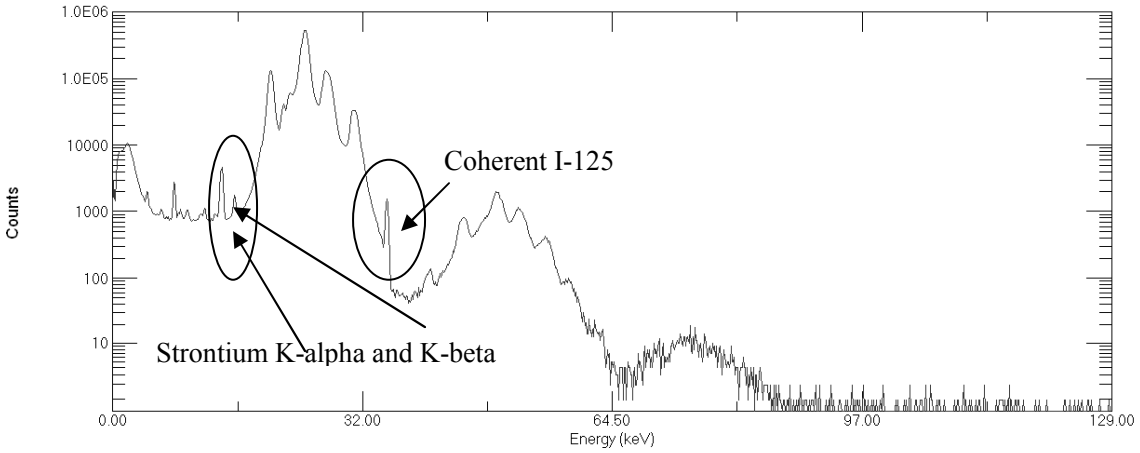

Figure 2.9: Sample raw spectrum obtained for a strontium supplementing individual (30 minute measurement in the ankle). The circled regions highlight the strontium alpha and beta X-rays at 14.2 and 15.8 keV, respectively and the coherent peak at 35.5 keV.

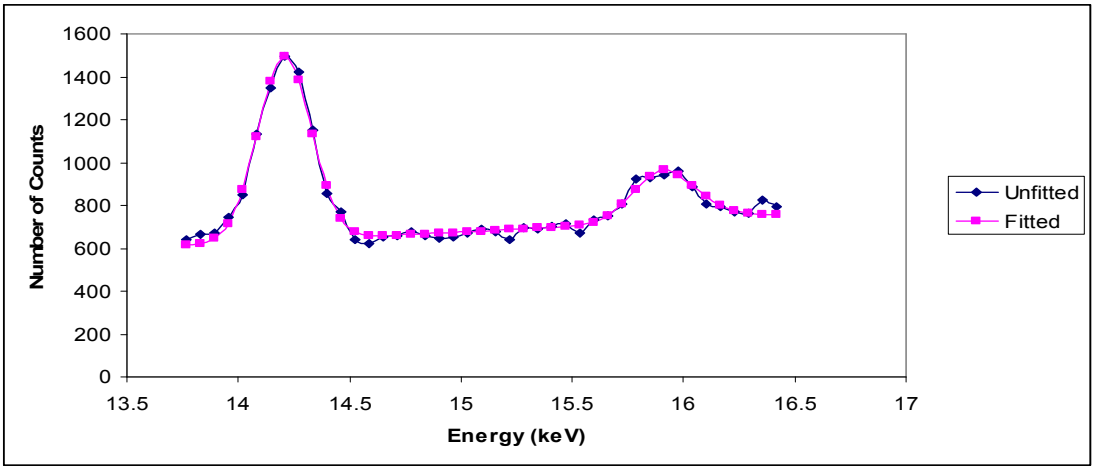

Figure 2.10: Sample spectrum showing the unfitted counts (blue) and the fitted counts (pink) of the two strontium X-ray peaks at 14.2 and 15.8 keV to be used in the analysis of the strontium signal.

The fitting of the spectrum obtained in this work and further analysis is discussed further in chapter three. Of interest, is the fitting results obtained when strontium signals begin to rise 20-30 times higher than the previously observed strontium levels, particularly considering that previous work done on fitting was performed on low baseline strontium levels. The next chapter provides more information on this fitting approach.

CHAPTER THREE: SPECTRAL FITTING IN IVXRF MEASUREMENTS

3.1 Introduction

Since the area under the strontium peaks contains information relative to the bone strontium levels in an IVXRF measurement, quantitative analysis of the strontium peaks should take into account relevant spectral features and employ a fitting routine that best models the shape of the strontium peak. As described in chapter two, although both strontium K-alpha and strontium K-beta peaks are observed, the strontium K-alpha peak at 14.2 keV which includes the combination of both the K-lines at alpha 1 and alpha 2 is used for the analysis of bone strontium levels in measuring the individuals with the IVXRF system. However, if the strontium K-beta peak at 15.8 keV (includes the combination of both the K lines at beta 1 and beta 3) is fitted and used to calculate the ratio of strontium K-alpha to strontium K-beta, then, theoretically, a value of 4.4 ± 0.4 is expected but was not observed for the natural bone strontium readings. This is further discussed in section 3.3.

As in XRF measurements, the peaks resemble a Gaussian peak and thus could be fitted using a Gaussian function, as shown in equation 3.1. However, distortion of the Gaussian peak may arise due to incomplete charge collection while tailing may become an issue at high counts.

(Equation 3.1) $$G(x) = \frac{A}{\sqrt{2\pi\sigma^2}} * \exp\left(-\frac{(x - x_o)^2}{2\sigma^2} \right)$$

where A is the peak area, x is the channel number and x_o and σ are the centroid and Gaussian width (Gaussian standard deviation), respectively.

To account for this distortion, several functions have been suggested in the literature. Campbell and Jorsch (1979) analyzed various functions to fit experimental peaks recorded in Si(Li), Ge(Li) and Ge detectors that included looking at a combination of the background, step function and tail function. The Hypermet function which consists of a combination of the Gaussian, tail and step function was proposed by Campbell and colleagues (1985) as best describing a full energy peak for Si(Li) detectors. The step function which takes into account the height differences on either side of the peak, and the tail function which takes into account the amplitude and shape, are shown in equations 3.2 and 3.3, respectively. Figure 3.1 illustrate the contribution of the Gaussian, tail and background components in the fitting function.

(Equation 3.2) $$S(x) = S * erfc\left(\frac{x - x_o}{\sqrt{2\sigma}}\right)$$

where S is the amplitude of the step function and x, x_o and σ are the same as defined in equation, 3.1.

(Equation 3.3) $$T(x) = T * \exp\left(\frac{x - x_o}{\beta}\right) * erfc\left(\frac{x - x_o}{\beta} + \frac{\sigma}{\sqrt{2}\beta}\right)$$

where T is the amplitude of the tail function, β is the coefficient that determines the shape of the tail function and x, x_o and σ are the same as defined in equation, 3.1.

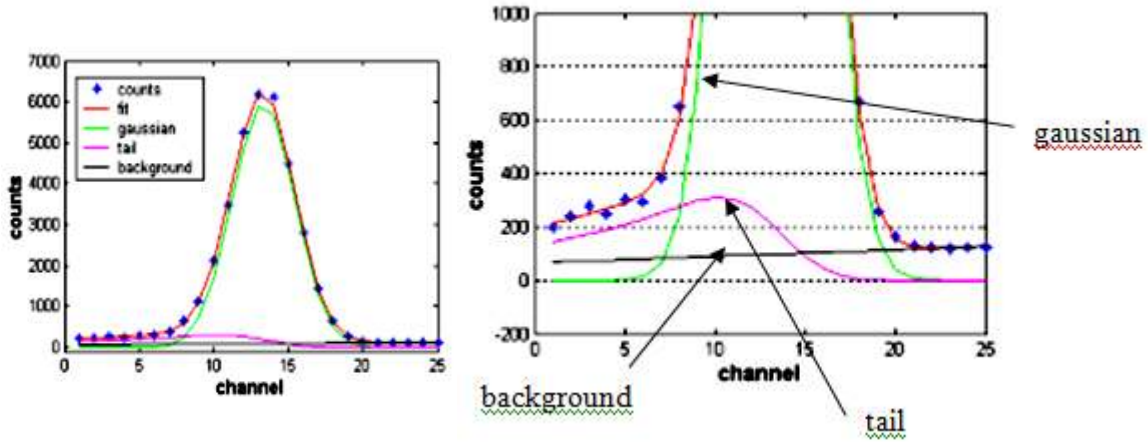

Figure 3.1: Contribution of the Gaussian, tail and background components to the fitting function (Zamburlini, 2008c).

The Hypermet function is expressed as a sum of these functions as : $G(x) + S(x) + T(x)$. On the basis of these functions, Zamburlini (2008c) investigated the best fitting routine to be used and concluded that while the Hypermet function together with the background gave the best results visually, the best fitting function was one consisting of the sum of the Gaussian and tail function. With respect to the IVXRF measurements, as Zamburlini (2008c) concluded, the model best fitting this description would be one in which the $K_{\alpha 1,2}$ and the $K_{\beta 1,3}$ peaks are fitted with the sum of the Gaussian and tail function and the $K_{\beta 2}$ peak fitted as the Gaussian.

However, while the fitting routine incorporating seven parameters has been shown to be satisfactory in the case of the strontium IVXRF measurements, of question is the use of the same fitting function to analyze high counts, as in the case of the low levels of strontium in the measured individuals who have been supplementing with strontium over a long period and show high bone strontium levels. This is of question since the fitting routine work was based on low strontium levels.

3.2 Fitting Comparison

Using the different fitting functions having 7, 9 or 11 parameters, the fitting of the strontium K-alpha at 14.2 keV and the strontium K-beta peak at 15.8 keV was used to compare and determine the best fitting function.

For the seven parameter model (G + B), the assumptions are:
(i) position of alpha1 and beta1 unlinked;
(ii) position of beta1 and beta2 linked;
(iii) amplitude unlinked for all three peaks;
(iv) tail for the alpha1 and beta1 peaks;
(v) gaussian width different for alpha and beta, but the same for the two betas.

The parameters are:
P(1) - position of strontium alpha peak
P(2) - area of strontium alpha peak
P(3) - width strontium alpha peak
P(4) - area of strontium beta peak
P(5) - width strontium beta peak
P(6) - amplitude of the background exponential
P(7) - exponent of the background exponential

Similarly, for the 9 parameter model and the 11 parameter model, (G+B+T), the same assumptions apply but due to the addition of the tail function, additional parameters are added to the 9 (P8 and P9) and 11 parameter routine (P8, P9, P10 and P11):

P(8): tail amplitude
P(9): beta coefficient of the tail
P(10): tail amplitude of the beta peak
P(11): beta coefficient of the tail (beta peak)

Measurements obtained from a subject's ankle were used in this comparison: the baseline measurement, a 4 month measurement and a high measurement (> 3years). Note that the ankle data were chosen as it shows a higher strontium level compared to the finger after a few months of supplementation. Figure 3.2 shows the spectrum acquired at

these time periods, which demonstrate the continued increase of the strontium signal in the ankle.

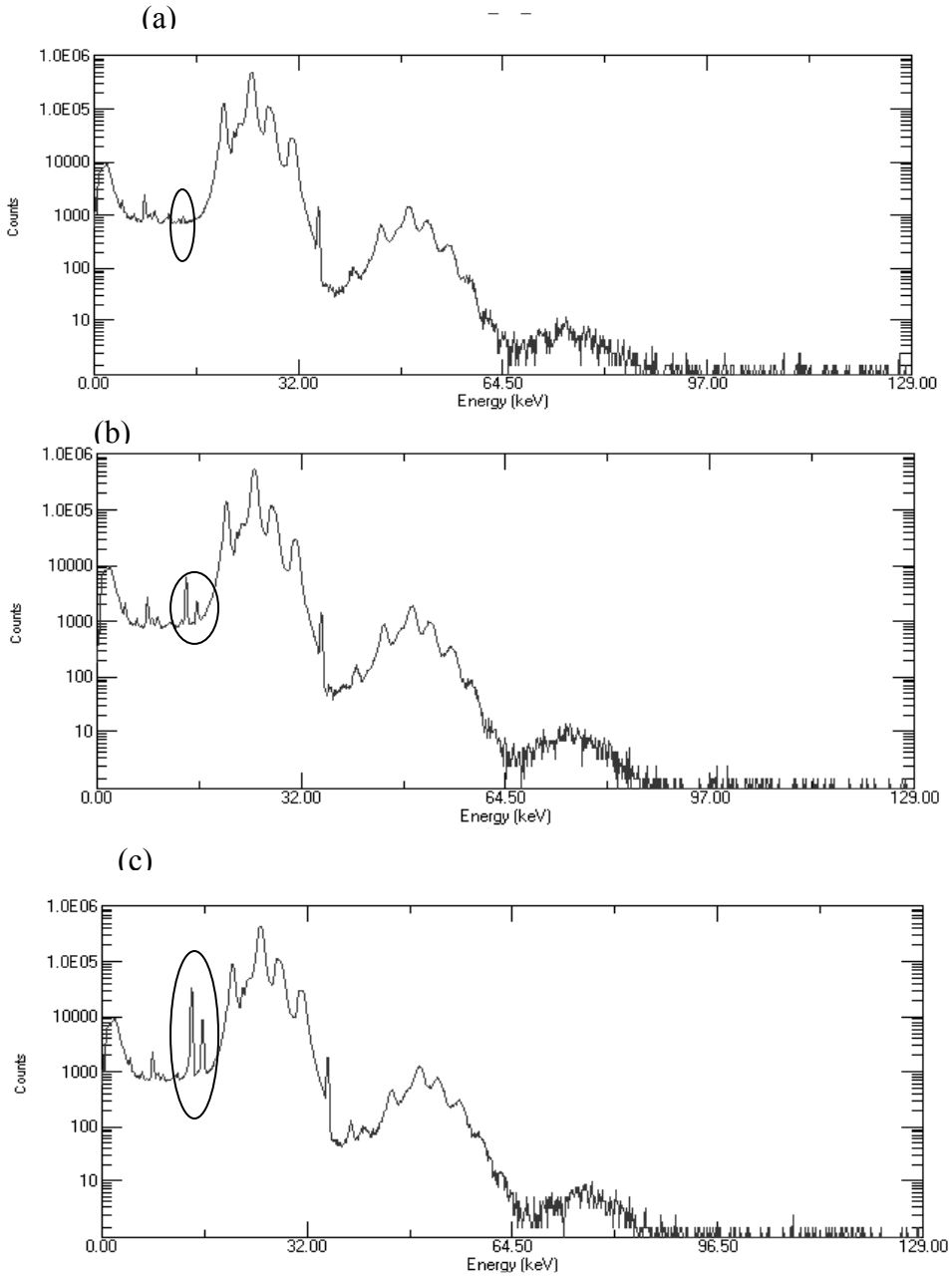

Figure 3.2 (a), (b) and (c): Spectrum acquired for a subject's ankle at baseline, 4 months and 3 years. The circled peaks are the strontium K-alpha and strontium K-beta peaks at 14.8 and 15.2 keV.

The chi square which looks at the goodness of the fit is reported in Table 3.1.

Time	Number of parameters	strontium K-alpha (uncorrected)	strontium K-beta (uncorrected)	χ^2
Baseline	7	1312 ± 87	557 ± 133	1.3981
4 months	7	15557± 130	3589 ± 97	1.4533
3 years	7	95449 ± 263	23449 ± 155	1.8211
Baseline	9	1301 ± 199	506 ± 193	1.4349
4 months	9	15376 ± 256	3473 ± 118	1.0122
3 years	9	91939± 693	21307 ± 266	1.1377
Baseline	11	1328± 410	222± 170	2.7711
4 months	11	15067 ± 297	3183 ± 220	2.6569
3 years	11	88374 ± 806	20178 ± 321	6.0719

Table 3.1: Comparison of fitting routine for three strontium levels in an individual's ankle.

The results as per Table 3.1, show that for high strontium levels (i.e. > 3 years), the fitting chi square improves when a nine parameter model is used. The tailing is expected to be more prominent at higher strontium levels such as in the case of ankle bone strontium measurements of 3 years. The larger values observed for the strontium K-alpha fitted area for the 7 parameter model compared to the 9 parameter and 11 parameter fitting routine (i.e. ankle measurement) is due to the lack of the tail function. As discussed previously, the 7 parameter fitting routine uses a Gaussian + Background fitting function, thus the counts in the tail are added to the peak area. Addition of the tail function at higher strontium levels seem to improve the overall fitting for the 9 parameter model and as expected addition of the tail function results in higher uncertainties. Comparison of the 11 parameter model to the 7 and 9 parameter fits shows much higher chi square values (χ^2 >1). The higher chi square values may be due to the guesses inputted for the beta peak tail amplitude and beta coefficient, which in turn define the shape function. However,

given the results in Table 3.1 for the highest strontium signal observed among the baseline subjects up until the last measurement, the fitting routine using the 9 parameter fit seems adequate. An example of a 9 parameter fit, showing both strontium peaks fitted is shown in figure 3.3 below. Based on the fitted peaks, only the strontium K-alpha peak (after the two step correction method has been applied) was used to report individual's strontium levels as a non-dimensionless number, since absolute strontium concentrations cannot be obtained, as discussed in chapter 7.

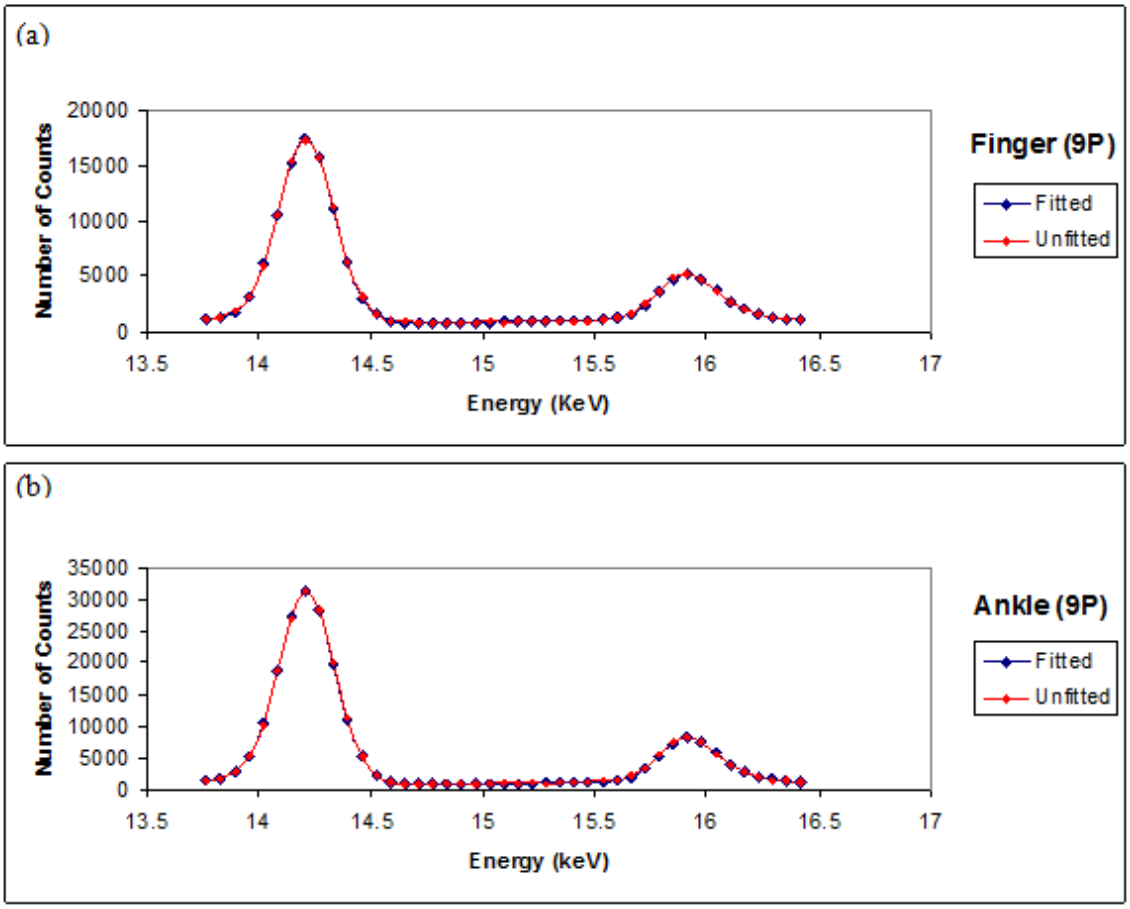

Figure 3.3 (a) and (b): Example of a 9 parameter fitting (subject R8) showing the fitted strontium K-alpha and K-beta peaks.

3.3 Strontium K-alpha and Strontium K-beta ratio

If it is considered that the emission probability for the strontium K-alpha photon is seven times greater than that of the strontium K-beta photon, then theoretically, it is expected that the ratio of the strontium K-alpha and the K-beta peaks is approximately equal to seven. However, experimentally, this ratio is lower when factors such as bone volume and photon attenuation due to overlying soft tissue are considered. Zamburlini et al (2007) calculated this lowered ratio to be 5.2, based on the assumptions that strontium is uniformly distributed in hydrated cortical bone and that bone thickness is infinite at this energy. Based on this calculated expectation, experimentally when the ratios were analyzed for baseline subjects in this study and in previous work by Zamburlini and colleagues (2007a) and Heirwegh (2008), the average observed ratio was between 2 and 3. For example, for the finger baseline measurements, the average ratio was 3.2 ± 0.7 and 2.7 ± 0.5 for the ankle, respectively. Similarly, Heirwegh (2008) observed ratios between 2.6 and 3.2 in his measurements of cadaver fingers (including overlying soft-tissue) and Zamburlini and colleagues (2007a) observed ratios of 2.9 ± 0.7 and 2.7 ± 1.0, for the finger and ankle respectively. This was a perplexing observation, especially as Zamburlini (2008c) found that strontium was uniformly distributed in bone through Particle Induced X-ray Emission (PIXE) analysis performed on five male cadaver index fingers. Moreover, Monte Carlo simulation of the bare bone EDXRF measurements predicted the ratio to be 4.4 ± 0.4 (Zamburlini, 2008).

However, since the strontium K-beta peak is not used in the analysis of this work, the results obtained in this work were not affected by the unexpected lower ratio. Nevertheless, the lower than expected ratio was thought to be due to the fitting routine underestimating or overestimating one of the strontium peaks, due to an overlap of another element such as rubidium or zirconium being present in the measurement sample. Table 3.2 below illustrates their similar emissions.

Element	Characteristic X-ray (keV)
strontium	**$K_{\alpha 1}$: 14.16, $K_{\beta 1}$: 15.83**
rubidium	$K_{\alpha 1}$: 13.39, **$K_{\beta 1}$: 14.96**
zirconium	**$K_{\alpha 1}$: 15.77**, $K_{\beta 1}$: 17.67

Table 3.2: K emission lines for rubidium and zirconium that may overlap with the strontium K lines.

Thus, it was hypothesized that:

(i) Since rubidium was observed in the spectrum of volunteer measurements, perhaps re-writing the fitting routine to analyze the strontium K-alpha, rubidium K-alpha and strontium K-beta and rubidium K-beta would improve the experimental strontium ratio.

(ii) Zirconium could be present in the system which would lead to the strontium K-beta being overestimated.

Both of these possibilities were thus tested and are discussed next.

3.3.1 Fitting Rubidium observed in Human Subjects

In humans, rubidium is generally present in all soft tissues and to a very small extent in bone and in the enamel of teeth, such that in reference man, the total body content is typically 360 mg (Underwood, 2012). In bone, the mass fraction of rubidium is about two orders of magnitude smaller than that of strontium (Zaichick, 2013). This work, which was presented at the European X-ray Spectrometry Conference held in Vienna, Austria

on June 2012, was performed to test whether rubidium may inadvertently affect the ratio. The fitting routine was re-written to analyze the rubidium K-alpha and rubidium K-beta peaks. To analyze the strontium K-alpha and rubidium K-alpha peaks, the following assumptions were made (personal communication, Dr. David Chettle):

(i) the positions of the strontium and rubidium K-alpha peaks are linked
(ii) the widths differ for the two peaks
(iii) separate amplitudes
(iv) single exponential background

Similarly, to analyze the strontium K-beta and rubidium K-beta peaks, the same above assumptions were made except that the widths are assumed to be same fixed width. The fitting routine was applied to a volunteer's data as shown in Table 3.3. As shown in Table 3.3 below, the observation that the ratio of strontium K-alpha to strontium K-beta approaches the expected ratio value of between 4 and 5 as the strontium signal increases is consistent with an overlapping spectral feature which is relatively constant in amplitude.

	Finger		Ankle	
Time (Days)	Current Fit Ratio	Alternate Fit Ratio	Current Fit Ratio	Alternate Fit Ratio
0	2.14 ± 0.56	1.90 ± 0.35	1.42 ± 0.70	5.13 ± 2.88
1	3.44 ± 0.88	4.51 ± 0.73	3.83 ± 0.56	3.89 ± 0.44
8	4.08 ± 0.32	4.42 ± 0.26	3.96 ± 0.20	4.33 ± 0.16
15	3.59 ± 0.28	4.30 ± 0.24	4.23 ± 0.16	4.20 ± 0.14
36	3.97 ± 0.18	4.68 ± 0.16	4.10 ± 0.13	4.39 ± 0.11
66	3.97± 0.15	4.46 ± 0.14	4.12 ± 0.11	4.50 ± 0.10
73	3.55 ± 0.17	4.05 ± 0.14	3.89± 0.07	4.42 ± 0.07
96	4.14 ± 0.17	4.44 ± 0.14	4.12 ± 0.06	4.31 ± 0.05
111	4.08 ± 0.18	4.42 ± 0.14	4.00± 0.06	4.26 ± 0.06
253	3.33 ± 0.08	4.40 ± 0.10	3.90 ± 0.04	4.36 ± 0.05
263	NA	NA	3.84 ± 0.17	4.26 ± 0.15
297	3.46 ± 0.07	4.30 ± 0.08	4.07 ± 0.04	4.25 ± 0.04
379	4.01 ± 0.06	4.19 ± 0.06	4.25 ± 0.03	4.36 ± 0.04
416	4.01 ± 0.07	4.21 ± 0.07	4.15 ± 0.05	4.23 ± 0.05
444	3.92 ± 0.07	4.09 ± 0.07	4.04 ± 0.04	4.14 ± 0.04
504	4.17 ± 0.06	4.31 ± 0.06	4.11± 0.04	4.18 ± 0.03
614	4.16 ± 0.05	4.23 ± 0.05	4.15 ± 0.03	4.29 ± 0.03
662	4.14 ± 0.05	4.25 ± 0.05	3.95 ± 0.04	4.08 ± 0.05
723	4.17 ± 0.06	4.32 ± 0.06	4.06± 0.05	4.19 ± 0.05
753	4.08 ± 0.05	4.17 ± 0.05	4.18± 0.03	4.36 ± 0.03
846	4.00 ± 0.05	4.21 ± 0.05	4.04± 0.04	4.22 ± 0.04

Table 3.3 : Ratios refer to the strontium K-alpha peak at 14.2 keV and strontium K-beta peak at 15.8 keV. The current fit refers to the usual fitting routine and assumes no linkage between the rubidium and strontium peaks whereas the alternate fit refers to the revised fitting routine as described in section 3.3.1 and assumes linkage. NA indicates measurement not available.

Figure 3.4 (a) and (b) include the graphical representation of the strontium K-alpha peak area over time using the current fitting routine and the alternate fitting routine for the finger and ankle bone site, as discussed above.

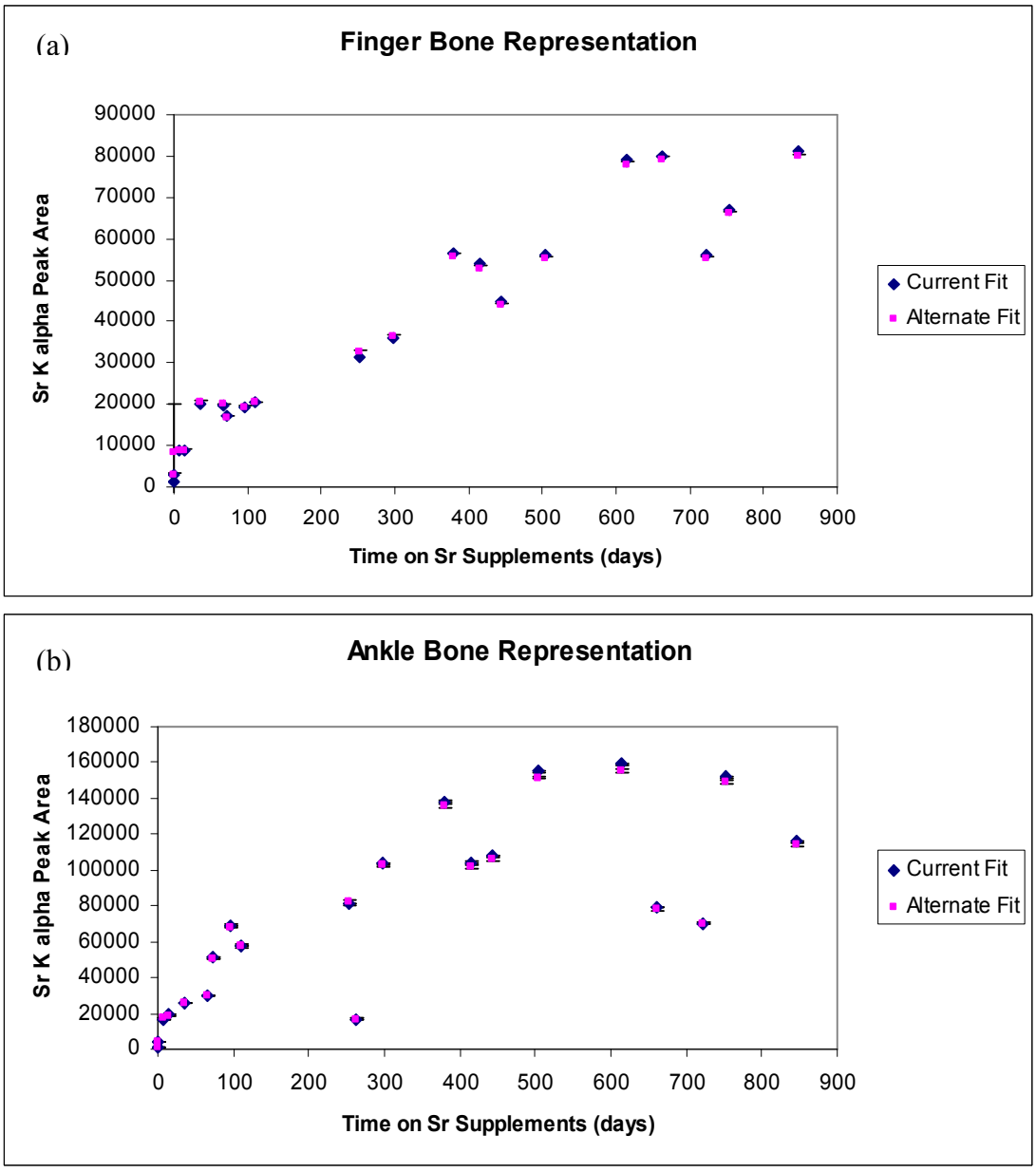

Figure 3.4 (a) and (b): Graphical representation for finger and ankle bone measurements in a baseline volunteer, respectively. The graph represents the strontium K-alpha peak area over time using the current and alternate fits. Note that the uncertainty is too small to be seen in the graph.

The results showed that the ratio for the finger and ankle bone measurements for both the current and alternate fit were within agreement of each other, taking into account uncertainty. For example, at baseline (t=0 days), finger and ankle ratios of 2.14 ± 0.56 and 1.42 ± 0.70 for the current fit was observed compared to finger and ankle ratios of 1.90 ± 0.35 and 5.13 ± 2.88 for the alternate fit. Overall comparison of the strontium K-alpha areas between the two fits indicated an excellent correlation of 0.998 and 0.999 for the finger and ankle, respectively. Thus, these results indicated that the problem was not due to rubidium peaks potentially affecting the strontium peaks and warranted further investigation. This raised the question of whether there any possible zirconium contamination within the system itself.

3.3.2 Zirconium Contamination of the IVXRF System

A background run for 1800 seconds real time on the system with the collimator in place and without was performed to check for possible zirconium contamination and indicated that there was no zirconium present in the system nor in the collimator. However, when the I-125 seed was placed in front of the detector, the system detected a peak at 15.77 keV as shown in figure 3.5. Colleagues at the Department of Physics (Ryerson University) initially observed this effect. A smaller peak at 17.67 keV suggested the presence of zirconium within the seed itself.

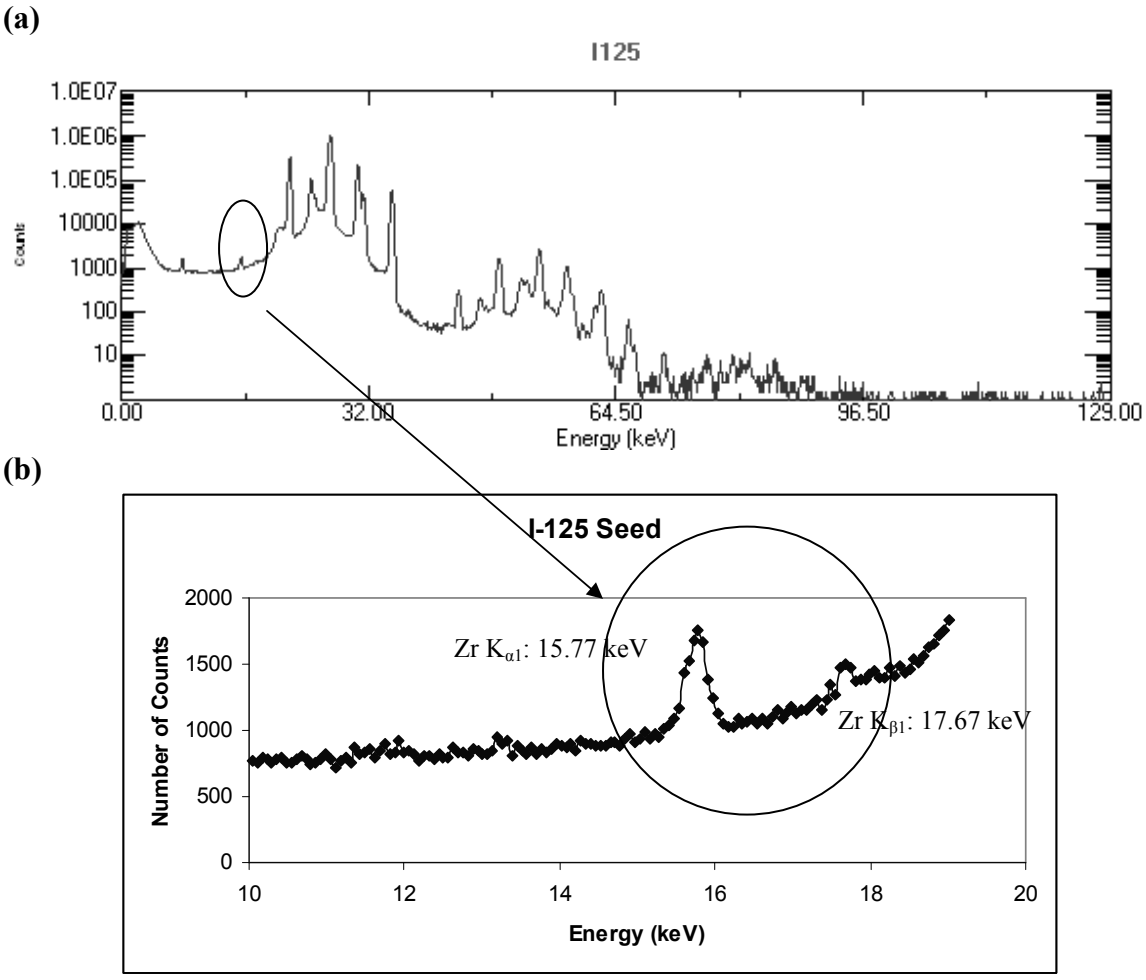

Figure 3.5(a) and (b): Spectrum of IsoAid® I-125 Advantage brachytherapy seed used as the photon excitation source for the IVXRF measurements.

Although, it is unclear why there might be zirconium present in the IsoAid I-125 seed, it is possible that it may be a byproduct of the manufacturing process.

I-125 seeds are manufactured according to the following reaction (Khalil, 2010):

$$^{124}\mathrm{Xe}\,(\mathrm{n},\gamma)\rightarrow{}^{125\mathrm{m}}\mathrm{Xe}(57s)\rightarrow{}^{125}\mathrm{I}\,(59.4\mathrm{d})$$

$$^{124}\mathrm{Xe}\,(\mathrm{n},\gamma)\rightarrow{}^{125\mathrm{g}}\mathrm{Xe}(19.9\mathrm{h})\rightarrow{}^{125}\,\mathrm{I}(59.4\mathrm{d})$$

The usual method of producing I-125 is by irradiation of Xenon-124 constituting 0.096% ^{124}Xe gas (Han et al., 2005), which is the target isotope to produce I-125 through neutron capture as shown in chapter two. As part of the irradiation process, ^{124}Xe gas may be loaded into capsules made up of zircaloy, a zirconium alloy or aluminum which are then subjected to neutron bombardment (IAEA, 2006, Han et al., 2005). As described in a patent by Zeigler et al (2002), newer I-125 seeds may comprise a radioactive carrier matrix which emits the radiation in a controlled manner. The carrier matrix itself is made up of a porous, inorganic material (porosity of about 15-40%) and can consist of TiO_2, Al_2O_3, ZrO_2, Y_2O_3, of which the pores contain I-125 and which is enclosed within a capsule (Zeigler et al., 2002).

Thus, because zirconium is present in the I-125 seed, obtaining a theoretical ratio of 5.2 for baseline subjects and low strontium counts will not be achievable. This is because the I-125 seed emits zirconium X-rays and a portion of these which is elastically scattered off the sample will enter the detector and closely overlap the strontium K-beta. However, as stated previously, since the IVXRF measurements uses the strontium K-alpha peak at 14.2 keV for analysis, the effect of zirconium overlapping the strontium K-beta peak does not impact the results obtained in this study. Although Zamburlini (2006) observed that strontium is uniformly distributed in bone, based on Table 3.3, it is not expected that the ratio will impart any information with respect to bone health in the volunteers.

In addition to observing the presence of rubidium and zirconium in the spectrum in humans and the radioisotope source, respectively, the presence of yttrium is another

element that was unexpectedly observed in excised human bone samples provided in collaboration with Albany state.

3.4 Presence of Yttrium in Excised Human Bone Samples

In collaboration with Wadsworth Center, Division of Environmental Health Sciences and the University at Albany, one of the objectives in this collaboration was to measure bone seeker elements such as strontium, lead, aluminum and fluorine in excised bone samples. At McMaster University, measurements of these elements are performed based on the techniques of XRF and IVNAA (*In-vivo* neutron activation analysis*)*. The Albany group's laboratory uses techniques based on inorganic mass spectrometry such as inductively coupled plasma-mass spectrometry (ICP-MS) to measure trace elements in human tissues and body fluids and so this collaboration provided for a unique opportunity to share results between two groups using different methods of analysis on the same set of bone samples.

In the excised human bone samples provided (age and pathology unknown), measurement with the XRF system detected the presence of yttrium. Studies involving radioactive isotopes of Y have suggested it to be a bone seeker element, such that Y is removed rapidly from the blood and deposited in the osteoid matrix of bone, where it can remain for a very long period of time (MacDonald et al., 1951). However, MacDonald and colleagues (1951) found that macro amounts of stable yttrium (intraperitoneal injection of yttrium chloride: 60 mg per kg of body weight) administered to thirty, young male rats over a period of at least five months did not accumulate in bone. They observed

that when dosages as large as 936 mg were administered, the amount of yttrium in bone ash never exceeded 330 ppm, whereas similar dosages of strontium showed a larger uptake by a factor of 100. Furthermore no correlation was seen between the bone burden of yttrium and dosage and attempts to fit the data with a single exponential function (linear line) did not fit the data adequately. The finding of yttrium in the Albany bone samples was unexpected since it is present in negligible amount in the human body. Nevertheless, yttrium was clearly distinguishable and seen for the five samples measured. Figure 3.6 shows a sample spectrum and figure 3.7 summarizes the yttrium results.

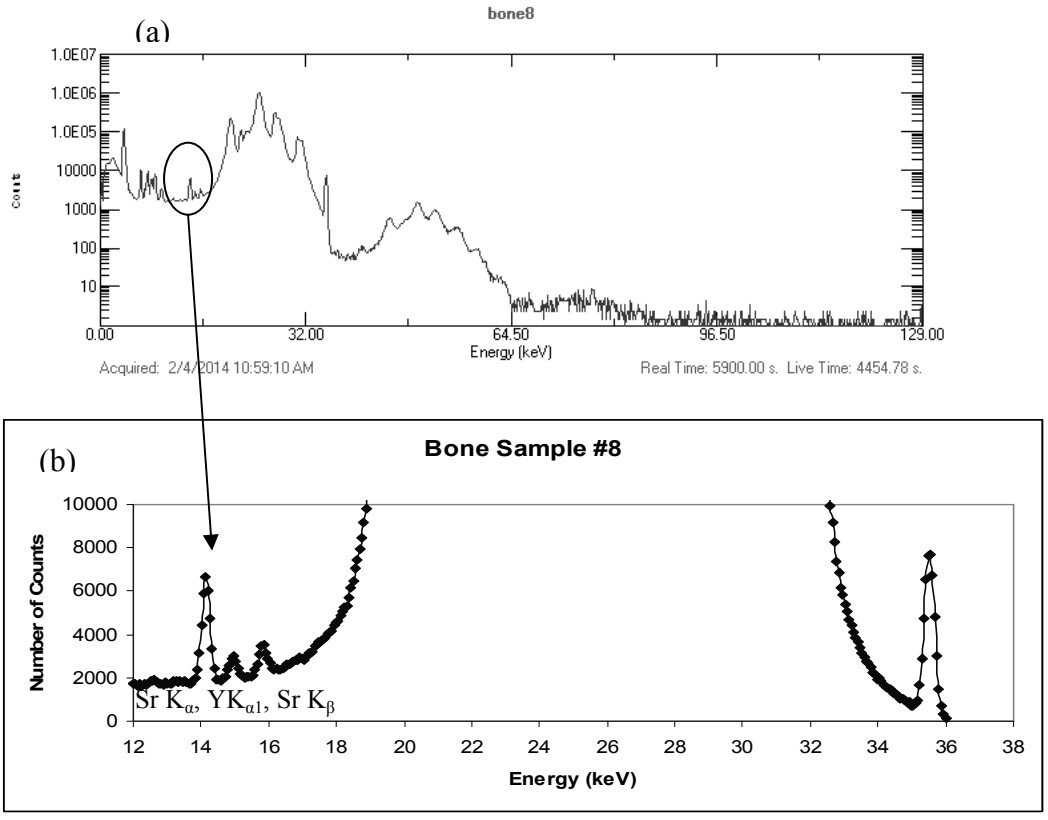

Figure 3.6 (a) and (b): Sample spectrum for bone sample #8, showing the presence of yttrium $K_{\alpha 1}$ peak at 14.96 keV.

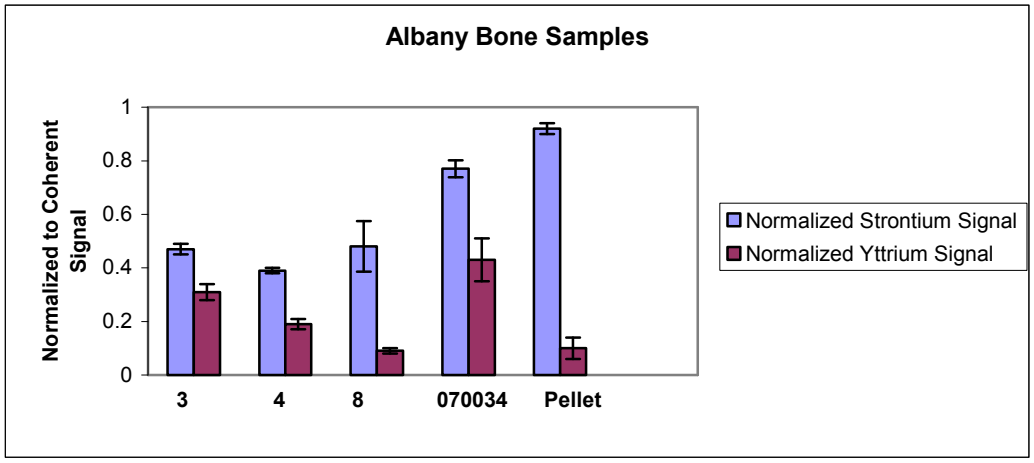

Figure 3.7: Comparison of normalized strontium K-alpha peak at 14.2 keV and Normalized yttrium $K_{\alpha 1}$ peak at 14.96 keV. Note the two peaks are normalized to the coherent I-125 peak at 35.5 keV to correct for experimental factors, as discussed in chapter two.

Upon discussing this result with the Albany group who supplied the bone samples, measurement of the bone samples on their part using ICPMS confirmed the presence of yttrium in the samples. While a direct comparison of strontium and yttrium concentrations is not possible, indirect comparison of the two techniques showed that they were both in agreement with respect to the yttrium levels and strontium levels. A visual representation of the results reported by the Albany group is shown in figure 3.8

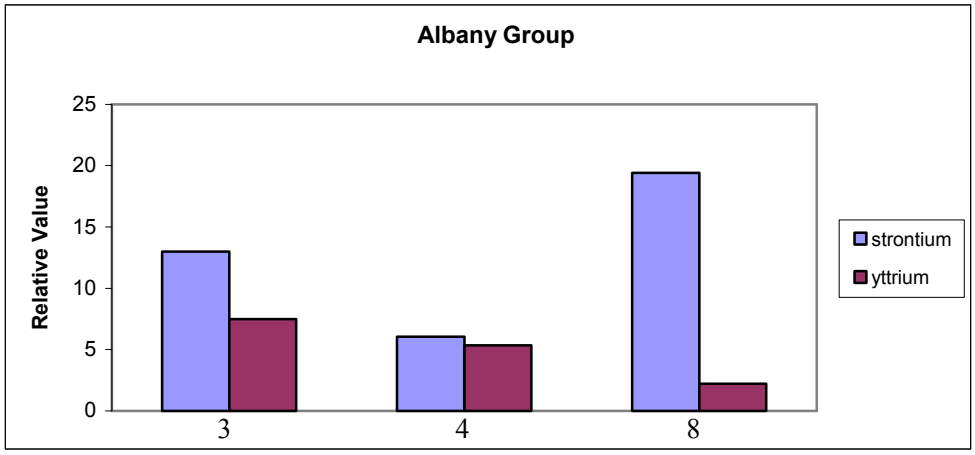

Figure 3.8: Visual representation of results reported by the Albany group. Note no uncertainty values were given by the group. Pellet and control samples were not reported by the group.

3.5 Conclusion

In conclusion, comparison of the fitting routines available show that the 9 parameter fitting routine is adequate to fit strontium levels, even at three years of continuous strontium intake. The observation that the strontium K-alpha to strontium K-beta ratio was smaller than the expected value of 4.4 ±0.3 is due to the presence of zirconium within the I-125 excitation source, and hence the overestimation of the strontium K-beta peak. However, because the strontium K-beta peak is not used to report bone strontium signals for subject measurements, the reported results are not impacted as they pertain to the reporting of the strontium K-alpha peak (including the two step correction method). Indirect comparison of strontium and yttrium levels in excised bone samples provided by the Albany group showed agreement and point to the sensitivity and capability of the IVXRF system.

CHAPTER 4: OVERLYING SOFT TISSUE MEASUREMENTS AND PHANTOM MEASUREMENTS

As discussed in chapter two, in order to obtain the bone strontium signal in the IVXRF measurements, a two step-correction method is applied in which the first step corrects for soft tissue attenuation. Thus, this highlights the importance of using an imaging modality in conjunction with the IVXRF system. Heirwegh (2008) investigated different imaging modalities such as CT, MRI and US (Ultrasound) and concluded that a 55 MHz ultrasound system provided for the least % relative error of 3.2%. However, given the resources and feasibility of available imaging systems and based on Heirwegh's results, a 10 MHz system was used for the overlying soft tissue measurements. During the development of the IVXRF system, participants were brought to Mohawk College in Hamilton and then later to the Mohawk-McMaster Institute of Applied Health Sciences to undergo soft tissue measurements and so the use of the mobile US system throughout this study eliminated the need for participants to travel between locations.

4.1 Portable Ultrasound Measurements

4.1.1 Method and Materials

The portable US system used in this work was made available to this study by the Department of Physics at Ryerson University. The portable US unit consists of a Telemed EchoBlaster 128 EXT-1Z kit and linear probe (model HL 9.0/40/1Z8Z) having a transponder frequency of 10 MHZ. Corresponding software consisted of the EchoWave 2.94 software in which images were recorded and measured in a standard 800x 600

software window. Prior to the IVXRF measurements, US were performed at the finger and ankle bone measurement sites as described in chapter two. Images in two transducer planes: sagittal and transverse were acquired with the aid of a gel pad. The average of the readings was used for the soft tissue correction. The gel pad was used for the measurements as it enhanced visual representation of the soft tissue overlying bone as shown in figure 4.1 below.

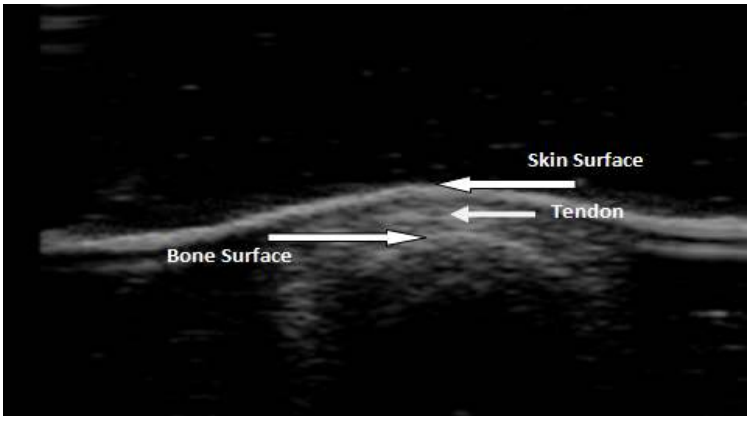

Figure 4.1: Transverse view with gel pad of an ultrasound measurement. Note that the overlying soft tissue thickness is determined as the distance from the bone surface to the skin surface (Moise, 2010).

Examples of images in both transverse and sagittal planes with and without the gel pad are available in Moise (2010).

4.1.2 Reproducibility of Ultrasound Measurements of Overlying Tissue

The reproducibility of the US measurements was investigated in previous work (Moise, 2010) in an individual. For this individual, the (mean ±SD) US reading for the finger and ankle was (0.31±0.04)cm and (0.19±0.007)cm, respectively, with the use of a gel pad. By contrast, measurements were also performed without a gel pad and showed US readings of (0.30±0.04)cm and (0.18±0.008)cm, for the finger and ankle, respectively.

Analysis of the coefficient of variance (CV), which is defined as the standard deviation over the mean, for the finger and ankle was 12.9% and 3.7%, respectively with the use of a gel pad and 13.3% and 4.4%, respectively without the use of the gel pad. As reported, the lower % CV calculated for the ankle indicates that the ankle measurements are easier to acquire, most likely due to the easier geometry of the ankle to measure (i.e. flatter, wider surface to manipulate the probe) compared to the finger. It was observed that US measurements had a strong reproducibility as determined by the standard deviation and that there was agreement within uncertainty between the gel pad and non gel-pad readings.

In this study, the average overlying soft tissue thickness ± SD for 21 volunteers (18 females, 3 males), at the finger and ankle was found to be (0.27± 0.02) cm and (0.21± 0.02) cm, respectively. Figure 4.2 shows the mean readings for all volunteers including a comparison between the male and female volunteers.

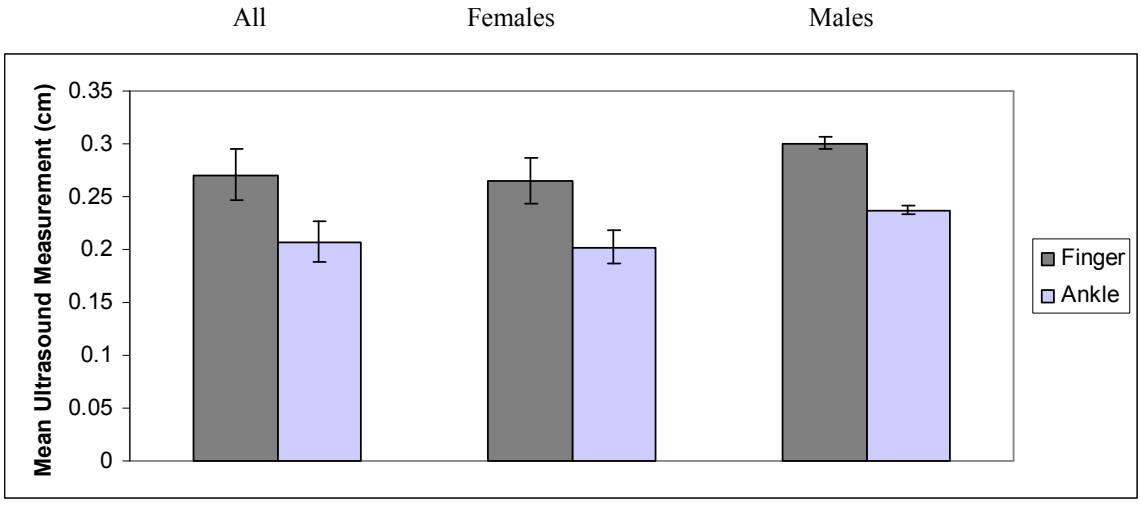

Figure 4.2: Mean ultrasound measurements for all volunteers, female volunteers and male volunteers. The uncertainty refers to the standard deviation.

The mean finger measurements are in agreement with those found by Pejović-Milić and colleagues (2004) who reported a mean reading of (0.29 ± 0.07)cm in ten healthy individuals (five females, five males) and previous graduate student Zamburlini (2008c) of (0.26 ±0.04) cm and (0.25 ± 0.07) cm, for the finger and ankle, respectively. The mean ultrasound reading for the female volunteers was observed to be (0.27 ±0.02)cm and (0.20 ±0.02)cm for the finger and ankle, respectively. For the male volunteers, the mean readings were (0.30 ±0.01) cm and (0.24 ±0.005) cm, respectively, which within uncertainty do not show any statistically significant differences between the female and male volunteers.

However, of question would be whether ultrasound measurements would be influenced by body mass, such that if a volunteer gained or loss weight, the overlying soft tissue thickness would change as well. Since weight of an individual was not taken during the study, statistical analysis of this was limited to an individual whose weight was shared as recorded in her BMD test results. In this subject, between 2008, 2010 and 2012, her weight changed from 54 kg to 53 kg to 56 kg, but her measurements at both bone sites were still within agreement as shown in table 4.1 below.

	Finger	Ankle
Weight (kg)	Mean Ultrasound Reading (cm)	Mean Ultrasound Reading (cm)
54	0.248	0.193
53	0.24	0.185
56	0.253	0.19

Table 4.1: Mean ultrasound measurements in an individual at different weights.

Assuming that the body mass is equally distributed in increased soft tissue mass throughout the body (~4% change in body mass), comparison of the ultrasound readings in Table 4.1 with the calculated COV (12.9% and 3.7% for the finger and ankle, respectively) does not indicate any clear correlation between the body mass and readings. For example, the COV for the ankle measurements was calculated to be 3.7%; therefore, for an ankle measurement of 0.19cm, the associated change would be 0.007cm, which is still within the range of uncertainty. Thus, while it is not expected that an increase in overall body mass might be a problem for increased soft tissue mass at the fingers and ankles (personal communication, Dr. Gregory Wohl), a question would be whether water retention and ankle swelling would present with a significant issue. Given that body weight was not taken during the course of the study, in order to help answer the question of correlation, future work could look at the relationship between body mass index (BMI) and ultrasound measurements.

Nevertheless, the results compared to those observed by Zamburlini (2008c) and Heirwegh (2008) indicate that the portable US system is an effective and useful imaging modality to measure overlying soft tissue thicknesses. Furthermore, US presents with the advantage of not exposing the patient to ionizing radiation.

4.2 Phantom Measurements

In addition to performing ultrasound measurements on individuals, a phantom measurement check is also performed. In this work, a set of plaster of Paris phantoms is available for use as calibration standards, as shown in Table 4.2 below and the corresponding calibration curve is shown in figure 4.3.

Phantom ID	CaSO4.1/2H2O (g)	Ca (g)	Sr added (mg)	ppm Sr/Ca	ppm Sr/CaSO4.2H2O
1/6	5.0366	1.391	0.17	119.84	27.90
1/3a	5.0571	1.396	0.33	238.72	55.57
1/3b	4.7827	1.321	0.33	252.41	58.76
1/2	5.1601	1.425	0.5	350.93	81.69
2/3	4.8979	1.352	0.67	492.95	114.75
1	5.4569	1.507	1	663.68	154.49
2	5.2677	1.455	2	1375.04	320.08

Table 4.2: Phantom calibration standards currently used in the IVXRF measurements. (Information provided through personal communication, Moise (2010)).

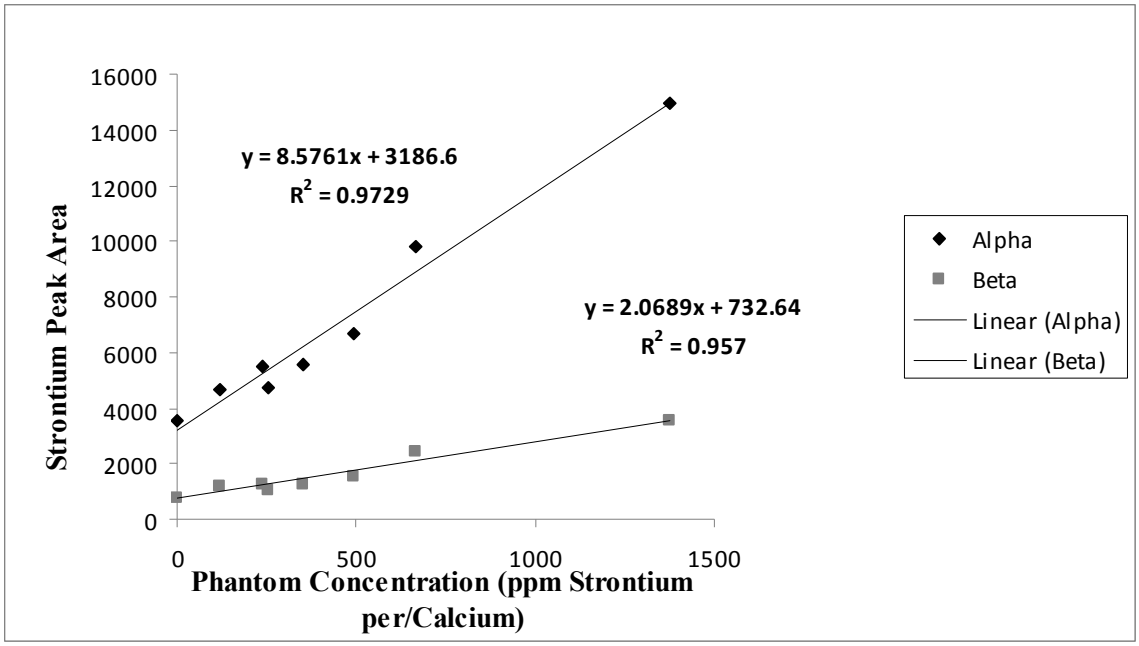

Figure 4.3: Calibration curve for phantom set currently used. Note that that the curve shows inherent strontium contamination within the phantoms. This is discussed further in chapter 7.

Since the phantom was used to perform system checks, the following section looks at the reproducibility of the phantom measurements.

4.2.1 Method and Materials

For the IVXRF system checks, the 1/6 phantom was used. The phantom was run for 1800 seconds real time and before each human bone strontium measurements. The same photon excitation source: I-125 brachytherapy seeds were used. The pulse processing and count sorting was performed using Ortec® DSPEC PLUS^{TM} Digital Gamma Ray Spectrometer and Maestro^{TM} software, respectively. A typical phantom spectrum collected is shown in figure 4.4 below.

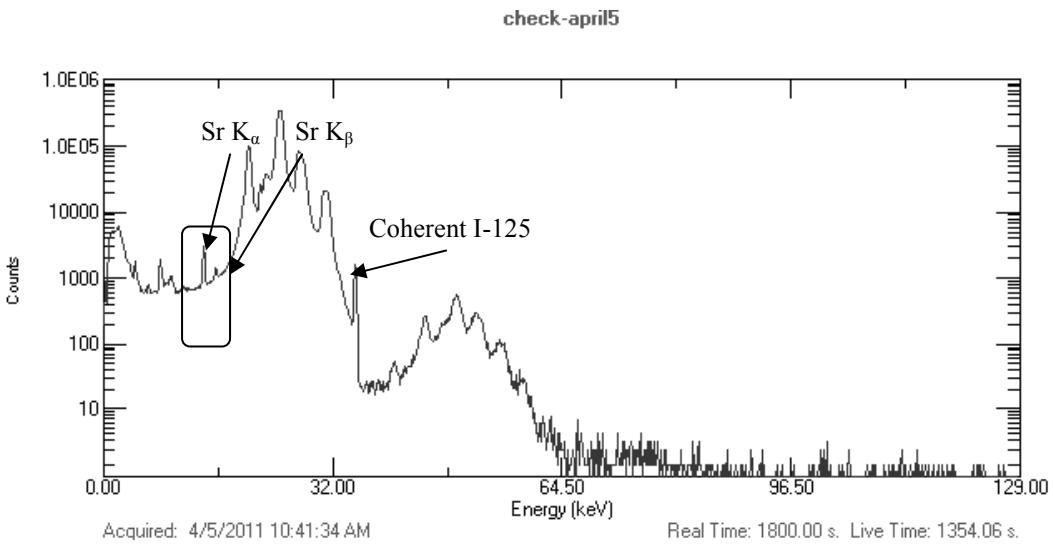

Figure 4.4: Typical raw spectrum of phantom 1/6 collected during a system check.

Similar to the human bone strontium measurements, the phantom 1/6 , strontium K-alpha and strontium K-beta peaks at 14.2 keV and 15.8 keV, respectively were fitted using an in-house non-linear least squares method program. To correct for differences in

positioning and changes in source activity over time, coherent normalization to the I-125 peak at 35.5 keV was performed.

A total of 364 measurements were performed with the phantom over a long term period of five years, spanning the length of the Ryerson and McMaster University Strontium in Bone Research study.

4.2.2 Results

Figure 4.5 shows a plot of the 364 measurements over five years.

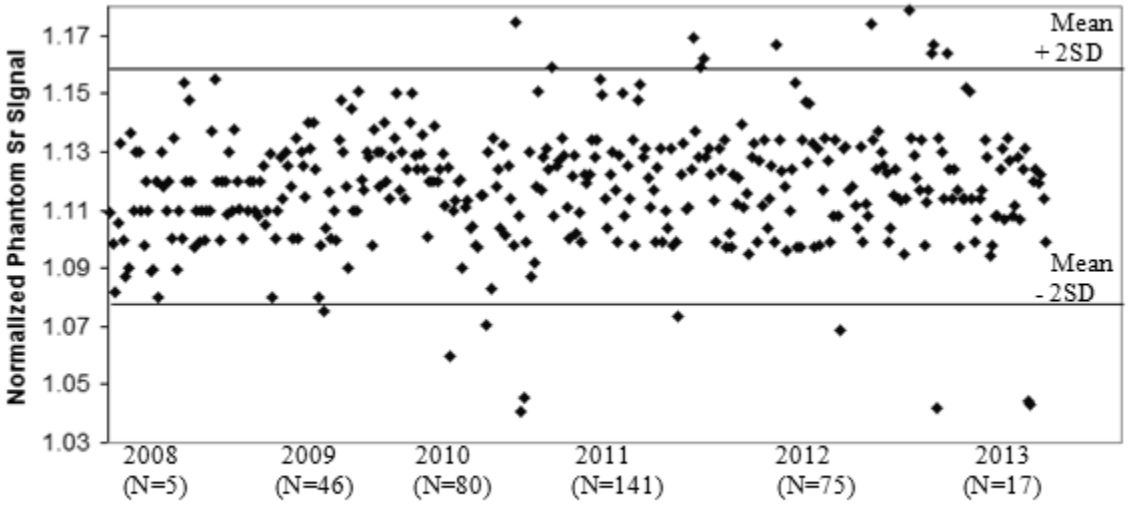

Figure 4.5: Reproducibility of Bone Phantom Measurements (N= 364) between 2008 and 2013. The normalization refers to the phantom peak area normalized to the coherent I-125 peak, to correct for positioning.

4.2.3 Conclusion

The reproducibility of phantom (1/6) is defined in this case as the standard deviation from the mean of all experimental measurements spanning over a period of five years. A total

of 364 measurements were performed, having a mean ± SD of 1.1198 ± 0.02171. The low standard deviation indicates an excellent reproducibility. Although, some values fall outside the mean ± 2SD as expected, the uncertainty associated with the measurements (uncertainty in statistical counts) are within agreement. The results also indicate that the coherent normalization corrects well for the positioning and source activity.

CHAPTER 5: MEASUREMENTS OF STRONTIUM IN BONE USING THE IVXRF SYTEM

5.1 Introduction

The advantage of using XRF to measure elements in the human body is its non-invasive nature and the capability to perform measurements both *in-vivo* and *ex-vivo*. As described in chapter two, the application of XRF has been used to study various elements in the human body, such as lead and strontium in human living subjects (Chettle, 2011). Since strontium is a ubiquitous element of interest, the ability to measure strontium in living bone would allow us to help answer several questions relating to its kinetics and action in bone. However, in order to answer such questions, a method allowing for frequent measurements, over a long period of time and in a non-invasive way should be used.

In the literature, the only bone strontium measurements over a period of three years of living human subjects was reported by Bärenholdt and colleagues (2009) who used the technique of DPA. This study included thirty two osteoporotic females taking a daily dose of 2 g of the drug Protelos© and their study was an extension of the five year SOTI (Spinal Osteoporosis Therapeutic Intervention) and TROPOS (Treatment of Peripheral Osteoporosis Study studies (Meunier & Reginster, 2003, Reginster et al., 2005). These studies were two major, phase III double- blind randomized placebo controlled international trials illustrating the benefits of Protelos© in reducing the number of new vertebral and peripheral fractures in post-menopausal osteoporotic women (Bärenholdt et al., 2009). As stated by the authors, the aim of their study was to look at the magnitude

and kinetics of strontium uptake in the ultra distal radius bone in osteoporotic females that had taken Protelos© over a long term period. Of their participants, 17/32 had taken Protelos© for 4-5 years before enrollment in the study and by the end of their study, the longest intake was 7-8 years. DPA and DXA BMD measurements were performed on the non-dominant radius every six months during the study as participants were taking Protelos © and continued measurements three-six months after treatment withdrawal. The authors concluded the following: (i)the highest strontium content was found in subjects having taken Protelos© for the longest period (7 to 8 years), (ii) at the end of treatment the variability in strontium content was pronounced among the individuals such that a mean of 1.1% strontium was measured, (iii) stopping treatment resulted in a decline of bone strontium content, but 73% and 67% of the content remained after three and six months respectively, in the ultra distal (UD) radius and (iv) that strontium containing drugs may affect BMD scores for several years, even after stopping treatment (Bärenholdt et al., 2009). Thus, their study raises several questions. The first is that while they observed that the rise in bone strontium content was most marked initially, as shown in figure 5.1 below, it is assumed that their results are comparative of both types of bone tissue rather than measuring cortical and trabecular bone, separately.

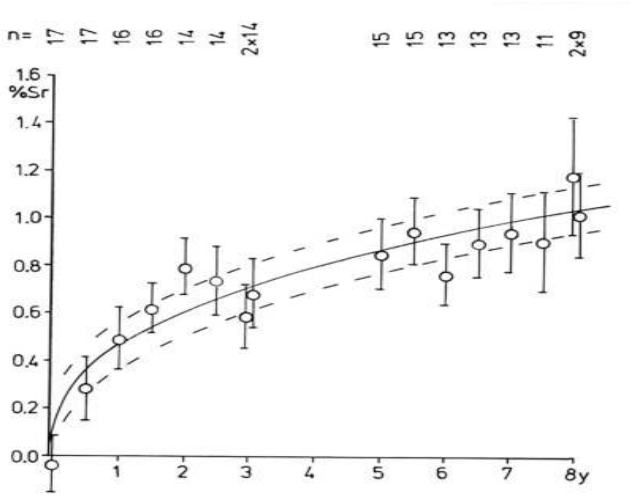

Figure 5.1: Bone strontium content, expressed as % strontium, as measured by DPA at the non-dominant UD radius in osteoporotic women having an average age of 80 years. (Bärenholdt et al, 2009).

Measurement at two different sites would be of interest, since in the literature, cortical and trabecular bone show different rates of strontium uptake (Dahl et al, 2001, Zamburlini, 2008c, Heirwegh, 2008, Moise et al, 2012). Furthermore, any observations in between six months are not performed and would have been of interest, if one considers that the bone remodeling cycle takes between 90-120 days for completion (Keaveny et al, 2004). The second question of interest is whether strontium levels will reach a plateau.

Plateau levels have been estimated based on serum plasma levels, BMD measurements and bone biopsies (Dahl et al, 2001, Boivin et al., 2010 and Doublier et al., 2011). The given values from these studies range from weeks for the animal model to months and years in the human model. Based on rat studies, in which rats were orally administered strontium ranelate and assessment of bone strontium levels at the femur, Dahl and colleagues (2001) concluded that bone strontium levels reached a plateau within four weeks. They also observed that plateau levels were lower in female rats than in

males, postulating that the plateau level was affected by gender difference in the absorption process. Interestingly, differences in non-steroidal anti-inflammatory drug (NSAIDs) metabolism were also observed between genders in rats. It was learned that male rates metabolize NSAIDs much faster than female rats, whereas female rats metabolize NSAIDs at about the same rate as humans (personal communication, Dr. Gregory Wohl). By contrast, a time interval of 2-3 years has been suggested for humans (Boivin et al., 2010, Doublier et al., 2011 and Cortet, 2009). In using the IVXRF system to assess bone strontium levels in an osteoporotic woman, self-supplementing with strontium citrate, Heirwegh (2008) suggested that bone strontium levels would reach a plateau within 2-6 months, for the finger (primarily cortical bone) and ankle (primarily trabecular bone). While there seems to be a variable range of times suggested for bone strontium to plateau in the literature, it should be noted that these estimates are based on few measurement points (for example, bone biopsies are based on a single individual measurement) or performed based on *ex vivo* analysis.

Hence, one of the objectives of the work reported in this chapter was to observe whether bone strontium levels reach a plateau based on frequent measurements, ranging from weekly, to biweekly to monthly in the same individual and over a long term period of at least three years.

5.2 First Baseline Subject Case Study

The initial recruitment of a volunteer self administrating strontium citrate supplements was initiated in December 2008, as part of the Ryerson and McMaster University Strontium in Bone Research Study. With approval from the Ryerson and McMaster

University Research Ethics Board (REB # 2007-212-1 and 07-402, respectively), a 68 year old female volunteer was referred by her bone specialist for bone strontium measurements. Unlike previous volunteers that were measured with this system (Heirwegh, 2008 and Zamburlini, 2007a) this volunteer had no prior history of strontium intake and thus a measurement could be obtained representing her natural bone strontium level, termed here as the baseline reading. The volunteer, 68 year old osteoporotic woman was planning to self-supplement with 680 mg of strontium citrate and agreed to be measured on a frequent basis. After her initial baseline reading in December of 2008, a second measurement was taken in January of 2009, 24 hrs after she began strontium supplementation, followed by frequent measurements on a biweekly to weekly to monthly basis. She was followed over two years. Her published results in the journal Bone follow (Moise et al., 2012)

The manuscript has been formatted to fit the style of this thesis.

Author contributions:

H.Moise performed all the bone strontium measurements, corresponding data analysis and writing the manuscript draft.
J.D. Adachi assisted in recruitment of the individual and reviewed the final draft.
D.R. Chettle assisted with interpretation of data analysis, reviewing and revising the manuscript. Funding was provided by D.R. Chettle beginning September 2010, made possible through an NSERC research grant.
A. Pejović-Milić assisted with interpretation of data analysis, reviewing and revising the manuscript. She is also the corresponding author. Funding by A. Pejović-Milić was provided during December 2008 to the end of August 2010, made possible by NSERC and CFI/ORF research grants.
Both A. Pejović-Milić and D.R. Chettle supervised and provided guidance

Monitoring Bone Strontium Levels of an Osteoporotic Subject due to Self-Administration of Strontium Citrate with a Novel Diagnostic Tool, *In Vivo* XRF: A Case Study

H. Moise[1,#], J.D. Adachi[2], D.R. Chettle[3], and A. Pejović-Milić[1,*]

[1] Department of Physics, Ryerson University, Toronto, M5B 2K3, Canada
[2] Department of Medicine, McMaster University, Hamilton, L8N 1Y2, Canada.
[3] Medical Physics and Applied Radiation Sciences, McMaster University, Hamilton, L8S 4K1, Canada.
[*] Corresponding Author: anamilic@ryerson.ca
[#] Presently PhD student at McMaster University, Medical Physics and Applied Radiation Sciences

ABSTRACT

A previously developed *in vivo* x-ray fluorescence (IVXRF) I-125 based system was used to measure bone strontium levels non-invasively in an osteoporotic female volunteer. The volunteer was recruited in December 2008, as part of the Ryerson and McMaster University Strontium in Bone Research Study and measured at twice weekly, weekly and monthly intervals. Thirty minute measurements were taken at the finger and ankle bone sites, representing primarily cortical and trabecular bone, respectively and the strontium K-alpha x-ray peak at 14.16 keV was used in the analysis. Since the volunteer had no prior history of strontium based medications or supplementation, baseline natural strontium levels were obtained followed by a 24 h measurement of first intake of strontium citrate supplements (680 mg Sr/day). While the baseline levels of 0.38 ± 0.05 and 0.39 ± 0.10 for the finger and ankle, respectively, were on par with those previously reported in Caucasians among twenty-two healthy non-supplementing strontium individuals by our group, an increase began to be seen after 24 h of 0.62 ± 0.14 and 0.45 ± 0.12 for the finger and ankle, respectively. By 120 h, the increase was statistically

significant at 0.68 ± 0.07 and 0.93 ± 0.05, respectively. Further increases occurred within an interval of 90 – 180 days, with the most recent, after 800 days, at the finger and ankle being 7 and 15 times higher than the initial baseline reading. The intriguing results show bone strontium incorporation and retention follow a pattern, suggesting strontium levels, at least in the ankle, do not plateau within two to three years and will continue to increase over time, as an individual takes strontium supplements. The ability of this IVXRF system to monitor and measure bone strontium levels over time provides a useful diagnostic tool to help gain insight into strontium bone kinetics.

KEY WORDS: Strontium, X-Ray Fluorescence, Bone, In-Vivo, Osteoporosis

1. INTRODUCTION

Bone diseases such as osteoporosis and osteopenia are worldwide health issues that are becoming increasingly prevalent. Osteoporosis Canada has estimated that 1 in 4 women and at least 1 in 8 men over 50 are living with osteoporosis [1]. While the causes of osteoporosis remain debatable, it is a progressive disease marked by a loss in bone density, mass, strength and an increased risk of fractures. As bone is constantly being remodeled, with one bone remodeling cycle taking approximately 120 days for completion, there is a continuous uptake of old bone (resorption) followed by the deposition of new bone [2]. There are two main different types of bone tissue, cortical and trabecular bone, with cortical bone making up the compact portion of bone and trabecular the spongy portion. Thus, bone will undergo different bone remodeling rates depending on the type of bone tissue. Osteoporosis occurs due to an imbalance in the

bone remodeling cycle, and thus the aim in the treatment of osteoporosis is to rebalance the bone cells' activity through resorption reduction and increasing bone strength and density. Current treatment includes the use of prescription medications such as bisphosphonate drugs, dietary and lifestyle changes and the use of supplementation. Strontium supplementation, in addition to calcium and vitamin D is one current therapy that is gaining attention and popularity.

In studies using strontium ranelate, improvements in bone mineral density, bone fracture risk and osteoporotic symptoms were reported [3-6]. However, in North America, while the strontium ranelate based drug (Protelos®) is unavailable for purchase, other strontium salts such as strontium citrate and strontium carbonate are available without a prescription through health food stores. However, while previous studies have shown beneficial effects due to strontium ranelate intake and Boivin et al. have shown that strontium from ranelate supplementation is located in bone formed during the period of treatment [6], how strontium is incorporated and retained in bone over time as an individual takes other types of strontium salts has not yet been shown in available literature to date.

Currently, there are three techniques that can be used to investigate bone strontium content. Boivin et al [6] used bone biopsy, which permits direct chemical assay of the strontium in bone. However, the technique is somewhat invasive and does cause pain, so it cannot be used frequently on the same person. Another method, referred to as dual photon absorptiometry (DPA) was developed by Nielsen et al [7] has the advantage of being non-invasive and may be used to determine both bone strontium and calcium

concentrations. This technique has been shown to be accurate, but it has a standard error of estimate of about 0.5 % Sr with respect to calcium in terms of molar ratio (about 10900 μg Sr/g Ca) and so is unable to detect bone strontium levels in normal volunteers. This technique was used in a recent study by Bärenholdt et al.,(2009) [8], who found a mean level of 1.1% Sr in subjects who had been treated with strontium ranelate for 7 -8 years. Some of the technical aspects of DPA compared to the alternative x-ray fluorescence method have been reviewed by Zamburlini et al. [9].

To measure bone strontium levels, an *in-vivo* x-ray fluorescence system (IVXRF) has been developed by our group [10,11] that is non-invasive, presents with minimal risk and negligible radiation exposure, thus allowing for repeated bone strontium measurements over time.

The IVXRF method exposes the organ or site of interest, to an external source of photons followed by the photoelectric effect. The strontium IVXRF system developed uses I-125 in the form of brachytherapy seeds as the photon excitation source and is able to detect strontium K-alpha x-rays at 14.16 keV which relate to bone strontium levels. This technique offers satisfactory precision, in that bone strontium levels can be detected in all subjects so far examined, including bone strontium in normal volunteers, which is too low to be detected by DPA. However, absolute quantification of bone strontium concentrations using IVXRF is not yet satisfactory. The behavior of the low energy photons from the brachytherapy seeds and the emitted Sr x-rays varies between calibration standards and the living soft tissue and bone of the finger or ankle sites at which measurements are made. Although some allowance can be made for these

differences, at present the measurement accuracy and hence absolute quantification is limited to ±40%. Nevertheless, preliminary studies by our group [10,11] have shown the system to be sensitive and capable of measuring strontium non-invasively and with negligible risk, *in-vivo* in human bone. Also, for relative measurements, that is examining changes in a person with time or comparing one person with another, the system has been shown to be satisfactory.

A major limitation of the Sr IVXRF system is the attenuation of the strontium signal by the overlying soft-tissue at the measurement bone site [12]. Corrections for soft-tissue attenuation based on ultrasound soft-tissue thicknesses were previously evaluated by our group [12,13] and more information about numerical modeling of bone strontium measurements using the Electron Gamma Shower 5 (EGS5) Monte Carlo simulation is available in the literature [12,14].

Thus, given the advantages of the bone Sr IVXRF system and the ability of the system to determine bone strontium levels, in this work, the IVXRF system was used to monitor an osteoporotic individual taking strontium citrate supplements over time, in order to assess the sensitivity of the system and to observe how bone strontium levels change over time at two different bone sites, representing cortical and trabecular bone.

2. MATERIALS AND METHODS

Prior to the IVXRF measurements, ultrasound measurements were performed at both bone sites to determine the soft tissue thicknesses overlying the bone sites. A portable ultrasound system, made available by the Department of Physics at Ryerson University was used. The portable ultrasound system consists of a Telemed EchoBlaster 128 EXT-

1Z kit with a linear HL 9.0/40/1Z8Z probe of 10MHz frequency (Telemed Lithuania). The corresponding software included the EchoWave 2.94 software from which images were recorded (standard 800 x 600 software window). Ultrasound measurements were taken at the finger and at the ankle bone, representing the bone measurement sites. Overlying soft tissue thicknesses did not change over time in this subject and the average soft tissue thickness readings taken in the two transducer planes; sagittal and transverse were used for correction purposes.

2.1 Bone Strontium IVXRF System

The IVXRF system compromises an Ortec® Ametek-AMT Si(Li) detector with a 16mm active crystal diameter and 5.65 mm sensitive thickness, which has an energy resolution of 230 eV at 5.9 keV. Prostaseed® I-125 brachytherapy seeds (Core Oncology, USA) were used as the excitation photon source, having an approximate initial activity of 24 MBq. The detector and measurement set-up and placement of I-125 seeds is shown in Fig 1. The pulse processing and count sorting was performed using the Ortec® DSPEC PLUS^{TM} Digital Gamma Ray Spectrometer and Maestro^{TM} software, respectively.

The spectra obtained with the IVXRF system were then subsequently analyzed using a modified in-house nonlinear least squares, Marquardt based, fitting routine.
However, in order to obtain the bone strontium signal, a two step correction method, previously proposed and reported by our group [14] was applied. This two step correction method takes into account overlying soft tissue photon attenuation and experimental conditions that may affect the strontium signal obtained. This was performed by measuring soft tissue thicknesses overlying the bone sites through the use of a portable

ultrasound system prior to the IVXRF measurements and then normalizing the strontium peak observed at 14.16 keV to the coherent I-125 peak at 35.49 keV. The coherent normalization of the strontium peaks, best source selection, geometry, ideal anatomical bone sites for measurements and tissue correction factors have been previously reported [10,15,16].

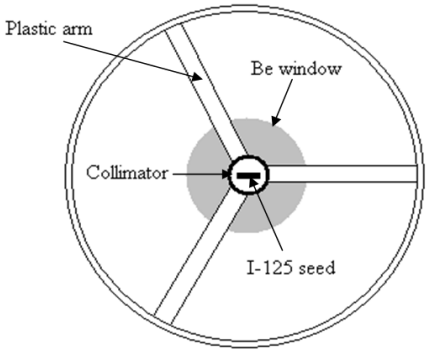

Figure 1. Detector and measurement setup using 180° interaction geometry (head-on view). The Be window, shown in gray, covers the active area of the Si(Li) detector [16].

2.2 Calibration

For system calibration, eight strontium doped plaster of Paris phantoms ranging in concentration of added strontium from 0 to 5.46 mg Sr/g Ca, resembling the finger bone shape were used.

Each phantom was run three times in random sequence for 1800 seconds live time. The dead time for the phantom measurements was kept between 15 and 45%. Energy calibration of the spectra was performed using the silver K x-ray peak at 22.17 keV and the coherently scattered I-125 peak at 35.49 keV. However, calibration of the system

with these phantoms to give absolute quantification of bone strontium concentration was not performed due both to inherent strontium contamination and limitations in absolute accuracy arising from the differences in photon transport through the plaster of Paris compared to the soft tissue and bone involved in an *in vivo* measurement.

2.3 Recruitment

Once ethics approval was obtained from the Ryerson and McMaster University Research Ethics Boards, a female subject suffering from osteoporosis was recruited through her physician, in December of 2008, to join the "Ryerson and McMaster University Strontium in Bone Research Study" to be regularly monitored over time, while taking strontium supplements of her choice.

The female volunteer, aged 68, had been diagnosed with severe osteoporosis of her lumbar spine, having a bone mineral density T-score of -3.2, as classified using the World Health Organization (WHO) classification system [17]. She decided to self-supplement with strontium citrate. Prior to starting the strontium citrate, a baseline reading of her natural bone strontium levels was obtained in December of 2008. This reading was recorded as Day 0. Following this first bone strontium measurement, in January of 2009, she then began taking strontium supplements, self- supplementing with two strontium citrate pills, each containing 340 mg of elemental strontium, for a daily dose of 680 mg Sr, and to date still continues to do so. The next bone strontium measurement was performed 24 hours after her very first strontium supplement dose. She was then followed twice a week, for four weeks, progressing to once a week over the second month and then once every two weeks for four months, and then currently,

monthly. To date, she has been measured for more than 2 and half years and on 32 occasions. Each measurement was performed in the morning or early afternoon, with her last dose taken the morning the day before.

Bone strontium measurements were performed at two bone sites for thirty minutes each (1800s clock time) at:

i) The dorsal side of the index finger at the center of the middle phalanx and

ii) The ankle at the most prominent part of the medial malleolus of the tibial bone

The finger to source distance was kept between 4 and 5 mm and the seed activity ranged from 24 to 39 MBq. The ankle to source distance was kept between 2 and 3 mm and the seed activity ranged from 13-26 MBq. Figs. 2 and 3 show the experimental set-up for a finger bone strontium measurement. A seed activity was chosen to keep the dead time between 30 and 50%. The effective dose with reference to a 30 MBq source and a 30 minute measurement time was previously experimentally determined by our group to be 0.05 and 0.09 μSv, respectively for the finger and ankle measurements [11]. The sum of these radiation doses (0.14 μSv) is equivalent to 20 - 30 minutes of natural background radiation in North America, where the natural background radiation is approximately 3000 μSv/year.

Figure 2. Human finger bone strontium IVXRF measurement.

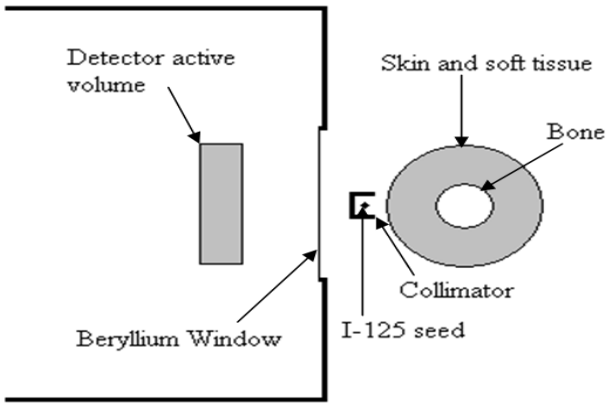

Figure 3. Side view of human finger positioning during the bone strontium IVXRF measurement [16].

3. RESULTS

Figs. 4 to 7 illustrate the subject's normalized bone strontium levels at the finger and ankle bone sites, respectively. The normalized peak areas refer to the strontium K-alpha peak after the 35.49 keV coherent normalization is applied.

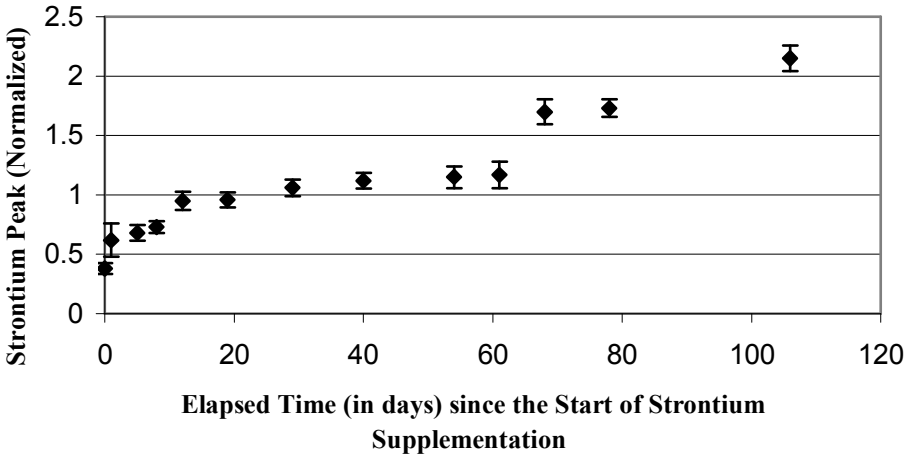

Figure 4. Subject's finger bone strontium measurement over the first 100 days. This graph is representative of primarily cortical bone. Alpha refers to the strontium K-alpha x-ray peak at 14.16 keV. Strontium peak areas have been corrected using the two step correction method (Zamburlini et al., 2007[11]). Errors are associated with the statistical uncertainty of the Sr x-ray and I-125 coherent counts.

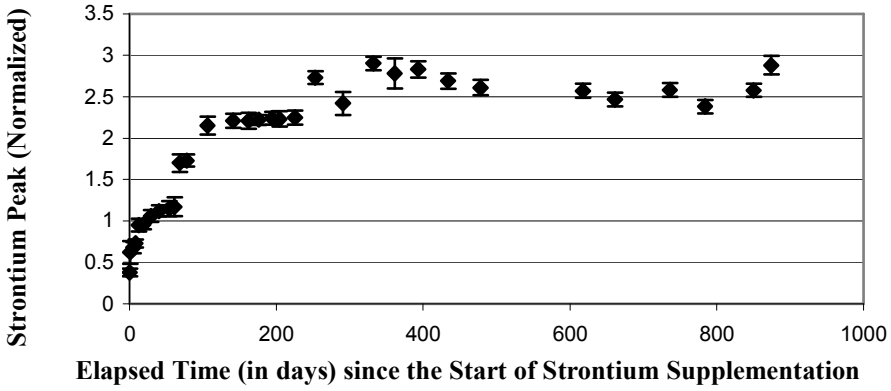

Figure 5. Subject's finger bone strontium measurement over time. This graph is representative of primarily cortical bone. Alpha refers to the strontium K-alpha x-ray peak at 14.16 keV. Strontium peak areas have been corrected using the two step correction method. Errors are associated with the statistical uncertainty of the Sr x-ray and I-125 coherent counts.

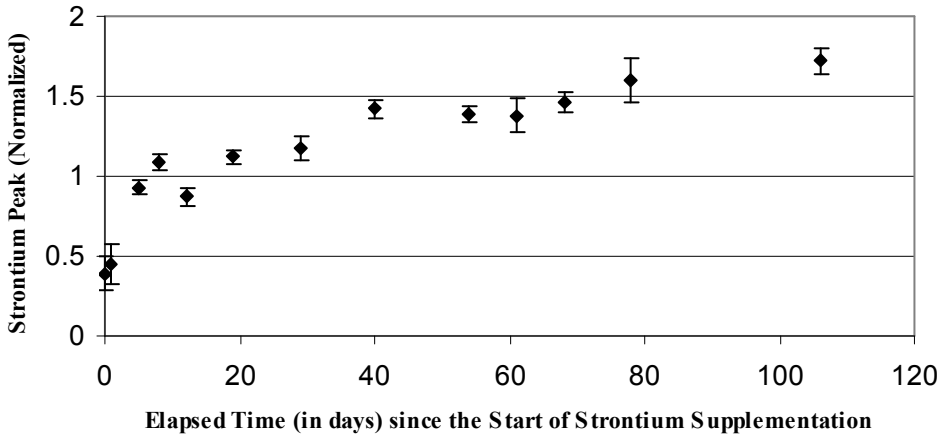

Figure 6. Subject's ankle bone strontium measurement over the first 100 days. This graph is representative of primarily trabecular bone. Alpha refers to the strontium K-alpha x-ray peak at 14.16 keV. Strontium peak areas have been corrected using the two step correction method. Errors are associated with the statistical uncertainty of the Sr x-ray and I-125 coherent counts.

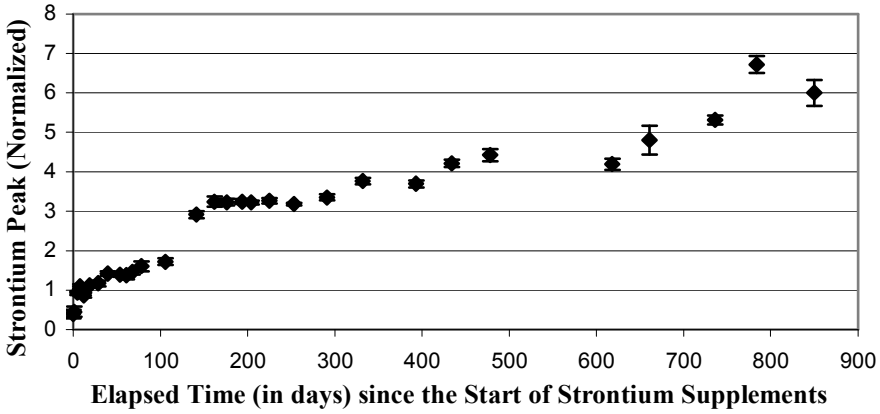

Figure 7. Subject's ankle bone strontium measurement over time. This graph is representative of primarily trabecular bone. Alpha refers to the strontium K-alpha x-ray peak at 14.16 KeV. Strontium peak areas have been corrected using the two step correction method. Errors are associated with the statistical uncertainty of the Sr x-ray and I-125 coherent counts.

The graphs show the change of strontium K-alpha x-ray peak normalized to the I-125 coherent peak, after soft tissue correction for photon attenuation has been made. They show that the baseline K-alpha strontium signal at 14.16 keV for this volunteer was 0.38 ± 0.05 and 0.39 ± 0.10 for the finger and ankle, respectively. At 24 hrs, after her very first intake in January of 2009, the strontium signal was 0.62 ± 0.14 and 0.45 ± 0.12, respectively. At the third visit, at 120 hrs, the levels had risen to 0.68 ± 0.07 and 0.93 ± 0.05 respectively.

4. DISCUSSION

The baseline values we observed for this volunteer are in agreement with the baseline values found among the Caucasian individuals among the twenty-two healthy volunteers, measured in a previous 2006 study [11]. The average normalized K-alpha baseline values for the Caucasian individuals were reported to be 0.43 ± 0.08 and 0.40 ± 0.13 for the finger and ankle, respectively. Thus, this person's natural bone strontium levels which arise mainly from the diet did not differ from healthy individuals despite the fact that she was osteoporotic.

Interestingly, as the volunteer was followed while she was self-supplementing with 680 mg of strontium citrate tablets per day, the results show that at her second visit, which represented the measurement taken 24 hrs after her very first intake in January of 2009, the strontium signal in the finger increased numerically. The increase continued and achieved statistical significance by the third visit at day five (120 hours). Further increase in bone strontium continued at both measurement sites.

The result suggests strontium bone uptake increases during a specific interval of time and then seemingly plateau. The consistent rising pattern observed in the early part of the study, as shown in figures 4 and 6 shows the measurements to be highly consistent. While it has been suggested that strontium levels plateau over time after the registered increase, the bone strontium levels, particularly at the ankle, keep rising over a long period of time.

The secondary increase in strontium levels was observed between 106 and 141 days, at both bone sites. At this time, the finger and ankle strontium signal have increased to 2.21 ± 0.09 and 2.91 ± 0.09, respectively. Compared to the natural baseline bone strontium levels, the strontium signal is approximately 6 to 7 times higher, respectively. This indicates that strontium supplementing individuals have significantly higher bone strontium levels than non-supplementing individuals after approximately only three months on strontium citrate.

Further bone strontium increases also can be seen on the graphs with the effect more pronounced in the ankle bone. Frequent measurements of this subject showed that bone strontium levels were higher in trabecular bone than in cortical bone, which is consistent with the literature and correlates with the observation that different bone skeletal sites will have differing bone strontium concentrations [18].

Recent measurements suggest that the Sr level in the finger may have reached a plateau. The mean and standard deviation of the 13 measurements since day 253 is 2.65±0.17. The standard deviation is larger than that attributed to individual measurements (typically ± 0.08 to 0.18), but this is not surprising, since the latter account

only for counting statistics. On the other hand, the Sr levels in the ankle continue to rise, having doubled during the period of time for which the finger Sr levels have changed very little.

Whether bone strontium levels will continue to increase in this individual, and if they do increase whether this should be of concern, as high strontium levels have been shown to cause skeletal abnormalities in animals and rickets and osteomalacia in adults [18-21] remains to be addressed. Furthermore, continued measurements at regular intervals may help to give insight into bone strontium kinetics and clarify the present observation that finger Sr appears to have reached a plateau, while ankle Sr has continued to increase. Equally, future studies may show whether a similar pattern can be observed in other people.

4.1 Conclusions

As noted in the Introduction, this *in-vivo* bone strontium measurement technique permits relatively precise measurements that can be used for monitoring changing strontium levels in an individual, or for comparing one individual with another. However, the absolute quantification is not yet fully satisfactory, being approximately ±40%. The table below compares results from this subject at baseline, the apparent plateau level for the finger and a mean of the two most recent ankle measurements. The table gives the concentration of strontium in terms of μgSr/gCa and in terms of molar %, which takes into account the different atomic masses of strontium and calcium, and therefore reflects the ratio of numbers of atoms of the two elements. Also shown are the precision which

can be used for comparing one measurement with another, and the accuracy, or the uncertainty in absolute concentration (Table 1)

Table 1
Concentration of strontium in terms of μgSr/g Ca and in terms of molar percent concentration

Sample	Sr concentration μgSr/g Ca	Measurement uncertainty (precision)	Absolute uncertainty (accuracy)	Molar %	Precision	Accuracy
Baseline finger	375	49	151	0.0172	0.0022	0.0069
Baseline ankle	385	99	154	0.0177	0.0045	0.0071
Plateau finger	2614	168[2]	1051	0.120	0.00768	0.048
Recent ankle	6315	148	2538	0.289	0.00677	0.1156

[2]The uncertainty for the plateau value is not actually a measurement uncertainty, it is the standard deviation of 13 measurements over 21 months.

In conclusion, the source-based bone strontium IVXRF system has been shown to be sufficiently sensitive to detect normal bone strontium levels and is then capable of following the changes in bone strontium levels in an osteoporotic individual over time. Although, a current limitation of the IVXRF system is that absolute quantification of strontium with respect to calcium has an uncertainty (limit in accuracy) of ±40%, the IVXRF system is sensitive and capable not only of measuring bone strontium changes over time in a direct manner, but also of comparing strontium levels in one individual with those in another. Furthermore, significant advantages of this diagnostic tool are that it is non-invasive and painless, and poses minimal risk to subjects by exposing them to a negligible radiation dose. A 30 min measurement gives a whole body effective dose of 0.05 μSv and 0.09 μSv for a finger and ankle bone measurements, respectively, which together are about 1-10% of the radiation dose a patient receives undergoing a DEXA measurement [22]. In terms of radiation risk it is equivalent to 20 to 30 minutes of natural background radiation. Thus, these significant advantages allow for repeated bone strontium measurements on the same patient over time. In doing so, information may be

obtained that may help answer how strontium is incorporated and retained in bone over time.

Future work includes continuing monitoring of this individual using the IVXRF system described here, in order to answer such questions as whether bone strontium levels will continue to increase or plateau at some time. In addition, measurements of healthy individuals will be useful to answer whether there is a difference in bone strontium uptake and retention compared to osteoporotic individuals. Once more volunteers join this study, the information gained will also allow study of bone strontium kinetics due to taking strontium based medications and/or supplements, besides observing bone strontium intake by finger and ankle bones reported in this case study.

5. ACKNOWLEDGEMENTS

This work was supported by NSERC and CFI/ORF research grants to APM and an NSERC grant to DRC. We express our thanks and gratitude to the volunteer who participated in this case study.

6. REFERENCES

[1] Osteoporosis Canada: Osteoporosis and You [Internet]. Ontario: Osteoporosis Canada; c2011[updated 2011 Aug 22; cited 2011 Aug29]. Available from: http://www.osteoporosis.ca.

[2] Marie PJ, Ammann P, Boivin G, Rey C. Mechanisms of action and therapeutic potential of strontium in bone. Calcified Tissue Int 2001;69:121 -129.

[3] Meunier PJ, Roux C, Seeman E, Ortolani S, Badurski JE, Spector TD, Cannata J, Balogh A, Lemmel EM, Nielsen SP, Rizzoli R, Genant HK, Reginster JY. The effects of strontium ranelate on the risk of vertebral fracture in women with postmenopausal osteoporosis. New Engl J Med 2004;350:459-468.

[4] Hwang JS, Chen JF, Yang TS, Wu DJ, Tsai KS, Ho C, Wu H, Su LS, Wang CJ, Tu ST. The effects of strontium ranelate in asian women with postmenopausal osteoporosis. Calcified Tissue Int 2008; 83:308-314.

[5] Neuprez A, Hiligsmann M, Scholtissen S, Bruyere O, Reginster JY. Strontium ranelate: the first agent of a new therapeutic class in osteoporosis. Adv Ther 2008; 25:1235-1256.

[6] Boivin G, Farlay D, Khebbab T, Jaurand X, Delmas PD, Meunier PJ. In osteoporotic women treated with strontium ranelate, strontium is located in bone formed during treatment with a maintained degree of mineralization. Osteoporosis Int 2010; 21: 667-677.

[7] Nielsen SP, Bärenholdt O, Bärenholdt-Schipler C, Mauras Y, Allain P. Noninvasive measurement of bone strontium. J Clin Densitom 2004;7:262-268.

[8] Bärenholdt O, Kolthoff N, Nielsen SP. Effect of long-term treatment with strontium ranelate on bone strontium content. Bone 2009;45:200-206.

[9] Zamburlini M, Pejović-Milić A, Chettle DR. Spectrometry methods for *in vivo* bone strontium measurements. X-Ray Spectrom 2008;37:42-50

[10] Pejović-Milić A, Stronach IM, Gyorffy J, Webber CE, Chettle DR. Quantification of bone strontium levels in humans by *in vivo* x-ray fluorescence. Med Phys 2004; 31:528-538.

[11] Zamburlini M, Pejović-Milić A, Chettle DR, Webber CE, Gyorffy J. *In vivo* study of an x-ray fluorescence system to detect bone strontium non-invasively. Phys Med Biol 2007;52:2107-2122.

[12] Zamburlini M, Pejović-Milić A, Chettle DR. Evaluation of geometries appropriate for I-125 *in vivo* bone strontium x-ray fluorescence measurement. J Radioanal Nucl 2006;269:625-629.

[13] Pejović-Milić A, Brito JA, Gyorffy J, Chettle DR. Ultrasound measurements of overlying soft tissue thickness at four skeletal sites suitable for *in vivo* x-ray fluorescence. Med Phys 2002;29:2687-2691.

[14] Zamburlini M, Pejović-Milić A, Chettle DR. Coherent normalization of finger strontium XRF measurements: feasibility and limitations. Phys Med Biol 2008;53: N307-N313.

[15] Zamburlini M. *In vivo* measurement of bone strontium with x-ray fluorescence. 2008 Ph.D. Dissertation. McMaster University.

[16] Heirwegh C. *In vivo* quantification of bone strontium using x-ray fluorescence. 2008 M.Sc. Thesis. McMaster University.

[17] WHO Geneva. Study group on assessment of fracture risk and its application to screening for postmenopausal osteoporosis.Technical Report Series (World Health Organization) 1994.

[18] Dahl SG, Allain P, Marie PJ, Mauras Y, Boivin G, Ammann P, Tsouderos Y, Delmas PD, Christiansen C. Incorporation and distribution of strontium in bone. Bone 2001; 28:446-453.

[19] Ozgür S, Sumer H, Kocoğlu G. Rickets and soil strontium. Arch Dis Child 1996;75:524-526.

[20] Cabrera WE, Schrooten I, De Broe ME, D'Haese PC. Strontium and bone. J Bone Miner Res 1999;14: 661-668.

[21] Cohen-Solal M, Augry F, Mauras Y, Morieux C, Allain P, Vernejoul MC. Fluoride and strontium accumulation in bone does not correlate with osteoid tissue in dialysis patients. Nephrol Dial Transpl 2002;17: 449-454.

[22] Bezakova E, Collins PJ, Beddoe AH. Absorbed dose measurements in dual energy x-ray absorpiometry (DXA). Br J Radiol 1997;70: 172-179.

5.2.1 Discussion and Conclusion of First Baseline Subject

This work presented for the first time in the available literature, frequent *in-vivo* measurements over a two year span in the same individual, using the novel IVXRF system. Based on her results, several observations were made:

- Her natural bone strontium levels, the baseline reading, were on par with those of Caucasian subjects observed by Zamburlini and colleagues (2007a) who measured twenty-two test subjects as part of a pilot study
- Bone strontium levels increased in the first 24 hrs at both bone sites.
- Trabecular bone showed a higher bone strontium signal compared to cortical bone.
- A plateau was thought to have been reached in cortical bone after a year but no plateau was observed in trabecular bone.
- A pattern of increase and uptake was observed at both sites, with increases occurring within an interval of 90 to 180 days.

As a result, several questions were raised. First, if these observations would be seen in a wider cohort of individuals. Second, if the long-term measurements would be able to provide more information about bone strontium kinetics. Third, if there would be any further changes in the bone strontium levels of the 68 yr old female volunteer over a longer time period than two years.

To answer these questions, further subjects were recruited to the study to be monitored and followed as they self-administered with strontium supplements. The recruitment of these subjects and the results were published in a second paper in Bone (Moise et al., 2014), which follows.

5.3 Long-Term Measurements in a Wider Cohort of Individuals

Please note that the following journal article was reprinted from Bone, Vol 61, Helen Moise, David R Chettle and Ana Pejović-Milić, Monitoring Bone Strontium Intake in Osteoporotic Females Self-Supplementing with Strontium Citrate with a Novel In-Vivo X-Ray Fluorescence Based Diagnostic Tool**,** Pages 48-54., Copyright (2014), with permission from Elsevier.

The manuscript has been formatted to fit the style of this thesis

Author contributions:

H.Moise performed all the bone strontium measurements, corresponding data analysis and writing the manuscript draft.
D.R. Chettle assisted with interpretation of data analysis, reviewing and revising the manuscript. Funding was provided by D.R. Chettle beginning September 2010, made possible through an NSERC research grant.
A. Pejović-Milić assisted with interpretation of data analysis, reviewing and revising the manuscript. She is also the corresponding author. Funding by A. Pejović-Milić was provided during December 2008 to the end of August 2010, made possible by NSERC and CFI/ORF research grants.
Both A. Pejović-Milić and D.R. Chettle supervised and provided guidance.

Monitoring Bone Strontium Intake in Osteoporotic Females Self-Supplementing with Strontium Citrate with a Novel In-Vivo X-Ray Fluorescence Based Diagnostic Tool

Helen Moise[a], David R Chettle[a] and Ana Pejović-Milić[b,*]

[a] Medical Physics and Applied Radiation Sciences, McMaster University, Hamilton, L8S 4K1, Canada.
[b] Department of Physics, Ryerson University, Toronto, M5B 2K3, Canada
[*] Corresponding Author: anamilic@ryerson.ca

ABSTRACT

Ten female volunteers were recruited as part of the Ryerson and McMaster University Strontium (Sr) in Bone Research Study to have their bone Sr levels measured as they self-supplemented with Sr supplements of their choice. Of the ten volunteers, nine were suffering from osteopenia and/or osteoporosis. Non-invasive bone Sr measurements were performed using an *in vivo* x-ray fluorescence (IVXRF) I-125 based system. Thirty minute measurements were taken at the finger and ankle, representing primarily cortical and trabecular bone, respectively. For analysis, the 14.2 keV Sr K-alpha peak normalized to the Coherent peak at 35.5 keV was used.

Baseline readings, representing natural bone Sr levels were acquired since all volunteers had no previous intake of Sr based supplements or medications. Once Sr supplements were started, a 24 hr reading was taken, followed by frequent measurements ranging from weekly, biweekly to monthly. The longest volunteer participation was 1535 days.

The mean baseline Sr signal observed for the group was 0.42 ± 0.13 and 0.39 ± 0.07 for the finger and ankle, respectively. After 24 hrs, the mean Sr signal rose to 1.43 ± 1.12 and

1.17 ± 0.51, for the finger and ankle, respectively, representing a statistically significant increase ($p=0.0043$ & $p=0.000613$). Bone Sr levels continued to increase throughout the length of the study. However the Sr signal varied widely between the individuals such that after three years, the highest Sr signal observed was 28.15 ± 0.86 for the finger and 26.47 ± 1.22 for the ankle in one volunteer compared to 3.15 ± 0.15 and 4.46 ± 0.36, for the finger and ankle, respectively in another. Furthermore, while it was previously reported by our group, that finger bone Sr levels may plateau within two years, these results suggest otherwise, indicating that bone Sr levels will continue to rise at both bone sites even after 4 years of Sr intake.

KEY WORDS: Strontium; *In-Vivo* X-Ray Fluorescence; Bone, *In-Vivo*; Osteoporosis

1. INTRODUCTION

Strontium (z=38) (Sr) is an element that can be found in nature and in the human body. A divalent cation, belonging to the group IIA elements in the periodic table, it has an atomic radius of 1.13Å, slightly larger than that of calcium (Ca), which is 0.99 Å [1] and in the human body it readily substitutes for calcium, having a great affinity for bone [2]. In the human body, more than 99% of the Sr burden is stored in bone and teeth [3]. In humans, the amount of stored Sr present in the body, primarily in bone, is between 300-400 mg in contrast to Ca which is present between 1000-1200 g in the average female [4]. By comparison to Ca, the amount of Sr in the human skeleton is 0.035 wt% of the Ca content [5]. Sr is obtained primarily through diet with an average daily intake of approximately 1-5 mg [4]. It is not thought to serve any primary purpose or essential role

in the human body, but studies involving both humans and animals have shown low doses of Sr to be a promising agent in the treatment of osteoporosis and osteopenia [6-8].

Osteoporosis and osteopenia are marked by an imbalance in the bone remodeling process, and such an imbalance may arise from a genetic or biological factor. Factors that influence bone turnover include, but are not limited to hormones (parathyroid hormone, vitamin D, sex steroids, growth hormones), growth factors, cytokines and other signaling molecules (receptor activator of nuclear factor-kB (RANK), RANK ligand, osteoprotegerin; insulin-like growth factor 1 and 2; Wnt signalling molecules) [9].
In turn, Sr incorporation into bone is influenced by several factors which include gender, dose, duration of treatment, plasma Sr level, skeletal site and age [2,10]. Thus, osteopenic or osteoporotic individuals are thought to benefit from Sr based treatment or supplementation [2].

While Sr Ran is unavailable in North America, other Sr salts, such as Sr citrate and Sr carbonate are available for purchase through health food stores. Although the bioavailability of ingested Sr is thought to be affected by the type of Sr salt [11], a study by Wohl and collaborators (2012) found no significant difference in bone Sr levels between rats administered with Sr Ran versus Sr citrate [12]. However, bioavailability is also affected by species and diet composition, especially with respect to Vitamin D, phosphorus, and calcium [11]. Although, Sr is touted as a possible therapy against bone diseases, such as osteoporosis and osteopenia, its long term action in bone remains unanswered.

Studies have indicated various times that it takes for Sr to plateau in bone based on animal and human supplementation with Sr Ran. The time period suggested include 4- 6 weeks [2] and a few years, averaging between 3- 5 years in osteoporotic women [8,13]. Although, it has been observed that there is a substitution of up to one atom in every one hundred of Ca being replaced by a Sr atom [14], there remain insufficient data available in the literature that looks at how Sr is incorporated and retained in human bone over a frequent time interval using non-invasive methods.

To help answer this question, an initial case study on a 68 yr old osteoporotic female, self- supplementing with 680 mg of Sr daily as Sr citrate was reported by our group [15]. Unlike previous methods used to determine bone Sr content, such as bone biopsies and dual photon absorptiometry (DPA), we use an *in-vivo* X-Ray fluorescence system (IVXRF) to measure bone Sr levels. Based on the principle of the photoelectric effect and the exposure of the bone site to an external source of photons, such as the radioisotope I-125 in the form of loose, sealed seeds, the IVXRF system is able to detect characteristic Sr K-alpha x-rays at 14.2 keV, which relate to information on bone Sr levels. The IVXRF system has been shown to be sensitive and capable of measuring bone Sr levels, non-invasively, with neglible radiation risk. Further information on this IVXRF system and its comparison to other methods of determining bone Sr content is available in the literature [16-18].

In our initial case study, frequent Sr measurements, progressing through bi-weekly, weekly and monthly intervals, were performed at the finger and ankle bone, representing primarily cortical and trabecular bone, respectively. While the human skeleton is

composed of approximately 80% cortical and 20% trabecular bone [9], it has been observed that Sr absorption is different between these two types of bone, with trabecular bone showing a higher Sr concentration than cortical bone, likely due to the fact that cortical bone has a slower turnover rate compared to trabecular bone [8]. Similarly, the initial case study found that Sr levels were higher at trabecular bone compared to cortical bone and that ankle levels continued to increase, even after 24 months of strontium supplementation [15]. This is in agreement with the findings available in the literature [6,8]. Thus, while our initial case study attempted to help answer the question of strontium incorporation at these two bone types, the purpose of this work was to follow-up on the initial case study, to confirm whether any similar patterns in bone Sr levels would be seen among a wider group of individuals and whether any variations in Sr signal either between individuals and/or over time would be observed.

2. MATERIALS AND METHODS

2.1 Ultrasound Measurements

Since the Sr signal coming from bone is attenuated by overlying soft tissue at the bone measurement site, with soft tissue photon attenuation being a concern when dealing with low energy photons in the order of 20 keV or less [19], ultrasound measurements were taken prior to the IVXRF measurements. Correction for soft tissue thickness attenuation has been previously evaluated by our group [19,20] along with the numerical modeling of the bone Sr measurements using the Electron Gamma Shower 5 (EGS5) [17,20].

A portable ultrasound system compromised a Telemed EchoBlaster 128 EXT-1Z kit with a linear HL 9.0/40/1Z8Z probe of 10 MHz frequency (Telemed Lithuania), with the corresponding software (EchoWave 2.94 software) from which images were recorded (standard 800 x 600 software window), was used to obtain the overlying soft tissue thickness. The ultrasound measurements were taken at the finger and ankle bone sites corresponding to the bone measurement sites. For correction purposes, the average soft tissue thickness readings in two transducer planes; sagittal and transverse were used. While soft tissue thicknesses varied between subjects, readings for each subject were consistent over time.

2.2 Bone Strontium IVXRF System

The Sr IVXRF system consists of an Ortec® Ametek-AMT Si(Li) detector with a 16 mm active crystal diameter and 5.65 mm sensitive thickness, which has an energy resolution of 230 eV at 5.9 keV. For the excitation photon source, Prostaseed® I-125 brachytherapy seeds (Core Oncology, USA), having an approximate initial activity of 24MBq were used. The pulse processing and count sorting was performed using the Ortec® DSPEC PLUS™ Digital Gamma Ray Spectrometer and Maestro™ software, respectively. The spectra obtained with the IVXRF system were then subsequently analyzed using a modified in-house nonlinear least squares, Marquardt based, fitting routine. However, since the Sr signal is affected by factors such as overlying soft tissue thickness attenuation and experimental conditions, a two step correction method [17] was applied. The two step correction takes into account the soft tissue attenuation of the Sr signal in the tissue overlying measured bone as indicated by the ultrasound and

normalization of the Sr signal at 14.2 keV to the coherent I-125 peak at 35.5 keV. As reported by Zamburlini and colleagues (2008), coherent normalization to the 35.5 peak, rather than to the silver 22.1 keV peak, was found to be effective in correcting for bone size with an overall accuracy of approximately 10% [17]. Thus, bone Sr measurements as reported in this work are reported as the ratio of the Sr K-alpha peak area to the I-125 coherent peak at 35.5 keV. Note that system calibration to obtain absolute bone Sr quantification was not performed due to inherent Sr contamination of bone phantoms (363 μg Sr/ g Ca) and limitations in absolute accuracy (±40%). Further details are reported in Moise et al, 2012 [15].

2.3 Subject Recruitment

With ethics approval from the Ryerson and McMaster Universities' Research Ethics Boards, recruitment of volunteers was made through flier distribution advertising the Ryerson and McMaster University Strontium in Bone Research Study in the local health food stores and naturopaths. Complementing the initial baseline case study in 2008, nine additional volunteers were recruited to join the study and to be monitored over time while they were self-supplementing with Sr supplements of their own (Table 1). The average age of the volunteers recruited was 64 years. All volunteers were female and with the exception of one, whose diagnosis was unknown at the time of the study, were diagnosed as having either osteoporosis, osteopenia or both. Their diagnosis was based on their bone mineral density test results, provided to them by their own physicians. For the one volunteer whose diagnosis was unknown, she chose to self-supplement with Sr citrate supplements for preventive reasons. The World Health organization (WHO) classifies

osteoporosis as having a T-score 2.5 standard deviations below that of a normal, healthy adult, while osteopenia is defined as a T-score between -1.0 and -2.5[21].

All volunteers were not taking Sr supplements at the time of recruitment and therefore, provided an opportunity to conduct baseline bone Sr measurements. Thus, prior to commencement of Sr supplements, initial baseline readings were acquired for each volunteer and this reading is denoted as day 0. With the exception of one volunteer, (S10 in table 1 below) who began taking 680 mg of Sr citrate based on her physician's recommendation, all other volunteers began self-supplementing with 341 mg of Sr citrate (341 mg elemental Sr) on a daily basis. The reading at Day 1 represents their bone Sr measurement taken 24 hrs after their very first Sr intake. Subsequent readings were performed on a regular monthly basis for most volunteers.

Volunteer ID (S #)	Age	Diagnosis	Calcium (mg/day)	Vitamin D (IU/day)
1	67	Osteopenia (hip)	1000	1000
2	74	Osteopenia (spine and forearm)	1500	1000
3	57	Osteopenia (hip and spine)	1200	1000
4	66	Unknown	500	800
5	53	Osteoporosis (hip and spine)	960	1165
6	66	Osteoporosis (spine) & Osteopenia (hip)	700	1200
7	53	Osteoporosis (spine)	1400	1000
8	70	Osteoporosis (spine) & Osteopenia (hip)	1000	500
9	63	Osteopenia (hip and spine)	1435	1600
10	68	Osteoporosis (spine)	500	1200

Table 1. Profile of the female volunteers self- administrating Sr based supplements daily. Note S1-S9 supplemented with 341 mg of elemental Sr/day whereas S10 took 680 mg of elemental Sr/day. All volunteers took Sr in the form of Sr citrate supplements. Amounts of Calcium and Vitamin D are amounts estimated from supplemental intake and do not include dietary intake.

Bone Sr measurements were performed at two bone sites, the finger and ankle, representing primarily cortical and trabecular bone. At the finger, the measurements were taken at the dorsal side of the index finger at the center of the middle phalanx and at the ankle, the measurements were taken at the most prominent part of the medial malleolus of the tibial bone.

Measurements at each site lasted for 30 minutes, with the finger to source distance kept between 4-5mm and the ankle to source distance kept between 2-3 mm. In order to keep the detector dead time maintained between 30-50% for both bone sites, between 1-3 seeds were used such that their activities ranged between 24 to 39 MBq. The whole body effective dose associated with the finger and ankle measurement was approximately 0.05 μSv and 0.09 μSv, respectively. This sum of radiation dose is equivalent to approximately 20-30 minutes of natural background radiation given that in North America the natural background radiation is approximately 3000 μSv/year [22].

3. RESULTS

The mean normalized bone Sr levels for both the ankle and finger prior to starting Sr supplementation (0 hrs) and after 24 hrs, within their very first intake is shown in Figure 1. The normalized Sr signal refers to the Sr K-alpha peak at 14.2 keV normalized to the I-125 coherent peak at 35.5 keV, after soft tissue correction for photon attenuation has been made. At 0 hrs, the baseline Sr signal was 0.42 ± 0.13 and 0.39 ± 0.07, for the finger and ankle, respectively. At 24 hrs, the normalized Sr signal at the same site rose to 1.43 ± 1.12 and 1.17 ± 0.51, respectively, which points to a factorial increase of 3 in Sr levels at

both bone sites. Bone Sr levels continue to increase in all individuals throughout the length of the study, as shown in Figures 3 and 5, which illustrate the average normalized bone Sr levels at the finger and ankle sites, respectively. Note the graphs show the normalized Sr signal normalized to the individual's own baseline Sr signal, so the initial signal is 1.0 by definition. These figures point to the wide variation of bone Sr levels observed among the ten volunteers; such that by the end of the study, compared to the individual's own baseline Sr signal, bone Sr levels have increased by a factor by as much as 72 and 85, in the finger and ankle, respectively for one volunteer (S6) and 8 and 11 times, for another volunteer (S10).

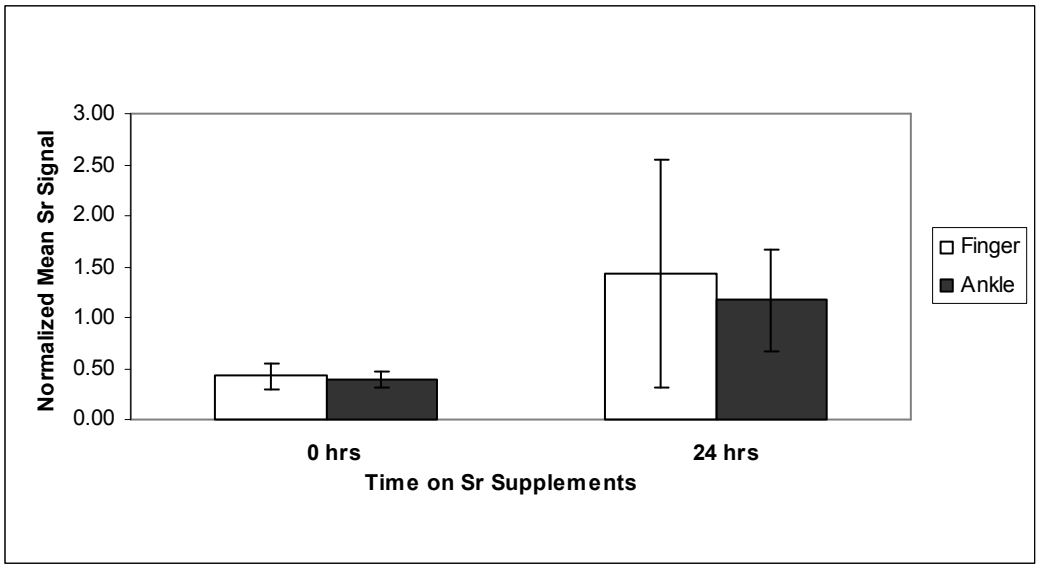

Figure 1. Mean normalized bone Sr signal of ten volunteers at 0 hrs (day 0) and at 24 hrs (day 1). The normalized Sr signal refers to the normalization of the K-alpha Sr peak observed at 14.2 keV to the I-125 coherent peak at 35.5 keV for each volunteer.

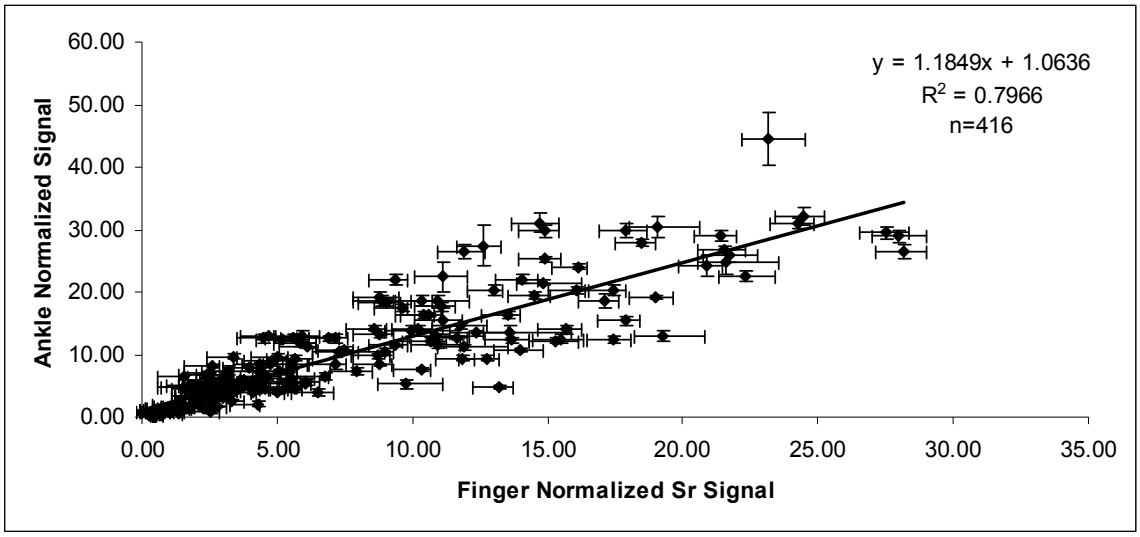

Figure 2. Graph showing a correlation (R^2=0.7966) between the Sr signal at the finger and ankle for the ten volunteers, for a total of 416 measurements.

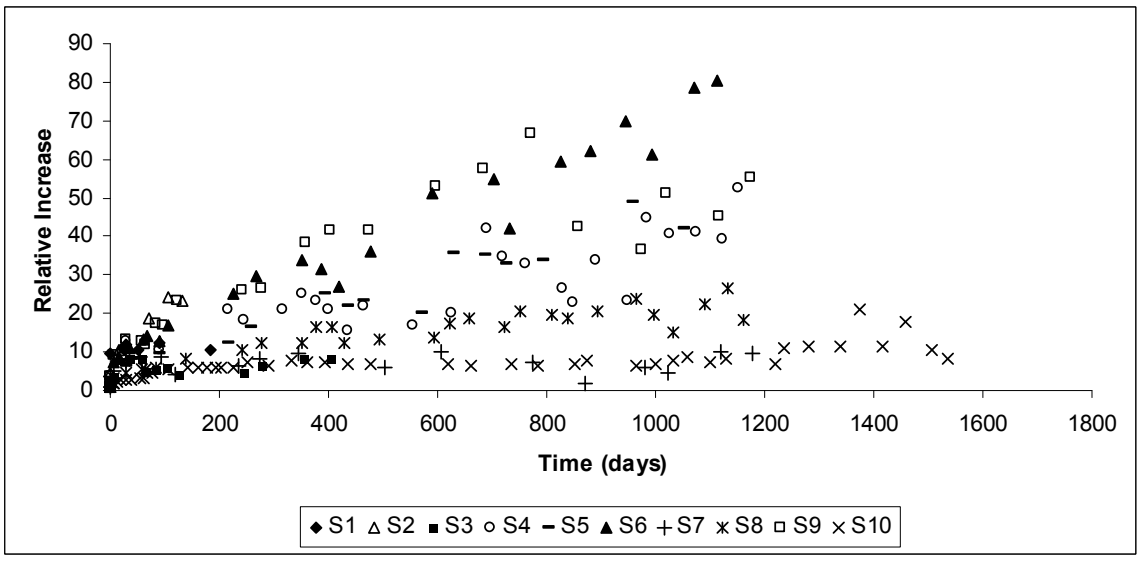

Figure 3. Bone Sr signal over time of ten volunteers in the finger (cortical bone) normalized to the individual's own baseline Sr signal

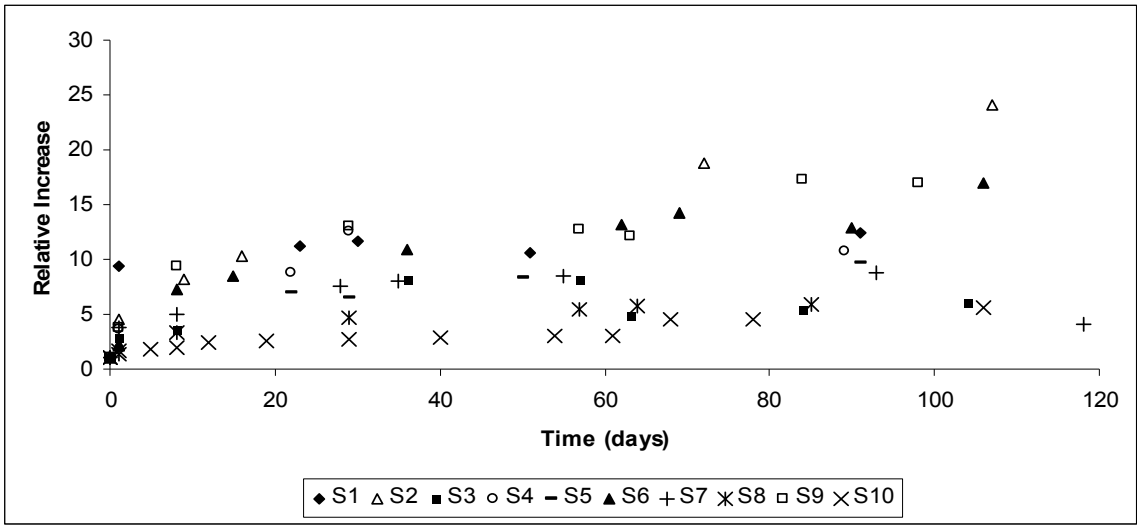

Figure 4. Bone Sr signal for the first 120 days, of ten volunteers in the finger (cortical bone) normalized to the individual's own baseline Sr signal

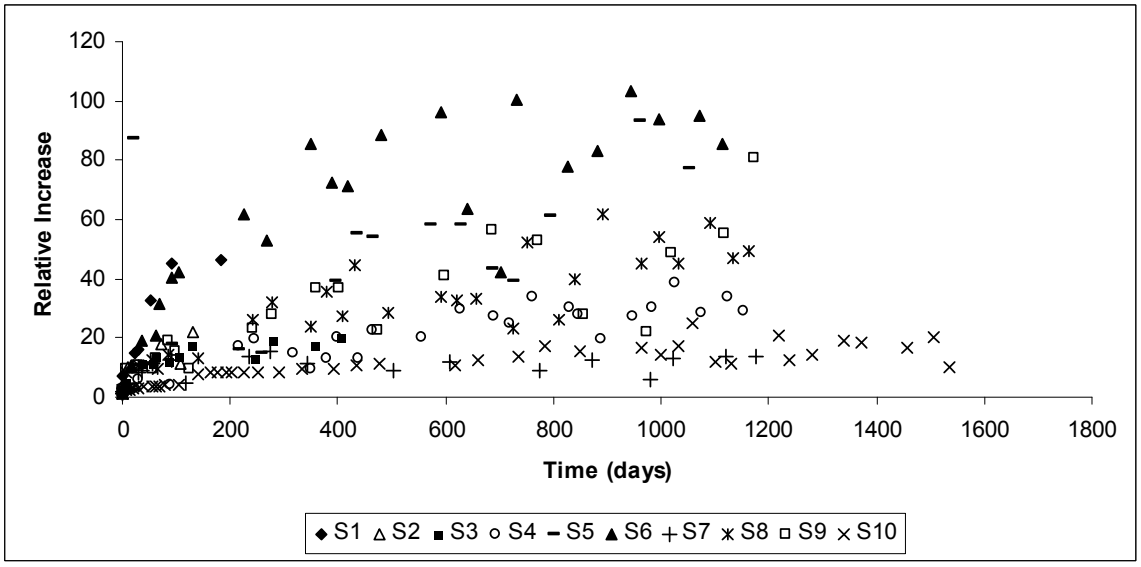

Figure 5. Bone Sr signal over time of ten volunteers in the ankle (trabecular bone) normalized to the individual's own baseline Sr signal.

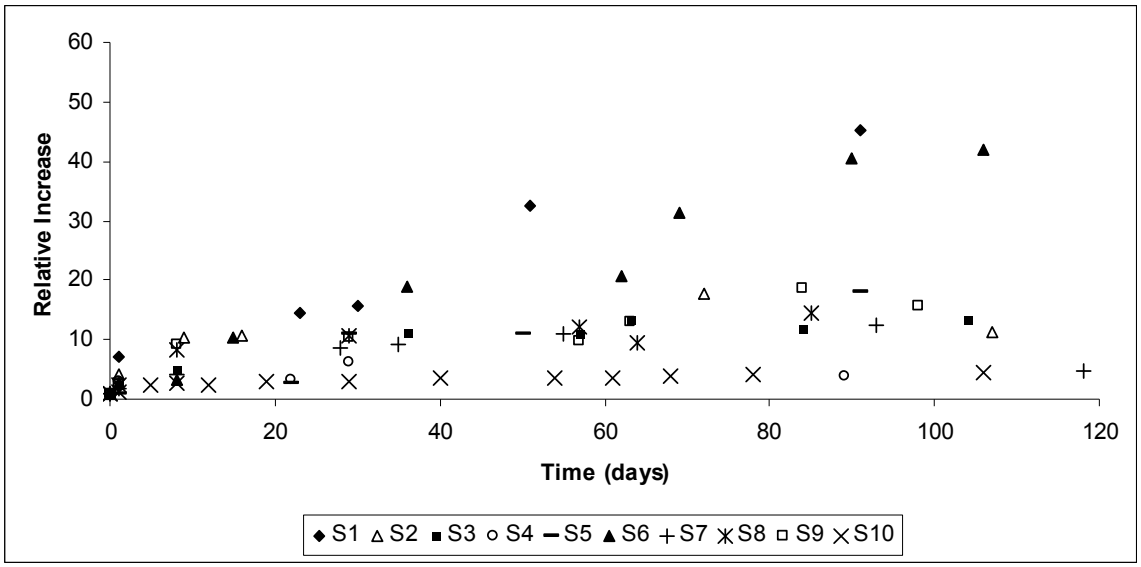

Figure 6. Bone Sr signal for the first 120 days, of ten volunteers in the ankle (trabecular bone) normalized to the individual's own baseline Sr signal

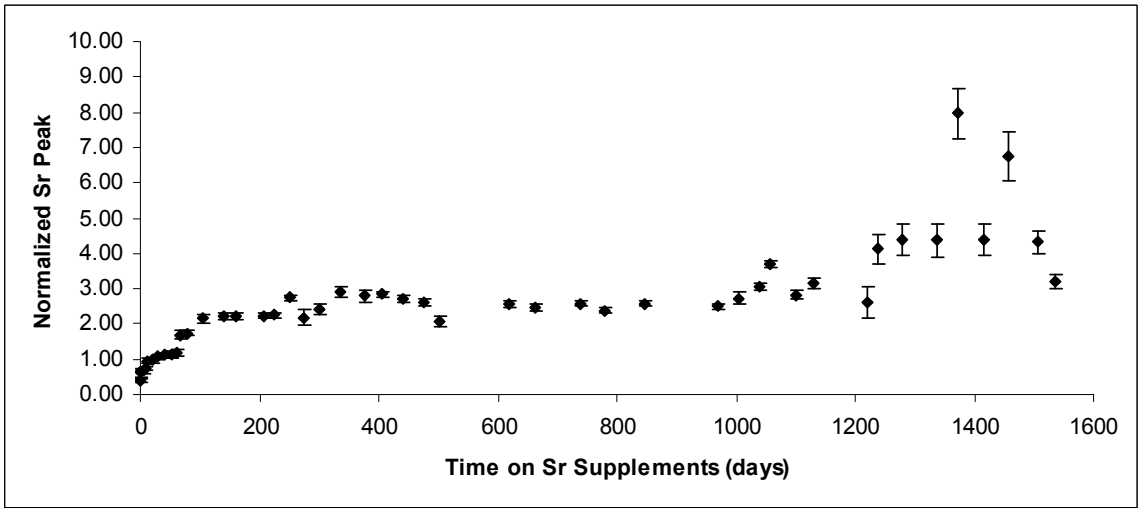

Figure 7. Updated finger bone Sr measurements for volunteer S10, since publication of her results in 2012 [15].

4. DISCUSSION

The use of a novel IVXRF system to measure bone Sr levels over time has been previously demonstrated in an initial case study that was reported by our group [15]. Continued measurements of this initial volunteer (identified as S10 in this paper) has been ongoing since the time of publication in 2012, along with the additional recruitment of nine other female volunteers. In this work, a total of 416 measurement occasions were performed on these ten volunteers and as shown in Figure 2, the correlation between finger and ankle bone Sr measurements shows a strong correlation of R^2= 0.7966, confirming the sensitivity and capability of the IVXRF system to measure bone Sr levels directly over time in different individuals. By comparison, in a study by Somervaille et al (1988), measurement of tibia bone lead (Pb) using the similar technique of IVXRF produced a correlation of R^2= 0.84 with a cumulative blood Pb index, indicating that the IVXRF technique provided a good indicator of long term exposure to Pb [23]. Thus, in addition to the strong correlation, the non-invasive nature of the IVXRF system gives it a strong advantage over other invasive methods such as bone biopsies.

From the ten volunteers recruited in this study, nine reported that they had established diagnosis of osteopenia and/or osteoporosis while one volunteer (S4) bone's condition was unknown in terms of being healthy or osteopenic. However, volunteer S4 decided to take Sr citrate primarily for preventive reasons. The remaining nine volunteers reported that they chose to self-supplement with Sr citrate based on their physician's advice or based on what they learned on their own of trying an alternative therapy instead of prescribed medications. The results of all ten volunteers are shown in Figures 3 and 5,

with the longest running volunteer participation being 1535 days (denoted as S10) and the shortest volunteer participation being 132 days (denoted as S1). Figures 3 and 5 represent the bone Sr signal normalized to the individual's own baseline value over time, with Figures 4 and 6, zooming in the time period for the first 120 days, show bone Sr finger and ankle bone measurements, respectively. The results showed that the mean normalized baseline bone Sr signal, at day 0, for all ten volunteers, having an average age of 64 years, did not differ between the finger and ankle bone ($p=0.214$), such that the mean normalized baseline bone Sr signal (± SD) observed was 0.42 ± 0.13 and 0.39 ± 0.07, for the finger and ankle, respectively. This is in agreement with the baseline Sr values previously reported and measured in a 2006 pilot study, involving twenty-two healthy subjects, having a median age of 31. In this study, the mean normalized Sr signal for the Caucasian individuals among the twenty-two healthy subjects were reported to be 0.43 ± 0.08 and 0.40 ± 0.13 for the finger and ankle, respectively. This suggests that natural bone Sr levels, which arise mainly from diet, do not differ among healthy and osteoporotic individuals, even despite the median age difference. However, after 24 hrs of very first intake of Sr supplement, the group's mean normalized Sr signal rose to 1.43 ± 1.12 and 1.17 ± 0.51 for the finger and ankle, respectively. A paired t-test (null hypothesis assuming that there is no difference between the baseline and 24hr Sr signal) showed a statistically significant increase between the baseline and 24 hr period ($p=0.0043$ and $p=0.00061$ for the finger and ankle, respectively). Interestingly, as the volunteers were continued to be measured on a frequent basis, as shown in Figures 3 and 5, two observations are noted. First, the frequent bone Sr measurements in all subjects

show that the Sr signal is higher in the ankle (primarily trabecular bone) than in the finger (primarily cortical bone), which is in agreement with literature findings that different bone sites will show different bone Sr concentrations. Second, a variation of the normalized bone Sr signal between the volunteers began to be more prominent after the second month of taking Sr supplements and this variation continues to be seen well after three years. At three years, the highest normalized bone Sr signal observed is for S6, of 28.15 ± 0.86 and 26.47 ± 1.22, for the finger and ankle, respectively whereas the lowest normalized bone Sr signal is observed for S10, who shows a normalized bone Sr signal of 3.15 ± 0.15 and 4.46 ± 0.36, for the finger and ankle, respectively. The remaining volunteers (S1-5, 7-9) fall between these two ranges. Why this wide variation occurs between the volunteers, remains unknown. Considering the bone health of the volunteers as shown in Table 1, the results do not point to any significant findings that would point to the Sr signal being affected by the condition of bone or age of the volunteer. Curiously, the one person who was taking 680 mg Sr/day showed the lowest increase in bone Sr, compared to the other subjects, who were taking 341 mg Sr/day.

While five factors such as gender, dose, duration of treatment, plasma Sr level, skeletal site and age have been suggested in the literature [2] as influencing Sr absorption, other factors such as Calcium (Ca), Vitamin D intake, time of Sr intake, water solubility and bioavailability of Sr have also been suggested in the literature as possible influencers of Sr absorption [11,24,25]. In terms of Ca and Vitamin D, Table 1 gives the estimated Ca and Vitamin D amounts as reported by the volunteers in terms of supplemental amounts. While these amounts may be higher if dietary Vitamin D and Ca are considered, the issue

of Ca intake influencing Sr absorption is not considered a factor in this study, since volunteers reported taking Sr supplements away from Ca, and the amounts of Ca intake reported by the volunteers seem to be below excessive Ca consumption (>2000mg/day) [26]. Thus, among these factors and the limited data available, considering the wide variation observed between the volunteers, it could be speculated that time of Sr intake may be a possible explanation for S10's lowest Sr readings compared to the other volunteers, despite taking the highest Sr dosage of 680 mg per day. Unlike the rest of the volunteers who took Sr supplements at night, S10 took Sr supplements in the morning. It has been suggested that bone resorption is most active at night and thus by having a sustained release of Sr ions present in the body at night, it could be expected that Sr can exert its greatest physiological effect of antiresorptive properties during this time [24]. However, speculation on these factors and whether they may contribute to the wide variation seen among the ten volunteers in this study is beyond the scope of this study, as the data collected here were limited to the volunteer's voluntary disclosure of their family history, bone density test results, supplement and/or medication intake and time of Sr intake. It would be important for future studies to look at the degree to which these factors influence Sr absorption in human bone. This could also include looking at the basal rate of bone formation and the collection of biomarkers for bone formation and resorption parameters.

Nevertheless, in addition to the variation observed among the Sr signal between the volunteers for both bone sites, it is interesting to note that regardless of the variation, a similar pattern of bone Sr absorption between subjects is observed, such that Sr levels

tend to increase over certain time intervals, averaging between 100-200 days. A similar observation was reported by our group in an initial case study, involving volunteer S10 [15]. In this initial case study, it was reported that increases occurred within an interval of 90-180 days and that Sr levels, at least in the ankle did not plateau within 2-3 years. While this observation was made for only one individual at that time, the results for all ten individuals confirm this finding, suggesting that Sr follows a pattern of uptake and retention.

However, interestingly, at the time of publication of the initial case study, S10's results for the finger (primarily cortical bone) showed no further increases after 800 days, which led to the conclusion that a plateau had been reached. Indeed, this turned out not to be the case. As the volunteer continued to be measured on her bone Sr levels, a statistically significant increase was observed after three years, as seen in Figure 7. Hence, this intriguing observation indicates that Sr levels in the finger did not reach a plateau as initially reported. Further to S10 results, the recent results of all ten subjects suggest that bone Sr levels at both the finger and ankle bone sites will continue to increase even after four years of Sr intake. Indeed, of interest would be the ability of the Sr IVXRF system to quantify the amount of Sr in bone, however current limitations do not allow for such measurements to be made [15]. In a study by Blake and Fogelman (2006), it was estimated based on the ICRP Sr retention function model that a person who took a daily dose of 2g of Sr Ranelate for three years ingested 745 g of elemental Sr and retained an average Sr retention of 14.0% [27]. Thus, since 2 g of Sr Ranelate is equivalent to 680 mg of Sr Citrate [28], this means that Sr supplementing individuals are consuming

between 100-700 times the normal dietary amount of Sr. Along with this estimate and the results in this study which indicate that Sr levels do not plateau; the question of Sr toxicity is raised. This is of concern since high Sr levels have been reported in the literature to cause detrimental effects in bone such as rickets and osteomalacia [29,30]. Hence, future work includes the development of a set of bone phantoms that would allow for the estimation of bone Sr content per g of Ca [31]. Likewise, future investigation of these data could help give some insight into Sr kinetics.

4.1 Conclusion

While bone Sr levels are reported in a dimensionless unit in this study, the observation that Sr levels continue to rise after four years points to the importance of monitoring individuals taking Sr supplements over a long-term period and the issue of correcting for bone mineral density test scores in such individuals. According to Blake and Fogelman, consumption of Sr supplements for more than six months may affect bone mineral density scores (BMD) for years afterwards, such that BMD scores are falsely increased. This is due to the fact that Sr atoms in bone attenuate X-rays more strongly than Ca atoms [27]. Hence, the IVXRF system thus emerges as a promising novel diagnostic tool to measure and monitor bone Sr levels over time without the risks of conventional methods.

5. ACKNOWLEDGEMENTS

This work was supported by an NSERC grant to DRC and APM, as well as CFI/ORF research grants to APM. HM is supported by a McMaster University research graduate stipend and scholarship. There are a few individuals we wish to acknowledge and thank. First, we would like to thank Dr. Jonathan Adachi of the Department of Medicine at McMaster University for the referral of some of his patients to the Ryerson and McMaster University Strontium in Bone research study. Second, to Dr. Michael Kolios of the Department of Physics at Ryerson University for the use of the mobile ultrasound system and third, most important of all, we wish to give our thanks to the volunteers for their time and participation in this study. This work could not be done without you, thank you.

6. REFERENCES

[1] Oliveira, J. P., Querido, W., Caldas, R. J., Campos, A. P., Abraçado, L. G., & Farina, M. (2012). Strontium is incorporated in different levels into bones and teeth of rats treated with strontium ranelate. *Calcif Tissue Int*, *91*(3), 186-195.

[2] Dahl, S. G., Allain, P., Marie, P. J., Mauras, Y., Boivin, G., Ammann, P. & Christiansen, C. (2001). Incorporation and distribution of strontium in bone. *Bone*, *28*(4), 446-453.

[3] Cabrera, W. E., Schrooten, I., De Broe, M. E., & D'Haese, P. C. (1999). Strontium and bone. *J Bone Miner Res*, *14*(5), 661-668.

[4] Argonne National Laboratory: StrontiumWorld Health: Strontium; Ward Dean, MD Accu-Cell Nutrition: Strontium Metagenics: Strontium and Bone Health (2006); Mark A. Kaye, DC. PDF book available at www.metadocs.com/pdf/pp_strontium.pdf

[5] Li, Z., Lu, W. W., Chiu, P. K., Lam, R. W., Xu, B., Cheung, K., ... & Luk, K. D. (2009). Strontium–calcium coadministration stimulates bone matrix osteogenic factor expression and new bone formation in a large animal model. *J Orthop Res*, *27*(6), 758-762.

[6] Neuprez, A., Hiligsmann, M., Scholtissen, S., Bruyere, O., & Reginster, J. Y. (2008). Strontium ranelate: the first agent of a new therapeutic class in osteoporosis. *Adv Ther*, *25*(12), 1235-1256.

[7] Marie, P. J., Ammann, P., Boivin, G., & Rey, C. (2001). Mechanisms of action and therapeutic potential of strontium in bone. *Calcif Tissue Int, 69*(3), 121-129.

[8] Doublier, A., Farlay, D., Khebbab, M. T., Jaurand, X., Meunier, P. J., & Boivin, G. (2011). Distribution of strontium and mineralization in iliac bone biopsies from osteoporotic women treated long-term with strontium ranelate. *Eur J Endocrinol*, *165*(3), 469-476.

[9] Peel, N. (2009). Bone remodelling and disorders of bone metabolism. *Surgery (Oxford)*, *27*(2), 70-74.

[10] Cabrera, W. E., Schrooten, I., De Broe, M. E., & D'Haese, P. C. (1999). Strontium and bone. *J Bone Miner Res*, *14*(5), 661-668.

[11] U.S Environmental Protection Agency: Integration Risk Information System. Strontium (CASRN 7440-24-6). URL: http://www.epa.gov/iris/subst/0550.htm. Accessed on August 20, 2013. Last updated on Thursday, August 09, 2012

[12] Wohl, G. R., Chettle, D. R., Pejović-Milić, A., Druchok, C., Webber, C. E., Adachi, J. D., & Beattie, K. A. (2013). Accumulation of bone strontium measured by in vivo XRF in rats supplemented with strontium citrate and strontium ranelate. *Bone*, *52*(1), 63-69.

[13] Boivin G, Farlay D, Khebbab T, Jaurand X, Delmas PD, Meunier PJ. (2010).In osteoporotic women treated with strontium ranelate, strontium is located in bone formed during treatment with a maintained degree of mineralization. *Osteoporosis Int*, *21*: 667-677.

[14] Blake, G. M., & Fogelman, I. (2007). Effect of bone strontium on BMD measurements. *J Clin Densitom*, *10*(1), 34-38.

[15] Moise, H., Adachi, J. D., Chettle, D. R., & Pejović-Milić, A. (2012). Monitoring bone strontium levels of an osteoporotic subject due to self-administration of strontium citrate with a novel diagnostic tool, *in vivo* XRF: A case study. *Bone*, *51*(1), 93-97.

[16] Zamburlini M, Pejović-Milić A, Chettle DR, Webber CE, Gyorffy J. (2007). *In vivo* study of an x-ray fluorescence system to detect bone strontium non-invasively. *Phys Med Biol* ,*52*:2107-2122.

[17] Zamburlini M, Pejović-Milić A, Chettle DR. (2008). Spectrometry methods for *in vivo* bone strontium measurements. *X-Ray Spectrom*,*37*:42-50

[18] Zamburlini M, Pejović-Milić A, Chettle DR. (2008). Coherent normalization of finger strontium XRF measurements: feasibility and limitations. *Phys Med Biol*,*53*: N307-N313.

[19] Pejović-Milić A, Brito JA, Gyorffy J, Chettle DR. (2002). Ultrasound measurements of overlying soft tissue thickness at four skeletal sites suitable for *in vivo* x-ray fluorescence. *Med Phys*, *29*:2687-2691.

[20] Zamburlini M, Pejović-Milić A, Chettle DR. (2006). Evaluation of geometries appropriate for I-125 *in vivo* bone strontium x-ray fluorescence measurement. *J Radioanal Nucl,* 269:625-629.

[21] WHO Geneva. Study group on assessment of fracture risk and its application to screening for postmenopausal osteoporosis.Technical Report Series (World Health Organization) 1994.

[22] Loftus, Michael L. Sanelli, P. C., Frush, D. P., & Applegate, K. E. Radiation Exposure from Medical Imaging. *Evidence-Based Neuroimaging Diagnosis and Treatment*. Springer New York, 2013. 63-79.

[23] Somervaille, L.J., Chettle, D.R., Scott, M.C., Tennant, D.R., McKiernan, M.J., Skilbeck A. & Trethowan, W.N. (1988). In vivo tibia lead measurements as an index of cumulative exposure in occupationally exposed subjects. *Brit J Ind Med 45*(3) 174

[24] Hansen, Christian, and Henrik Nilsson. "Strontium combinations for prophylaxis/treatment of cartilage and/or bone conditions." WIPO Patent Application PCT/DK2004/000327 filed May 6, 2004.

[25] Rousselet, F., El Solh, N., Maurat, J. P., Gruson, M., & Girard, M. L. (1974). [Strontium and calcium metabolism. Interaction of strontium and vitamin D]. *Comptes rendus des seances de la Societe de biologie et de ses filiales*, *169*(2), 322-329.

[26] Office of Dietary Supplements: National Institutes of Health. Dietary Supplement Fact Sheet: Calcium. URL: http://ods.od.nih.gov/factsheets/Calcium-HealthProfessional/. Accessed on November 14, 2013. Reviewed March 14, 2013.

[27] Blake, G. M., & Fogelman, I. (2006). Theoretical model for the interpretation of BMD scans in patients stopping strontium ranelate treatment. *J Bone Miner Res, 21*(9), 1417-1424.

[28] Blake, G. M., & Fogelman, I. (2006). Strontium ranelate: a novel treatment for postmenopausal osteoporosis: a review of safety and efficacy. *Clin Intervention Aging*, *1*(4), 367.

[29] Ozgür S, Sumer H, Kocoğlu G. Rickets and soil strontium. (1996). *Arch Dis Child*,*75*:524-526.

[30] Cohen-Solal M, Augry F, Mauras Y, Morieux C, Allain P, Vernejoul MC. (2002). Fluoride and strontium accumulation in bone does not correlate with osteoid tissue in dialysis patients. *Nephrol Dial Transplant*,*17*: 449-454.

[31] Da Silva, E., Kirkham, B., Heyd, D. V., & Pejović-Milić, A. (2013). Pure hydroxyapatite phantoms for the calibration of in vivo X-ray fluorescence systems of bone lead and strontium quantification. *Anal Chem*, *85*(19), 9189-9195.

5.3.1 Discussion and Conclusion of Long-Term Subjects

The second paper highlighted findings that would have not been evident had the bone strontium measurements not been continued. As illustrated in the second paper, one of the major findings reported was that for the initial study participant. Initially, as part of the Masters work, and as discussed previously, in section 5.2, it was thought at the time, that bone strontium levels in the finger, or rather cortical bone would plateau after a year of strontium supplementation while the ankle, representing primarily trabecular bone, would continue to increase. However, as the subject was measured throughout 2012 and 2013, a statistically significant increase in her bone strontium levels for the finger was observed after three years, which suggested the new conclusion that bone strontium levels would continue to increase at both bone sites, as long as the individual continued to take strontium supplements. This significant increase as observed with the IVXRF measurement was confirmed in the BMD test scores for that subject, who interestingly showed an increase of 11.8% in her femur site measurements, going from a BMD of 0.746 g/cm^3 to 0.834 g/cm^3(personal communication, 2013). This brings up and highlights the issue of strontium playing a role in artificially increasing BMD test values and the importance of correcting for BMD values in strontium supplementing individuals. As stated by Blake and Fogelman (2007), since strontium can replace the calcium in bone, DXA measurements of BMD can be overestimated because strontium, which has a higher atomic number (Z=38) attenuates the X-rays more strongly than calcium (Z=20). Neilsen and colleagues (1999), suggested that a 1% molar ratio of: [Sr/ (Ca+Sr)] caused a 10% increase in BMD values. This overestimation was confirmed by Blake and Fogelman

(2007), in their theoretical study of analyzing strontium ratios for different axial DXA systems.

Nevertheless, the second paper also highlighted these findings:

- Natural baseline strontium values for all ten subjects were on par with those reported by Zamburlini et al.,(2007a) within the same ethnic group (Causasian individuals). The mean normalized baseline strontium signal (± SD) for the ten subjects in the second paper were reported to be 0.42 ± 0.13, for the finger and 0.39 ± 0.07 for the ankle, in agreement with Zamburlini's reported values of 0.43 ± 0.08 and 0.40 ± 0.13, for the finger and ankle, respectively (Zamburlini et al., 2007a).

- Similar to the first paper (Moise et al., 2012), statistically significant increases in bone strontium levels were seen after 24 hrs ($p=0.0043$ and 0.000613 for the finger and ankle, respectively). By the end of the study, bone strontium levels continued to increase at both bone sites suggesting an absence of a plateau.

- All subjects showed a similar pattern of timed increases and uptake. However, while the pattern of uptake was similar, the strontium signal between the subjects showed a wide variation. For example, as discussed in the paper (Moise et al., 2014), by the third year, the lowest normalized strontium signal was observed to be 3.15 ± 0.15 and 4.46 ± 0.36, for the finger and ankle, respectively in one subject, whereas the highest was 28.15 ± 0.86 for the finger and 26.47 ± 1.22 for the ankle, in another subject.

In summary, while the paper answered the question that similar patterns would be seen in individuals and no plateau would be reached, it raised the question of the wide variation of strontium signal seen among the participants. However, based on the observations by the research group Bärenholdt et al (2009), whose study was introduced in section 5.1, such a variation in bone strontium content may be expected. Bärenholdt and colleagues (2009) concluded that bone strontium variations would not only be affected by the duration of treatment but also vary considerably between individuals. This

observation is partly explained by the differences in physiological make-up between individuals.

In Apostoaei's (2002) paper involving literature reviews, variations in the absorption factor (termed f_1) which represents the fraction of ingested strontium that is absorbed from the gastrointestinal tract and transferred to the plasma, were also observed in healthy adults. In trying to explain this variability, Apostoaei (2002) stated that despite the abundant information on strontium absorption from the gastrointestinal tract, the large variation of f_1, could not be explained by gender, age or calcium intake rate. Furthermore, Apostoaei (2002) states that in order to understand the large variation between individuals, the underlying physiological processes responsible for the uptake of strontium from the gastrointestinal tract should be investigated, and it is this physiological process that is most likely responsible for the large variability (Apostoaei, 2002). This is similarly echoed by Dahl and colleagues (2001) who stated strontium plasma levels as being correlated with bone strontium content, and ATSDR (2004) who cites various literature studies pointing to individual factors such as genetic makeup (genetic polymorphisms), health (renal disorders, diabetes, Paget's disease, rheumatoid arthritis or seronegative spondarthritis) and nutritional status (protein deficiency).

Hence, considering these conclusions and the observations as reported in the second paper by our research group, investigation of other biological and physiological factors, such as dietary intake, bioavailability, plasma serum analysis and bone formation markers, (e.g. alkaline phosphatase) may give more insight into the uptake and incorporation of strontium absorption. However, such analysis was beyond the scope of this study.

Another interesting observation reported by Bärenholdt and colleagues (2009) was their suggestion that their bone strontium uptake and retention data were representative of a power function model. While different models have been suggested in the literature for bone seeking elements including strontium, the long-term data collected over the last four years as part of this thesis work, were used to derive a model which is discussed in the next chapter.

5.4 Deer Bone Strontium Measurements

In addition to the *in-vivo* human bone measurements, animal (deer) bones of rib and vertebrae type have also been measured with this system. Although, the animal bones, found courtesy of Dr. Bill Prestwich (department of Medical Physics and Applied Radiation Sciences) were bones found in the Hamilton region within a forested area, details such as age of bone samples and related background were unknown. Nevertheless, the IVXRF system was able to detect a sufficiently high strontium signal in all samples.

5.4.1 Results

A total of seven bone samples were measured; five ribs and two vertebras. They were each measured for 1800 seconds (30 minutes) real time, using I-125 brachytherapy seeds as the photon excitation source, and the strontium alpha (Sr K_{α}) and beta peaks (Sr K_{β}) at 14.2 keV and 15.8 keV were fit using the seven parameter function, as described in chapter three. A sample raw measurement spectrum is shown for one of the rib bones and table 5.1 summarizes the results obtained for the seven samples.

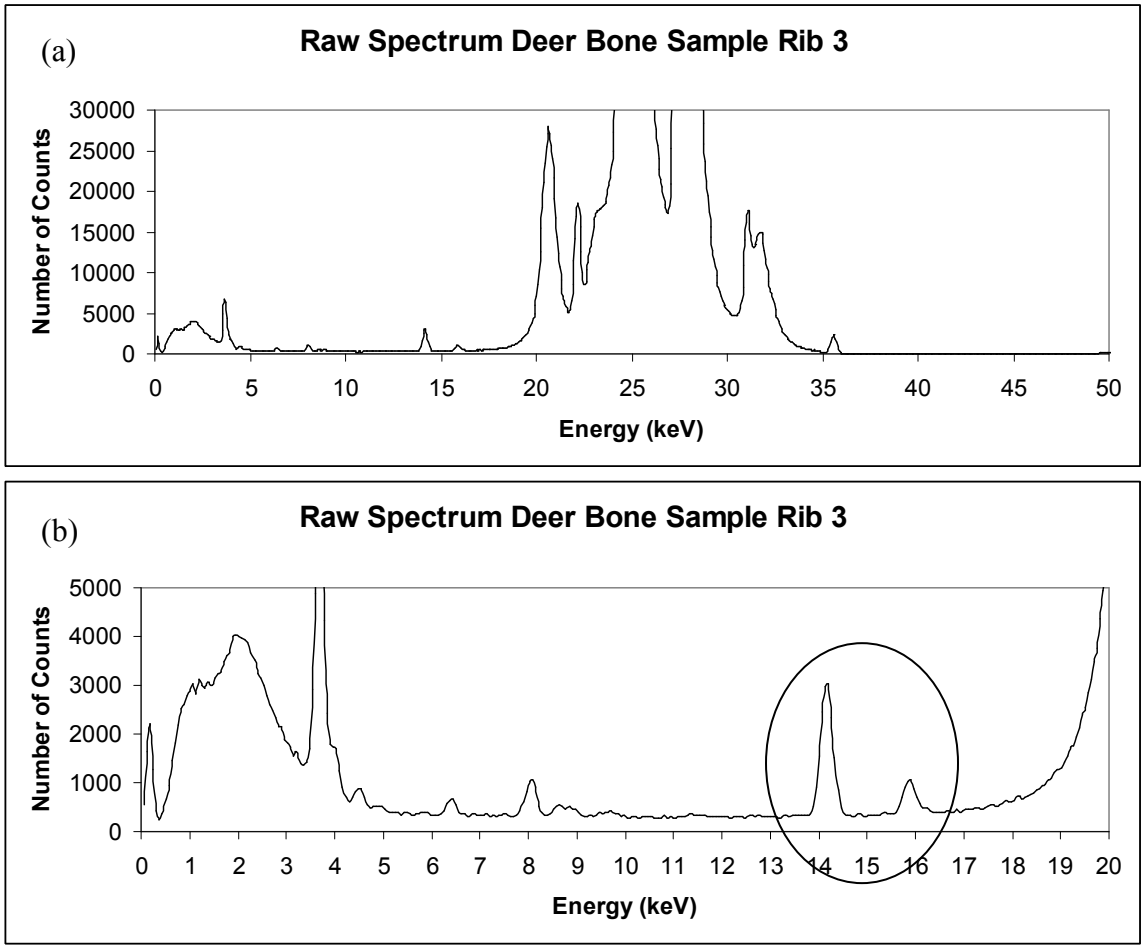

Figure 5.2(a) and (b): Sample measurement spectrum of deer bone rib 3 and highlighted portion showing the strontium K-alpha and K-beta peaks at 14.2 and 15.8 keV, respectively.

Bone Sample	Sr K_α (14.2 keV) Fitted	Sr K_β (15.8 keV) Fitted	Ratio (Sr K_α: Sr K_β
rib 2a	9866 ± 94	2325 ± 72	4.24 ± 0.14
rib 2b	11017 ± 100	2741 ± 76	4.02 ± 0.12
rib 3	7655 ± 85	1924 ± 65	3.98 ± 0.14
rib 4	9442 ± 92	2334 ± 70	4.04 ± 0.13
rib 5	12182 ± 103	2831 ± 77	4.30 ± 0.12
vertebrae 1	13189 ± 106	3050 ± 79	4.32 ± 0.12
vertebrae 9	10922 ± 99	2747 ± 77	3.98 ± 0.12

Table 5.1: Summary of deer bone measurements.

5.4.2 Discussion

As shown in Figure 5.2b, both strontium K-alpha and K-beta peaks are clearly observed. Although the deer bones were found approximately 2-3 years ago, the observable strontium signal for all samples raises the question of whether the strontium signal arises as a result due to soil contamination and uptake by the dead, exposed bones or rather by the natural strontium levels present in bone. Furthermore, it should be considered that the higher strontium signal not only results due to the absence of overlying soft tissue but, perhaps also the vegetarian diet of the deers. Similarly, as cited by Schoeninger and Peebles (1981), skeletal remains from agricultural humans are expected to have higher strontium content compared to hunter-gatherers within the same geological area, because plants will have higher strontium levels compared to animal products. Nevertheless, as stated in chapter one, the relative strontium content in plants is also dependant on the strontium soil levels. Hence, this also raises the question of geological and geographical environment influencing bone strontium levels in both animals and humans, and of which is explored further in chapter seven.

CHAPTER 6: KINETIC MODELING OF ELEMENTAL STRONTIUM

6.1 Introduction

The developments of the models available in the literature used to describe the retention of radionuclides in the human body have been mainly based on experimental data of radioactive isotopes in the human body (Shagina et al., 2003). While early literature studies have shown strontium to be a promising therapy in the treatment of osteoporosis, the findings shifted to a focus on understanding the health effects of strontium radioisotopes, such as Sr-90 (Pertinez et al., 2013). Thus, until recent years, available data in the literature on strontium retention in humans has been restricted to experimental findings based on single intake, Sr-90 due to global fall-out and measurements of dial painters (Degteva and Kozheurov, 1994). However, as stable strontium has been shown in the literature to be beneficial at low doses in the treatment of osteoporosis, refinement of past models, including those based on bone seeker elements such as calcium and lead were proposed to help gain further insight into strontium kinetics and health effects in bone.

6.1.1 Bone Volume Seekers and Development of Strontium Model

Since strontium is a bone seeker element such as calcium, it is thought that an understanding of the behavior of one of the elements would help give insight into the other. One of the important developments in modeling was that given by the International Commission on Radiological Protection (ICRP) Task Group based on literature data ranging from 15 minutes to 50 years, such as those from global fall-out and radiotracer

studies. Their publication of the ICRP 20 model of alkaline earth metabolism in adult man has marked an important step towards improving our understanding of the distribution and retention of such elements in the human body (Johnson and Myers, 1981). The six parameter ICRP 20 model, as shown in equation 6.1 applies to strontium and to other bone volume seekers such as calcium and its radioisotopes, barium and radium (Marshall et al.,1973).

Equation 6.1 $$R = (1-p)e^{-mt} + p\varepsilon^{b}(t+\varepsilon)^{-b}[\beta e^{-r\lambda t} + (1-\beta)e^{-\sigma r\lambda t}]$$

where:

R = the fraction of injected activity remaining in the body following a single intravenous injection
ε = time related to turnover of an initial pool (between 0.3 and 3 days)
b= power function slope which is related to the diffusion of activity from bone to blood and excretion of part of that activity from the body. The values range from 0.1-0.5.
λ= the rate of apposition and resoprtion in cortical bone (2.5% per year)
□= the ratio of turnover rates of both trabecular and cortical bone
β= fraction of bone volume turnover activity in cortical bone of ~ 0.5
r= correction factor for redeposition of activity in new bone at resorption sites long after the injection (0.83-0.99)
m=the rate constant of a small early exponential in R (0.1-0.8 day^{-1})
p=the fraction of R not in the early exponential (0.6-0.8)
t= time (from 0 to any time after injection)

The above ICRP model is based on nine postulates from which equations were developed with respect to retention in organs as a function of time following an intravenous injection. The parameters of these equations were then fit to existing data on alkaline earth metabolism in man (Johnson and Myers, 1981).

However, while the ICRP 20 model provided a reasonable fit to existing literature data, such as those from Sr-90 studies, it provides for some impracticality to use in practice (Johnson and Myers, 1981). As cited by Johnson and Myers (1981), the two main difficulties with the model are:

(i) The recycling of material between organs via blood is not explicit in the model, when in reality blood concentration and excretion rates estimates may differ considerably from experimental values.

(ii) A power function is used to represent the diminution of material in mineral bone from availability for resorption on blood. As a result, it increases the computational difficulty for calculations other than those based on a single injection.

Furthermore, the model applies to a 'normal' individual and does not take into account the health differences between healthy and diseased bone. However, the ICRP task force states that assuming an annual bone loss of 1% in normal man, after age 50 and more in osteoporotic individuals, then the final exponential in radioisotope retention in these population could be 1% per year greater than the given steady state value (ICRP, 1973). In addition, the task force states that for osteoporotics, it is best to use the steady state model first and then increase the rate of radioisotope loss from the model by the rate of bone mass loss (ICRP, 1973).

The model also does not take into account age and was developed for use in the adult man. This is of interest since younger people (i.e. <25 yrs) retain the alkaline earth elements to a greater extent than older people do (Legget, 1992). However, the ICRP further refined their model and created a new model (ICRP 1993) that takes into account infants, children and adolescents (ATSDR, 2004). While it shares the similarity of dividing bone into cortical and trabecular components, it differs in the sense of having

different parameter values as per age, the diminution of activity in the bone volume is assumed to be first order, re-deposition and soft tissues are addressed explicitly rather than as whole body minus bone and blood (Legget, 1992). In addition, it assumes that 99% of the strontium that enters the body and is not excreted is stored in bone with 1% in soft tissue as shown in Figure 6.1 (ATSDR, 2004).

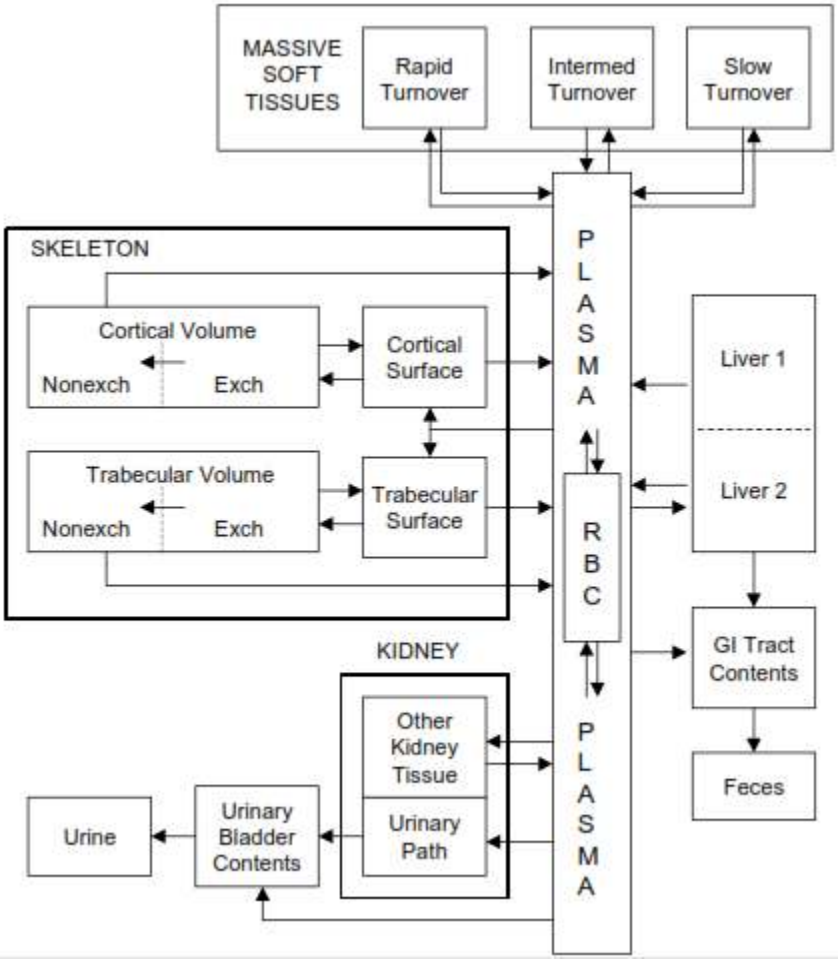

Figure 6.1: ICRP 1993 model of strontium biokinetics (ATSDR, 2004)

However, while the model added improvements, it should be noted that the model was designed to calculate Sr-89 and Sr-90 intake limits based on radiation dose to all

major organs (ATSDR, 2004). Nevertheless, the ICRP model also marked an important step towards our understanding of alkaline earth elements in terms of distribution and retention (Johnson and Myers, 1981).

6.1.2 Strontium Models in the Literature

The strontium models available in the literature are mostly based on *in-vivo* whole body counting (Reeve et al, 1983, Staub et al, 2003a,b), intravenous injection or oral administration of a single or multiple radiotracer (Bärenholdt et al, 2009, Staub et al, 2003a,b), urinary or fecal analysis (Bauer et al, 1958), and studies involving Sr-90 measurements. Power function models in the form of $y=x^a$ have been suggested to be useful in describing the retention of radioactive bone seekers (Nielsen et al., 2009) and while power and exponential models have been used to model the data, mathematical functions similar to the ICRP model discussed above have also been suggested for comparison and employed. For example, Johnson and Myers (1981) tried to substitute the $(t+\varepsilon)^{-b}$ rate variable with a second compartment for cortical and trabecular bone to represent diminution. Degteva (1994) devised an age dependant model based on Sr-90 whole body counting data using parameter estimates based on data from studies on populations who resided by the banks of the Tech river which was contaminated with fission products in 1945-1956, global fall-out data relating to strontium in human bone and single intake. More recent developments in modeling have included models incorporating a greater degree of physiological and mechanistic rationale, expanding on the compartments relating to strontium absorption (Pertinez et al, 2013) and looking at

strontium absorption within the osteoporotic population (Staub et al., 2003a,b, Bärenholdt et al, 2009). A few of these models are shown in Table 6.1 on the next page.

Group	Technique	Subjects	Model
Cohn et al (1962)	Sr-85: Excretion, *in-vivo* whole body counting	4 normal and 6 moderate osteoporotic individuals	$R = A_1 e^{-\lambda_1 t} + A_2 e^{-\lambda_2 t} + A_3 e^{-\lambda_3 t}$
Bärenholdt et al (2009)	Ca-47: *in-vivo* whole body counting, DPA and DXA of Sr	For Ca-47 (1 normal subject), for DPA and DXA (32 osteoporotic females from SOTI and TROPOS)	Based on Marshall's equations: $R = \left(\frac{t}{t_0}\right)^{-a}$ for initial few days $R = t_o^a \left(\frac{t + t_o}{a}\right)$ Retention of Sr to a time *t*, in terms of Ca: $\frac{M_{Sr}(t)}{M_{Ca}} = \frac{m_{Sr} * A * t_0}{M_{Ca} * (1-a)} * \left\{ \left(\frac{t}{t_0}\right)^{1-a} - \left(\frac{t - t_{Sr}}{t_0}\right)^{1-a} \right\}$
Degteva & Kozheurov (1994)	Sr-90: *in-vivo* whole body counting	Techa river residents exposed to global fall-out (1949-1956)	$R(\tau,t) = f_1(\tau)P(\tau)[R_c(\tau,t) + R_T(\tau,t)]R_{Ca}(\tau,t)$ $R_C(\tau,t) = \beta(\tau)\varepsilon(\tau)^{b(\tau)}[t+\varepsilon(\tau)]^{-b(\tau)} \exp(-\lambda_c t)$ $R_T(\tau,t) = [1-\beta(\tau)]\varepsilon(\tau)^{b(\tau)}[t+\varepsilon(\tau)]^{-b(\tau)} \exp(-\lambda_T t)$ $R_{Ca}(\tau,t) = \begin{cases} 1 & \tau + t \le 30\,\text{yrs} \\ Ca(\tau,t)/Ca(30) & \tau < 30, \tau + t \ge 30\,\text{yrs} \\ Ca(\tau,t)/Ca(\tau) & \tau \ge 30\,\text{yrs} \end{cases}$
Marcus (1977)	Pb: *vivo* whole body counting	Based on previous literature data in animals and humans	General compartmental model: $R(t) = \sum_{i=1}^{N} q_i \exp(-v_i t)$ Based on ICRP: $R(t) = q_1 \exp(-v_1 t) + q_2 \exp(-v_2 t)d^b(t+a)^{-b} + q_3 \exp(-v_3 t)d^b(t+a)^{-b}$
Bauer et al., (1958)	Sr-85: excretion and surface body counting	5 normal subjects	$E = \frac{1}{S_B + k' \int_0^t S_B dt}$ where $k' = 0.693/t_{1/2}$ and S_B =specific activity

Table 6.1: A few literature models incorporating power and exponential functions.

6.1.3 Issues with Literature Models

The advantage of using strontium as a tracer is that it not only parallels calcium in studying certain aspects of metabolism in man, it also has a pure gamma ray emission which permits body surface counting (Bauer et al., 1958). However, there are several questions and issues with using data based on whole body counting or excretion analysis. Some of the questions posed include (i) how much of the total store of the body's strontium or calcium is actually measured with the use of a radiotracer, (ii) past studies using excretion analysis (i.e. fecal analysis) are limited in time and are further limited by the problem of obtaining complete excreta collections over a long term period and (iii) since Sr-85 as a radiotracer presents with a short half-life of 65 days, studies are confined to a maximum of two years duration and so projections of long term retention values are extrapolated from existing short term data (Cohn et al., 1962).

While recent studies such as those by Bärenholdt and colleagues (2009) have looked at modeling strontium retention based on long term data in 32 post-menopausal osteoporotic women, using mean % strontium over 7 to 8 years, the fact that they used mean % strontium values rather than individual measurements to model the data raises the issue of the wide variability of strontium absorption between individuals. While this was recognized by the authors, they suggest as future work that measurement of parameters with respect to the power function model for individuals may be possible by whole body counting after an oral intake of Sr-85 followed by injection with Sr-85 six days later when the absorbed Sr-85 has passed the intestine. Cohn and colleagues (2014) suggest excretion studies performed over an initial portion of time followed by long term

whole body counting, such as over a year using the power and exponential functions to model the data.

However, in *in-vivo* radiotracer studies, there is often the assumption that the subjects are in a constant steady state with respect to the element being investigated which may not be correct, especially as these models have been widely used to obtain quantitative estimates of absorption and urinary excretion (Bauer et al., 1958, Staub et al, 2003a). Bauer and colleagues (1958) state that the assumptions are incorrect because it should be considered that (i) the rate of ingestion of strontium, iodine or iron usually varies with the time of day and (ii) the subjects may be in process of developing a new steady state such as anemia or osteoporosis. The use of normal subjects to develop a model would not be applicable to individuals suffering from bone diseases, metabolic disorders such as hypothyroidism, hyperparathyroidism and Paget's disease, those suffering from vitamin D deficiency, and those presenting with fractures (Bauer et al., 1958).

In addition, while it has been suggested that understanding the model of calcium may help understand strontium metabolism due to their similar biochemical properties (Dolphin and Eve, 1963), translating the calcium model into a strontium model or the other way around presents some important differences to consider such as (Bauer et al., 1958):

- Elimination mechanisms are more efficient for strontium than for calcium by a factor of approximately 4.
- The 'final' exponential for strontium is not reached until 3 days following administration, whereas in Ca-45 administration, Krane et al (1956) found that the blood activity started to fall exponentially after 1.5 days.

- The intracellular concentration of strontium in the fluid may be equivalent to the extracellular concentration whereas in calcium the concentration is higher in the extracellular

Hence, the complexities of modeling strontium is evident in the literature studies, especially as experiments have lasted over a longer period of time, and it has been necessary to add more compartments with longer half-lives (Marcus, 1977). Adding to the challenges of developing a model for strontium distribution and metabolism is the question of the physiological role of strontium, the absence of evidence for strontium homeostasis and the high dosages (as much as 1000 times the normal dietary intake) of oral strontium administration in some studies (Staub et al., 2003a).

Thus, in order to model strontium, the study necessitated long term collection of IVXRF data. The data collected over a period of four years was used for eight baseline female individuals. The results are discussed in the next sections.

6.2 Method and Materials

The eight baseline female subjects whose data were used for modeling purposes are shown in Table 6.2 below. The technique and method of the IVXRF system has been described in chapter two and five of this thesis. Although ten baseline subjects were recruited in the study, as profiled in chapter five, data over a span of at least a year were chosen for modeling purposes.

Subject #	Age	Diagnosis
1	66	Unknown
2	53	Osteoporosis (hip & spine)
3	66	Osteoporosis (spine) & Osteopenia (hip)
4	68	Osteoporosis (spine)
5	70	Osteoporosis (hip) & Osteopenia (spine)
6	63	Osteopenia (hip & spine)
7	53	Osteoporosis (spine)
8	57	Osteopenia (hip & spine)

Table 6.2: Profile of baseline subjects. Note that age is given for age at time of recruitment.

Modeling of the variation of the bone strontium IVXRF data with time was performed with Origin Pro 9.1. Parameter values were selected based on trial and error using both fixed and variable settings. Initial guesses were made based on the individual's data and data available in the literature with respect to half-life and uptake. Repeated fittings were performed for different parameter values until satisfactory fits were obtained for all data.

6.3 Results

Based on the attempts to model the baseline subjects' data on the literature models of strontium, calcium and lead uptake in bone as shown in Table 6.1 and of which a few model values are shown in Table 6.3 below, the choice of using a one model compartment expressed as an exponential, first rate order kinetic function was chosen.

Model	Parameters	Parameter Values	χ^2	Adj R^2
$y = a + be^{-\lambda t}$ $\lambda = \ln 2 / c$	a, b, c	b=11.69±1.81 c=1.55x10^{25}d	78.617	0.045
$y = a + \frac{b}{1 + ce^{-(\ln 2/d)x}}$	a,b,c,d	b=20.97±1.09 c=5.64±1.82 d=88.26±18.44d	7.875	0.879
$y = a + \frac{b}{1 + ce^{-(\ln 2/d)x}} + \frac{e}{1 + fe^{-(\ln 2/g)x}}$	a,b,c,d,e,f,g, h	b=8.90±6.07 c=4.04±4.06 d=23.80±23.37d e=11.98±6.36 f=263.59±1781.17 g=45.11±45.83d	7.804	0.879

Table 6.3: Examples of a few models attempted. Note that parameter '*a*' is taken to be the mean strontium baseline signal for all baseline subjects; 0.42 ± 0.13 and 0.39 ± 0.07, for the finger and ankle bone measurements, respectively.

6.3.1 One Compartmental Model

In this model, strontium retention is represented by a single compartment, as shown in figure 6.2 below.

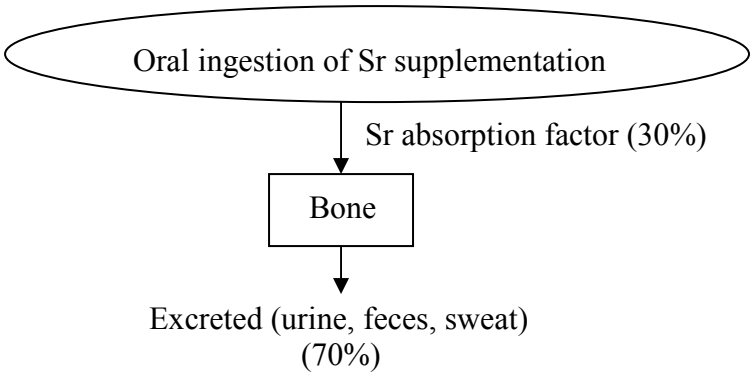

Figure 6.2: One compartmental model. Note that of the total amount of strontium ingested, roughly 30% (ICRP 82) will be absorbed from the GI tract and the remainder (70%) will be excreted.

The corresponding equation may be represented as equation 6.2, where the model includes three parameters listed as: A_o, A_1, and A_2.

Equation 6.2 $$y = A_o + A_1(1 - e^{-\lambda t})$$

Where the terms are defined as:

y= Normalized strontium signal at time, t in days
A_o= parameter relating to the mean baseline signal observed in the subjects enrolled in this study (N=10). The values (± SD) are taken to be 0.42 ± 0.13 and 0.39 ± 0.07, for the finger and ankle bone measurements, respectively.
A_1= parameter relating to bone uptake
$\lambda = \frac{\ln 2}{A_2}$
A_2= parameter equal to the half-life of strontium in bone (days)
t= time of strontium supplementation (days)

Table 6.4 below summarizes the parameter values obtained when this model was applied to the eight baseline subjects' data.

Baseline Subject ID #	Parameter A_1 (bone uptake)	Parameter A_2 (half-life in days)	Reduced Chi Square (χ^2)	Adjusted R^2
1	14.38 ± 4.93	654.73 ± 356.58	3.311	0.707
2	34.86 ± 14.12	910.44 ± 494.03	3.024	0.925
3	49.34 ± 16.10	1049.01 ± 456.67	4.084	0.946
4	3.96 ± 0.53	376.12 ± 125. 61	0.933	0.563
5	15.27 ± 1.04	263.33 ± 49.33	2.953	0.882
6	21.30 ± 1.36	177.87 ± 36.66	8.235	0.872
7	2.61 ± 0.45	190*	1.752	0.865
8	7.03 ± 0.72	442.68 ± 107.93	1.270	0.555

Table 6.4: Summary of modeling results for the finger bone, representing primarily cortical bone.* Note that for the data to converge, the parameter was left fixed in this case.

Graphical representations for subjects #2, 3 and 6 are shown in the subsequent figures.

The remaining graphs are available in the Appendix section.

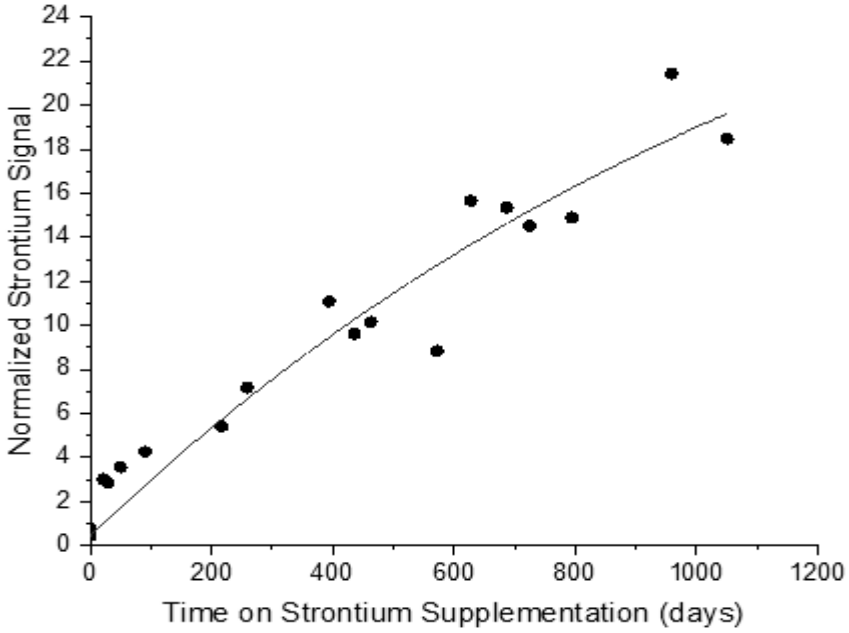

Figure 6.3 Graphical representation of finger one compartmental model for subject #2.

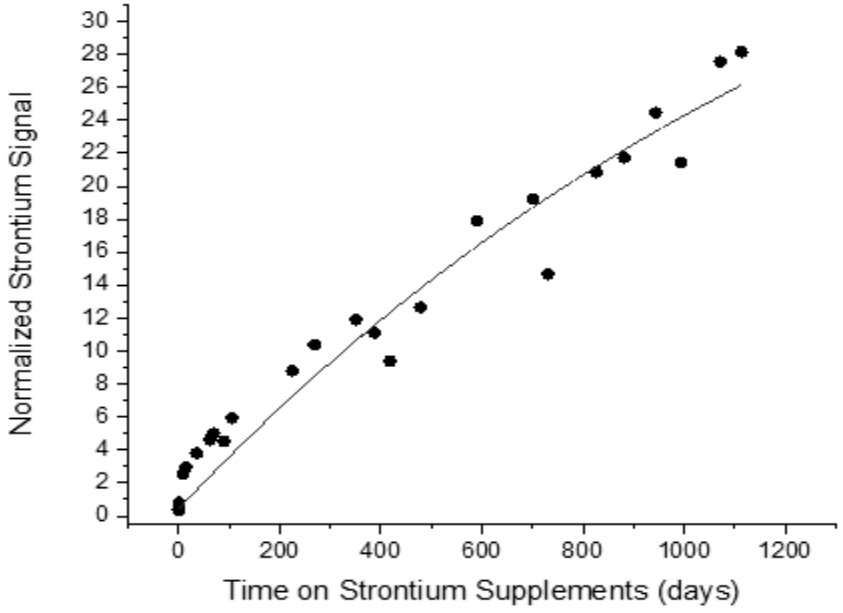

Figure 6.4: Graphical representation of finger one compartmental model for subject #3.

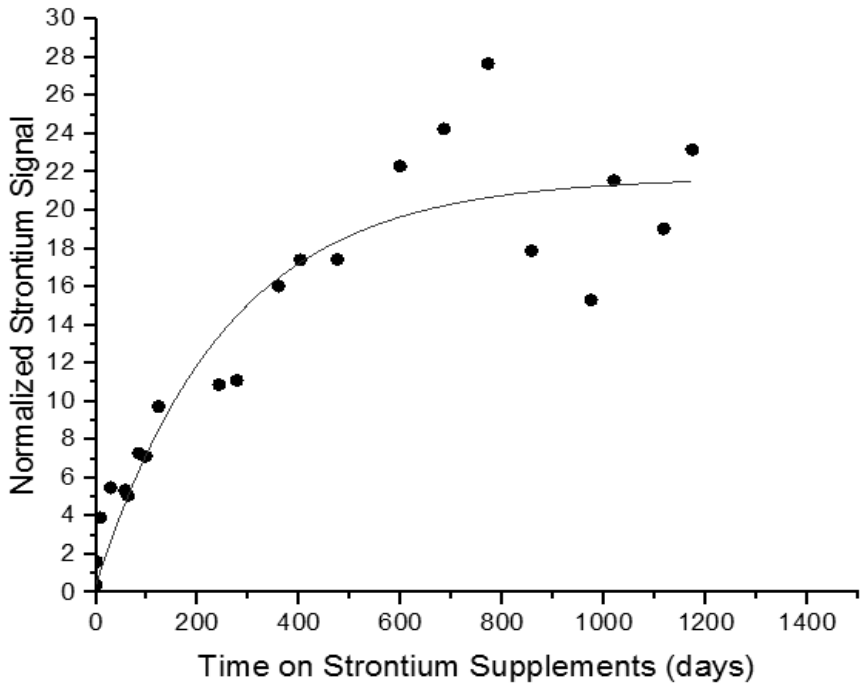

Figure 6.5: Graphical representation of finger one compartmental model for subject #6.

Similarly, the model was applied to the bone ankle measurements and Table 6.5 summarizes the results obtained for the ankle and the graphical representations for subjects 2, 3 and 6 are shown in figures 6.4, 6.5 and 6.6, respectively.

Baseline Subject ID #	Parameter A_1 (bone uptake)	Parameter A_2 (half-life in days)	Reduced Chi Square (χ^2)	Adjusted R^2
1	15.53 ± 2.45	435.67 ± 134.54	3.429	0.832
2	34.33 ± 11.39	526.18 ± 284.99	14.055	0.837
3	26.26 ± 1.39	127.99 ± 27.40	15.504	0.862
4	6.14 ± 0.43	275.66 ± 58.72	1.213	0.789
5	21.30 ± 2.80	328.03 ± 101.56	11.377	0.770
6	30.65 ± 5.82	313.64 ± 32.54	4.059	0.701
7	3.79 ± 0.28	14.77 ± 7.32	1.011	0.596
8	5.96 ± 0.38	35.32 ± 7.87	0.593	0.881

Table 6.5: Summary of modeling results for the ankle bone, representing primarily trabecular bone.

As above graphical representations are shown for subjects #2,3 and 6. Remaining graphs for the baseline subjects may be seen in the Appendix.

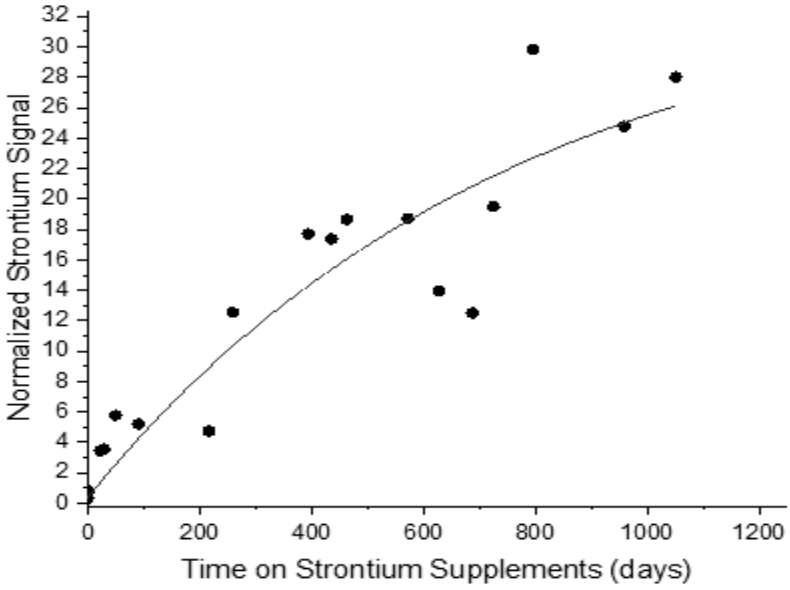

Figure 6.6: Graphical representation of ankle one compartmental model for subject #2.

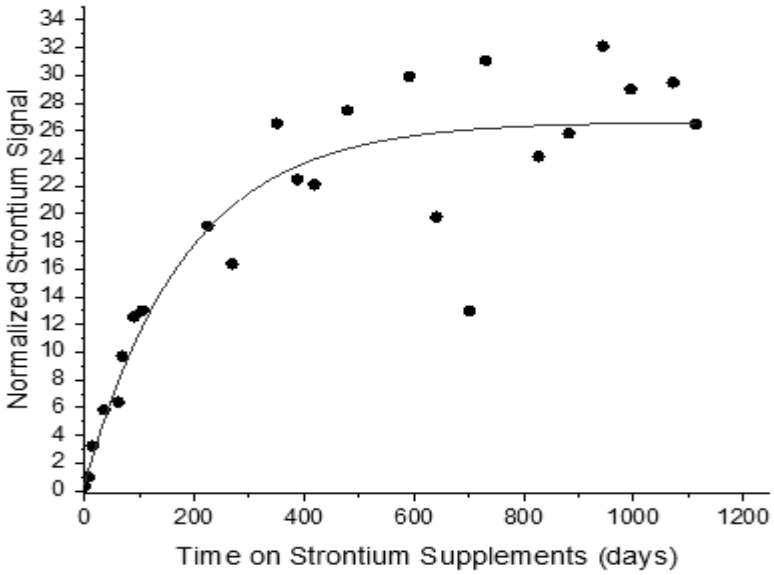

Figure 6.7: Graphical representation of ankle one compartmental model for subject #3.

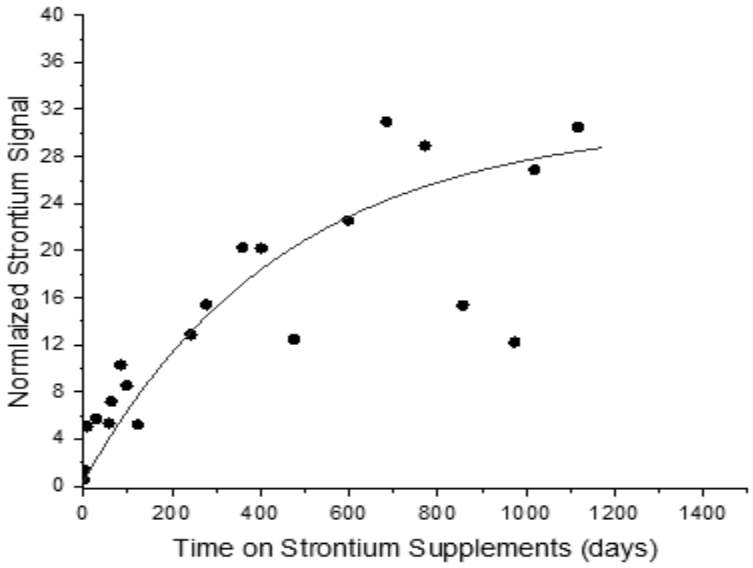

Figure 6.8: Graphical representation of ankle one compartmental model for subject #6

Although the one compartmental model was associated significantly with the variation in bone strontium in all cases, the goodness of fit varied quite widely. For finger bone strontium data, the reduced χ^2 ranged from 1.0 to >8 (illustrated in Table 6.4 and the adjusted R^2 ranged from ~0.56 to ~0.95. For ankle data, the reduced χ^2 ranged from <1.0 to ~16 and the adjusted R^2 ~0.60 to ~0.88. For subject #7, it was not possible to achieve a satisfactory fit that would allow both the uptake and half-life parameters to vary. Furthermore, as observed in figures 6.6 to 6.8, there is considerable variability of the values plotted and so fitting of the curves with this model also contributes to the large range of errors as observed in the Table values. Nevertheless, the one compartmental model showed that the average half-life ± SD for the first six baseline subjects at the finger was 572 ± 357 days and 335 ± 137 days for the ankle. The last two subjects (subjects 7 and 8) were individuals who missed the occasional dose of strontium and who

took strontium together with food likely to contain calcium (for example almond butter and orange juice), thus their values were not taken into account in calculating the average half-life.

The bone strontium uptake parameter, A_1, represents the percentage uptake of strontium based on the parameter half-life, A_2, and may be deduced from differentiating equation 6.2, as shown below. For simplicity, in the differentiation of equation 6.2, the parameters A_o , A_1 are denoted as "a' and 'b'. A_2 is represented by the exponential function and the half-life as 'c'.

$$\frac{d}{dt}(a+b\left(1-e^{-\ln 2t/c}\right))$$

$$=-b*\frac{d}{dt}\left(e^{-\ln 2t/c}\right)$$

$$=-be^{-(\ln 2t)/c}*\frac{d}{dt}\left(-\frac{\ln 2t}{c}\right)$$

$$=-b*\frac{-\ln 2}{c}*e^{-(\ln 2t)/c}$$

$$=\frac{b\ln(2)*e^{-(\ln 2t)/c}}{c}$$

or re-written as :

Equation 6.3 $$\frac{dy}{dt}=\frac{b\ln 2}{c}*e^{-(\ln 2)t/c}$$

And thus, taking into account the two parameters of b and c, relating to the uptake parameter (A_1) and half-life (A_2), the percentage uptake of strontium was calculated. However, in the determination of strontium uptake, a few assumptions were made. These assumptions were:

- In 'normal' man, it is estimated that calcium is present as 1kg calcium per 75 kg of body weight. Given the estimated weight of the average volunteer to be 60 kg, the whole body weight is then 800 g of calcium.

- Considering that the volunteers are osteoporotic and/or osteopenic, they are assumed to have an abnormal bone metabolism compared to the normal individual. Thus, for a 60 kg volunteer, the estimated calcium in the whole body is then: 1000 g calcium x60 kg x .8/75kg = 640 g calcium.

- In calculating the amount of calcium presented in each type of bone tissue, it is considered that the skeleton is made up of 80% cortical bone and 20% trabecular bone. Thus, in the above example, the amount of calcium in cortical and trabecular bone is 512 g and 128 g, respectively.

- As stated in the first chapter, the amount of strontium in reference man is 320 mg strontium per g calcium, which is equivalent to the mean normalized baseline strontium signal of 0.40 observed in the baseline volunteers in this study.

Therefore at t=0 days: $\frac{dy}{dt} = \frac{b \ln 2}{c}$

Based on these assumptions, and the evaluation at t=0, the percentage uptake of strontium in bone over the entire length of the study was calculated for the baseline subjects, as shown in Table 6.6

Subject #	Cortical (mg Sr/day)	Trabecular (mg Sr/day)	Total Uptake (mg Sr/day)	% Uptake
1	6.23 ± 4.01	2.53 ± 0.88	8.76 ± 4.11	2.57 ± 1.20
2	10.87 ±7.37	4.63 ± 2.94	15.50 ± 7.93	4.55 ± 2.32
3	13.35 ± 7.26	14.56 ± 3.21	27.91 ± 7.94	8.19 ± 2.33
4	2.99 ±1.08	1.58 ± 0.35	4.57 ± 1.13	0.67 ± 0.17
5	16.46 ± 3.28	4.61 ±1.55	21.06 ± 3.63	6.18 ± 1.06
6	33.99 ± 7.33	6.94 ± 1.50	40.94 ± 7.49	12.00 ±2.20
7	3.90 ± 0.67	18.21 ± 9.12	22.11 ± 9.15	6.48 ± 2.68
8	4.51 ± 1.19	11.98 ± 2.78	16.48 ± 3.02	4.83 ± 0.89

Table 6.6: Summary of bone strontium uptake in the eight baseline subjects based on the bone uptake and half-life parameters.

A discussion of the half-life and percentage uptake values compared to the literature ranges and possible physiological factors that may affect these parameters is presented later on.

However, unexpectedly, when weighted fits (to the measurement uncertainty) were compared with the unweighted fits there was a disagreement between the two parameter values. An example of this discrepancy is shown in Table 6.7 below, for subject #2.

	Unweighted Fit		Weighted Fit	
Bone Site	Uptake Parameter (A_1)	Half-life Parameter (A_2)	Uptake Parameter (A_1)	Half-life Parameter (A_2)
Finger	34.86 ± 14.12	910.44 ±494.03	81.29 ± 89.24	2408 ± 2987
Ankle	34.33 ± 11.39	526.18 ±284.99	32.78 ± 8.39	470 ± 218

Table 6.7: Comparison of unweighted fit to weighted fit for subject #2.

Thus, a two compartmental model was introduced to see if the fit would improve, as shown in figure 6.9.

6.3.2 Two compartmental model

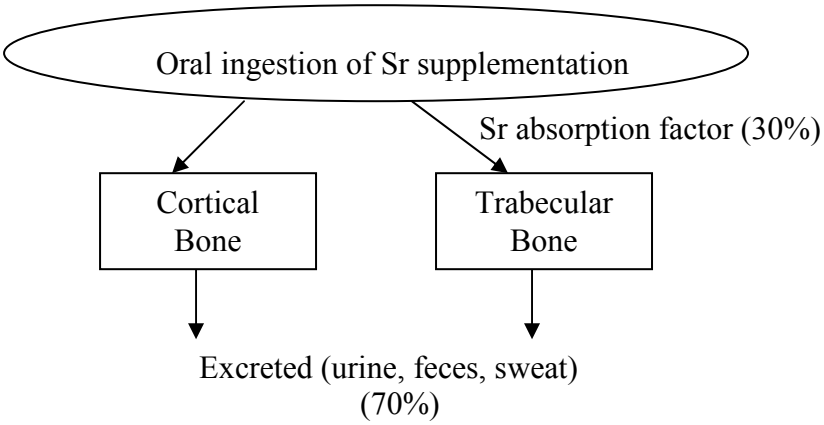

Figure 6.9: Two compartmental model. Note that of the total amount of strontium ingested, roughly 30% (ICRP 82) will be absorbed from the GI tract and the remainder (70%) will be excreted.

The modeling equation for the two compartmental model is then expressed as:

Equation 6.4 $$y = A_o + A_1(1 - e^{-\lambda_1 t}) + A_3\left(1 - e^{-\lambda_2 t}\right)$$

Where y is the normalized strontium signal and t is the time of strontium supplementation in days. The parameters A_o, A_1 and A_2 are the same parameters as defined previously in section 6.1.1. However, since the bone compartment is now split, parameters A_1 and A_2 represent the cortical bone compartment. Similarly:

A_3= parameter relating to bone uptake in second bone (trabecular) compartment

$\lambda_2 = \frac{\ln 2}{A_4}$

A_4 = half-life of strontium in days for the second bone (trabecular) compartment.

It was found that this model did not converge if all four parameters (2 uptake, 2 half-life) were free to vary. So, in order for the model to converge to the data, the parameters relating to bone uptake (A_1 and A_3) were fixed based on trial and error. Table 6.8 shows an example for subject # 5 of the model parameters as they were left fixed or variable

	A_1	A_2 (days)	A_3	A_4 (days)
method 1	V	V	V	V
method 2	V	F	V	F
method 3	F	F	V	V
method 4	F	V	F	V
method 1	2.21 ±1.02	3.00 ± 7.19	14.90 ± 1.92	408.38±145.01
method 2	44.33 ± 9.72	500	-37.87 ± 15.18	1000
method 3	10	500	-5.70×10^{13} $\pm 2.97 \times 10^{13}$	-5.70×10^{15} $\pm 2.97 \times 10^{15}$
method 4	10	171.11 ± 34.10	10	1222.13± 224.51

Table 6.8: Example of fitting trial and error for subject #5. The best method followed leaving the uptake parameters (A_1 and A_3) fixed while leaving the half-life parameters (A_2 and A_4) variable or solved by the program.

The bone uptake parameters were estimated based on the results obtained from the one compartment model. Tables 6.9 and 6.10 summarize the results obtained.

Baseline Subject ID #	A_1 bone uptake	A_2 half-life (days)	A_3 bone uptake	A_4 half-life (days)	Reduced Chi Square (χ^2)	Adj R^2
1	5	322.66 ± 205.35	10	1054.89± 379.38	3.285	0.710
2	15	623.42 ± 402.73	25	1677.07± 1071.47	3.016	0.925
3	15	306.10 ± 104.59	25	1110.99 ± 271.31	7.604	0.899
4	3	259.87 ± 68.69	5	6127.86± 2836.24	0.901	0.578
5	10	171.11 ± 34.10	10	1222.13 ± 224.51	2.816	0.782
6	15	120.13 ± 28.08	25	2468.76 ± 539.13	9.000	0.867
7	1.5	176.52± 233.15	4	1945.03 ±1263.06	2.088	0.912
8	5	423.78 ± 142.57	7	2000*	1.293	0.583

Table 6.9: Two compartmental model applied to finger bone measurements. *The second half-life for finger data for subject #8 had to be fixed in order for the fit to converge

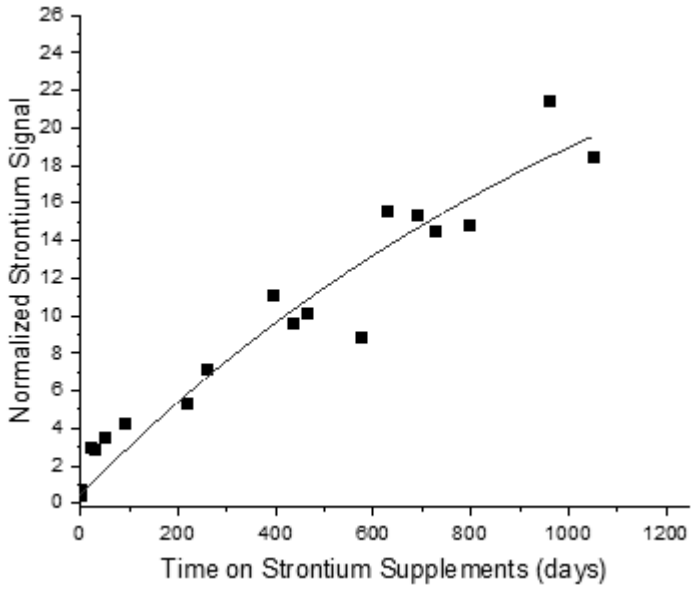

Figure 6.10: Two compartmental model fit for finger, subject #2.

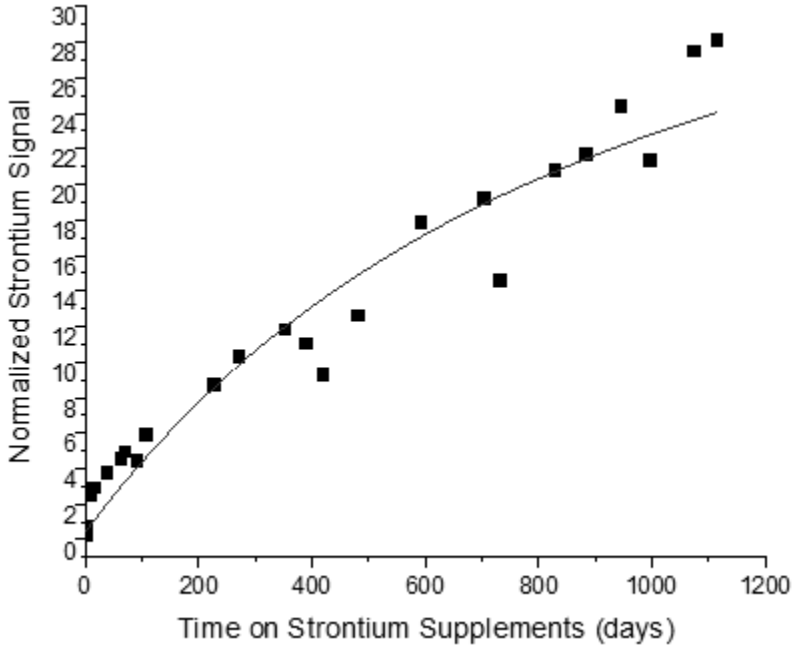

Figure 6.11: Two compartmental model fit for finger- Subject #3

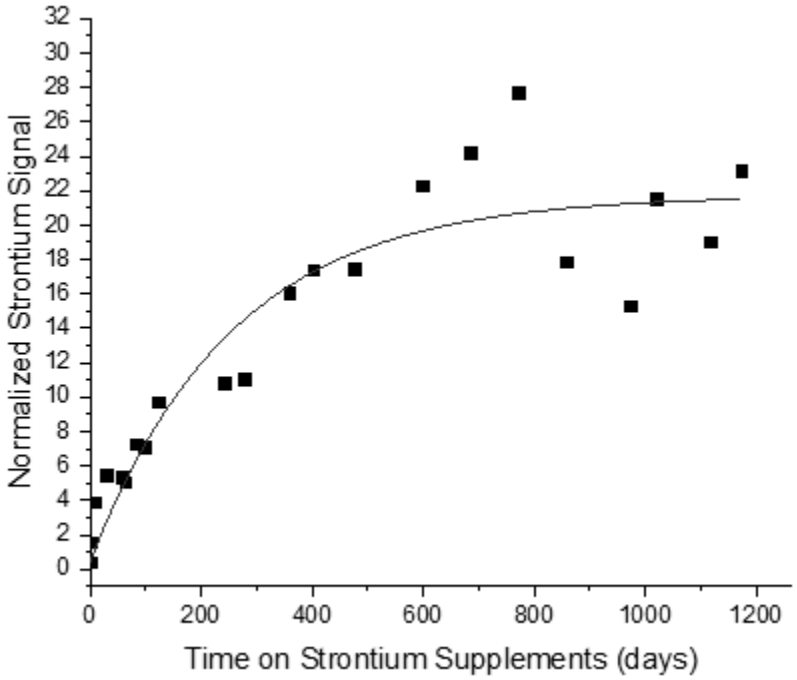

Figure 6.12: Two compartmental model fit for finger- Subject #6

Baseline Subject ID #	A_1 bone uptake	A_2 half-life (days)	A_3 bone uptake	A_4 half-life (days)	Reduced Chi Square (χ^2)	Adj R^2
1	5	180.72 ± 80.72	20	1476.38 ±172.02	3.430	0.839
2	20	361.48± 151.83	40	3091.98 ±1794.50	13.878	0.839
3	20	87.14 ± 20.30	25	2070.81 ± 454.69	14.725	0.869
4	3	138.40 ± 44.68	5	973.20 ±147.23	1.227	0.787
5	15	239.41 ± 71.13	15	1183.61 ± 561.28	11.164	0.892
6	20	202.56 ± 80.89	30	2295.08 ±1014.60	39.397	0.709
7	3	8.98 ± 6.69	2	1010.06 ± 545.04	1.070	0.596
8	5	25.37 ± 5.36	7	1348.84 ± 464.28	0.481	0.912

Table 6.10: Two compartmental model applied to ankle bone measurements

The ankle data for subject #6 showed a particularly high $\chi 2$ (nearly 40). But otherwise the goodness to fit measures showed a similar range of values to those observed for the single compartment model.

Graphical representations for subjects # 2, 3 and 6 are shown below. The remaining graphs are available in the appendix section.

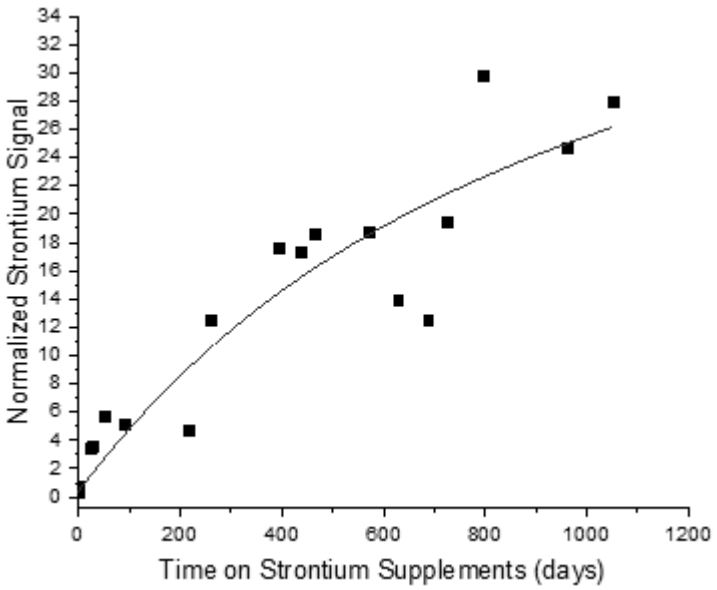

Figure 6.13: Two compartmental model fit for ankle- Subject #2

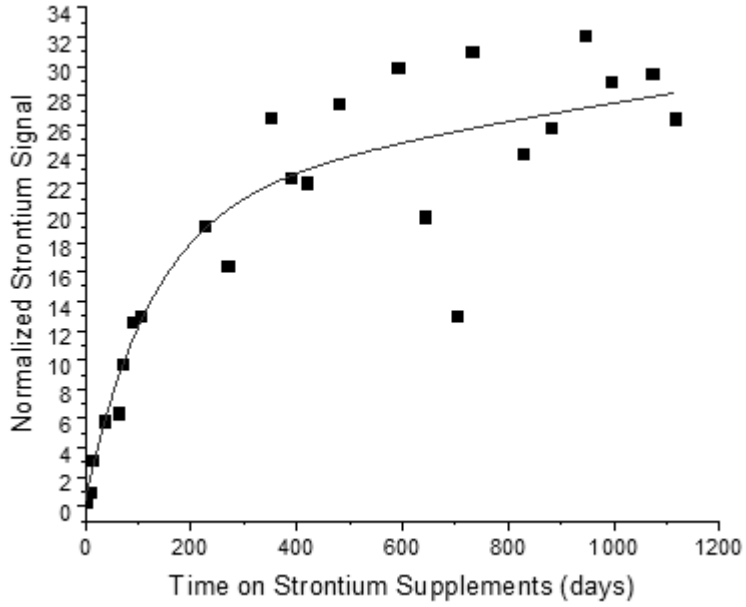

Figure 6.14: Two compartmental model fit for ankle- Subject #3.

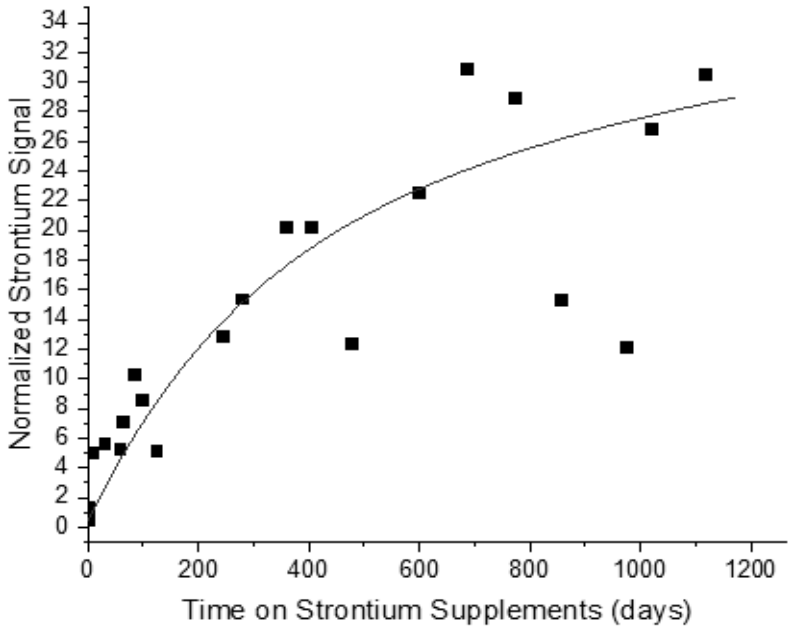

Figure 6.15: Two compartmental model fit for ankle- Subject #6.

6.4 Discussion and Conclusion

Applying the one compartmental model as shown in equation 6.2, to the eight baseline subjects gave an average half-life value ± SD of 508 ± 331 days and 232 ± 183 days for the finger and ankle bone, respectively. Although, the half-life in this work was based on measurements performed with the IVXRF technique, the values are within suggested half-life values for osteoporotic individuals presented in the literature. For example, in their study of ten individuals, six of whom were suffering from moderate osteoporosis, using the exponential model as shown in Table 6.1, applied to data obtained from excretion studies and whole body counting over a period of a year, Cohn and colleagues (1962) obtained half-life values between 210 to 982 days. For the six osteoporotic individuals, the mean half-life was 843 days (Cohn et al., 1962). Similarly a mean half-

life of 500 days was observed by Cowan and colleagues (1952), 178 days by (Smith et al., 1967) and as long as 1118± 450 days for cortical bone by Newton and colleagues (1977). However, although the half-lives obtained from the one compartmental model agree with some literature values, the one compartmental model shows no statistically significant difference between the finger and ankle bone half-lives (p=0.08796). However, analysis of the second parameter related to strontium bone uptake finger and ankle values show a correlation of 0.804, which is significant at the 95% level.

For the eight baseline subjects, the mean percentage uptake was 5.68 ± 3.46%, giving a range of 0.67 and 12% for the total % uptake. This falls within the range observed by Wohl and colleagues (2013) who observed an uptake of 2.7% in rats administered with strontium citrate over an 8 week period using the same technique of IVXRF.

Taking into account half-life and uptake parameter values, at first impression, the one compartmental model seems to be a possible fit, but when a comparison is made between the unweighted fits and weighted fits (weighted to the measurement uncertainty), there is disagreement between the parameter values of as much as 40%. An example is shown in Table 6.6 for the finger data for subject #2. As a result of this discrepancy, and considering that an exponential model would best describe the data, an additional compartment was added. While the results did not improve with the two compartmental model, the model indicated that there are two different half-lives for the two compartments, with one being longer than the other. The half-lives for both compartments for the finger data and ankle data show statistically significant differences (p=0.0147 and p=0.000711, for the finger and ankle, respectively). For the eight baseline

subjects, the mean half-life was 300 ± 163 days and 2200 ± 1661 days for the short and long compartments, respectively. This suggests that one compartment has a much quicker turnover compared to the other, which reflects the behavior of trabecular bone compared to cortical bone. This observation agrees with that stated in the literature in which elimination of strontium from the skeleton has two half-life components, that is, an initial half-life of 41 days followed by a slower half-life of three years (Marie et al., 2001).

In addition to the type of bone tissue, the half-life observed will also be affected by factors such as dietary consumption, such that the half-life is enhanced by vitamin D_3 intake and negatively affected by clodronate (Cohen-Solal, 2002). A discussion of the factors of strontium absorption and also factors affecting the observation of a wide variation of the strontium signal between the subjects in this study was presented in chapters one and five, respectively.

Due to the spread of the data, modeling the data to fit a specific function is very challenging and points to the possibility of a lack of a suitable model for the IVXRF data. Furthermore, even though a similar pattern of uptake is observed for the baseline subjects, attempting to model the data to resemble the pattern is not satisfactory, as shown in figure 6.16 below (model 3, Table 6.3)

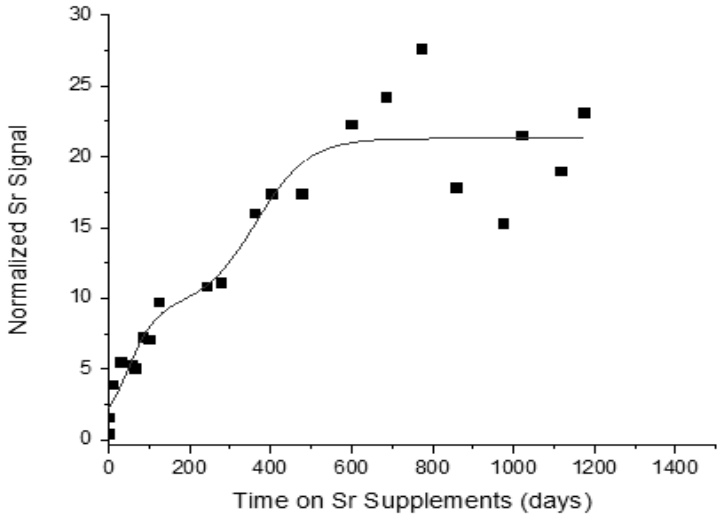

Figure 6.16: Unsatisfactory model fit due to scatter of data for subject #6 finger.

In the case of the second compartmental model, when all four parameters were left variable, the data either failed to converge or gave unrealistic parameter values. For example, when the data did converge, the half-life parameter was $>10^{18}$ years. This is in comparison to the longest half-life in the literature for strontium retention in the whole body which is $1.3x\ 10^4$ years (Cohn et al., 1962). A similar issue of choosing the best model to describe strontium kinetics was brought up by Cohn and colleagues (1962) who observed a wide divergence between the power function and exponential function models towards their *in-vivo* Sr-85 data of ten subjects. As stated by Cohn and colleagues (1962), when retention is represented by a series of exponentials, the half-life values for the long-lived compartments cannot be anticipated by the method of curve analysis used and hence a power function may be more appropriate. However, still, the power function did not adequately describe their data during the first thirty days. Furthermore, a wide divergence was seen in their half-life exponentials. On the basis of the exponential model,

Cohn and colleagues (1962) concluded that strontium should approach an equilibrium distribution after a long period (e.g. 40 years) when retention would then be dominated by a single exponential. But when their data were fitted with a power function to the period of 20 to 40 years, the half-life increased to 110 years, which is approximately 48 times greater than the one obtained through the exponential model, resulting in an inconclusive model.

Thus, taking into account the wide variation of the strontium signal observed between the subjects as discussed in chapter five, the pattern of the data and the inconclusive arrival of a specific model to represent all subjects' data, future work could consider a new, more controlled study. This should be considered since the wide variation observed is indicative of biological variance factors rather than technical or positioning factors as observed by the consistency of the baseline values. Furthermore, analysis of the strontium data as discussed in chapter two includes a normalization procedure, which also corrects partly for positioning. As reported in chapter four, systemic checks using a standard calibration phantom also indicated excellent reproducibility over a four year period: 1.1198 ± 0.02171 (mean normalized strontium signal ± SD, N=364). Thus, controlled study parameters may include ensuring subjects all take the same dosage of strontium, vitamin D and calcium intake, do not have additional metabolic conditions such as thyroidism or elevated bone turnover markers and sharing similar dietary consumption (i.e. vegetarians versus non-vegetarians). However, while these controls may help control variability of the strontium signal between subjects, the figures as presented in this chapter, also indicate variability of the signal within the subject as the study progressed.

Omitting the issue of technical and positioning issues, this variability may be explained by changes of strontium intake of the subject themselves (i.e whether strontium intake or dosage was consistent throughout the study). This is hypothesized since the strontium signal is proportional to the strontium levels in bone and missed dosages or irregular intake of strontium in between visits may influence the observed signal. This was observed for other participants who participated in the study. The data for these 'non'baseline' subjects (i.e those that had a prior intake of strontium supplements at the time of the study) are shown in chapter seven. Nevertheless, it should be also considered that in addition to these factors, physiological make-up relating to gastrointestinal absorption also depends on genetic make-up of the individual. These factors combined are issues thought to affect the half-life and uptake parameters and as such, poses additional challenges in understanding strontium kinetics.

CHAPTER 7: FUTURE WORK AND CONCLUSION

The work performed in this thesis was unique in the sense that it included for the first time in the available literature, bone strontium measurements performed in osteoporotic and/or osteopenic individuals measured with an in-house custom based IVXRF system over a frequent and long term basis. While there are data in the literature reporting bone strontium measurements, the available literature data are primarily based on invasive methods or *ex-vivo* studies on excised human or animal bone samples, thus presenting with experimental limitations as discussed in chapter one. Furthermore, while a non-invasive technique of DPA and DXA has been reported to be successful in measuring osteoporotic individuals (Bärenholdt et al., 2009), the limitation with their technique as reported by the authors is that it is not sensitive to measure natural bone strontium levels nor can the DPA method be used to monitor changes in % strontium changes in the individual subject. The IVXRF system on the other hand, as shown in this work is sensitive and capable of measuring diverse individuals over a long term period due to its non-invasive nature and negligible radiation risk and low MDL of 22-23 μg strontium per g calcium. However, one of the disadvantages with the current IVXRF system is that bone strontium levels cannot be quantified absolutely in terms of concentration.

7.1 Calibration Phantom Standards

Currently, the bone strontium results presented in this thesis work have been expressed as a dimensionless unit, although the normalized bone strontium level is proportional to the bone strontium content and the IVXRF system is able to track bone

strontium changes. As depicted in figure 7.1, the problem arises due to inherent strontium contamination within the calibration phantoms themselves. It is estimated that the strontium contamination is 360 μg strontium per g calcium.

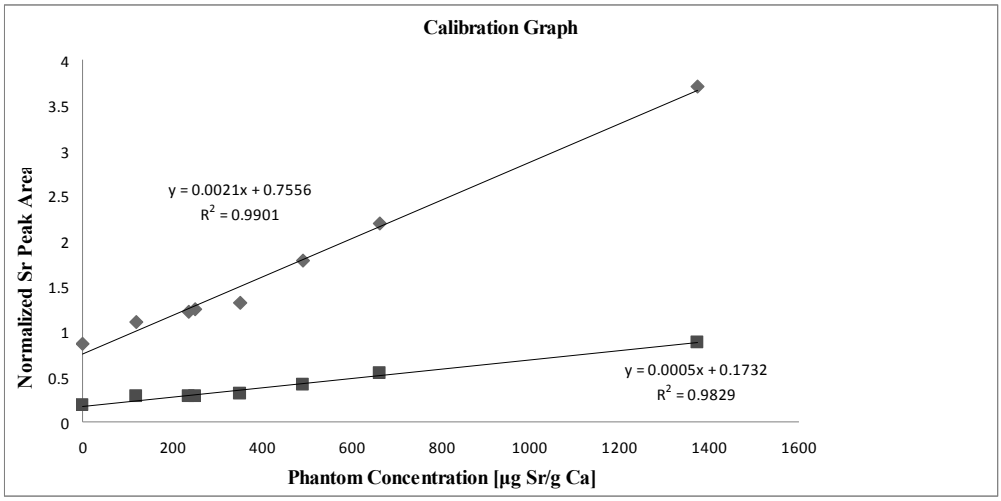

Figure 7.1: Calibration graph for current phantom standards.

Currently, the calibration phantoms are made of plaster of Paris (poP) which is problematic when purity is required. The two sources of contaminations are contamination of the whole material by the analyte and other metals and second, contamination of the material with other Ca chemical species (Da Silva et al.,2013). Furthermore, poP phantoms presents with the issue of nonequivalent matrixes, hence, replacing the current poP calibration phantoms with that made of hydroxyapatite (HA) would not only mimic the bone mineral apatite more closely with that of human bone, but would reduce the contamination problem to negligible levels. Da Silva and colleagues (2013) have created a new set of calibration standards which reduced the contamination to <0.7 μg strontium per g calcium. As a result, this presents a promising opportunity for

future work in being able to achieve absolute quantification of the bone strontium measurements made with the IVXRF system. Future work should look at measuring these calibration phantom standards with the current IVXRF system and looking at reporting bone strontium measurements in terms of concentration. Nevertheless, in spite of the limitation of quantifying bone strontium, the system is able to track successfully changes in bone strontium levels.

7.2 Measurements in Baseline Subjects

Using this system, ten baseline subjects were measured over a four year period at which it was concluded that bone strontium levels would not reach a plateau and would continue to rise as long as an individual self-supplemented with strontium, which raised the question of strontium kinetics. This is in disagreement with some literature studies involving animals and humans, ranging from 6 weeks in monkeys to 3 years in humans (Dahl et al., 2001, Boivin et al., 2010 and Doublier et al., 2011). The work also demonstrated that while strontium levels followed a certain pattern of uptake and retention, there was a wide variation of the strontium signal among the volunteers, such that after three years, the highest strontium signal observed was 28.15 ± 0.86 for the finger and 26.47 ± 1.22 for the ankle in one volunteer compared to 3.15 ± 0.15 and 4.46 ± 0.36, for the finger and ankle, respectively in another.

Based on the data collected through the continued measurements, modeling of the data was performed. However, based on the long term data, a model could not be satisfactorily derived due to the wide scattering pattern of the data. Power and exponential functions have been used in the literature to model bone seeker elements such as calcium and lead

but have been based primarily on data obtained from radiotracer studies. In this work an exponential model showed a promising lead but the end result was the arrival of an inconclusive model for the main reason suggested above. When the one compartmental, three parameter model was used, a mean half-life of (± SD) of 508 ± 331 days and 232 ± 183 days for the finger and ankle bone, respectively were obtained which is on par with literature ranges. However, analysis shows no statistically significant difference between the finger and ankle bone half-lives ($p=0.08796$) for the eight baseline subjects. On the other hand, analysis of the second parameter related to strontium bone uptake between the finger and ankle values shows a correlation of 0.804, which is significant at the 5% level. Applying a two compartmental model suggested that the two compartments of bone tissue (cortical and trabecular bone) will have two different half-lives, which is in agreement with literature findings. In this model (four parameters), the short and long compartments show half-lives of 300 ± 163 days and 2200 ± 1661 days, respectively. The half-lives for both compartments for the finger data and ankle data show statistically significant differences ($p=0.0147$ and $p=0.000711$, for the finger and ankle, respectively). Hence, because the result was an inconclusive model, future work should consider a new study that is restricted in subject criteria and in a more controlled environment. Because half-lives will be negatively affected by dietary consumption such as Vitamin D (Cohen-Solal, 2002) and a wide variation of the bone strontium signal is observed among the study participants, it is suggested that controlled study parameters include ensuring all subjects take the same amount of strontium dosage, same strontium salt, do not have additional metabolic conditions (such as hyperthyroidism) , and share similar dietary

consumption (i.e vegetarians versus non-vegetarians, Vitamin D and Ca). However, as reported in chapter five and in the literature, a wide variation among individuals regarding bone strontium uptake should not be unexpected because of the differences in genetic make-up of each individual and physiological factors related to gastrointestinal absorption. All of these factors pose challenges and add to the difficulty in trying to understand strontium kinetics.

7.3 Measurements in Non-Baseline Subjects

In addition to the baseline subjects recruited in this study, non-baseline (retention) subjects were also followed. Non-baseline subjects are those individuals defined as having a previous intake of strontium intake. Their profiles are shown in Table 7.1

Subject	Age	Gender	Diagnosis	Strontium Dosage and Time (months)**
R1	61	F	Osteoporosis (spine & hip)	Variable (680 mg/day in past, 341 mg/day during study) (8 m)
R2	51	F	Osteoporosis (spine)	341 mg/day (7m)
R3	52	M	Osteoporosis (spine & hip)	682 mg/day + Prolia (12m)
R4	55	F	Osteoporosis (spine)	341 mg/day (6m)
R5	68	F	Osteoporosis (spine)	341 mg/day (12m)
R6	54	F	Osteoporosis (spine)	341 mg/day (3m)
R7	57	M	Osteoporosis (spine, hip & neck)	Variable (341 mg/day to reduced intake) (<3m)
R8	76	F	Osteoporosis (spine)	341 mg/day (8m)
R9	62	F	Osteoporosis (spine & hip)	341 mg/day (12m)
R10	76	F	Osteoporosis (spine & hip)	341 mg/day* (<3m)
R11	64	M	Osteoporosis (spine)	682 mg/day (12m)

Table 7.1: Profile of non-baseline subjects measured during study. *Subject R10 initially took 341 mg elemental strontium per day in the form of strontium citrate supplements for ~ 8 months then switched to the strontium carbonate form. All remaining subjects took

elemental strontium in the form of strontium citrate. **The time denotes the estimated length of time subjects took strontium prior to joining the study.

Figures 7.2 and 7.3 summarize their normalized strontium signal over time.

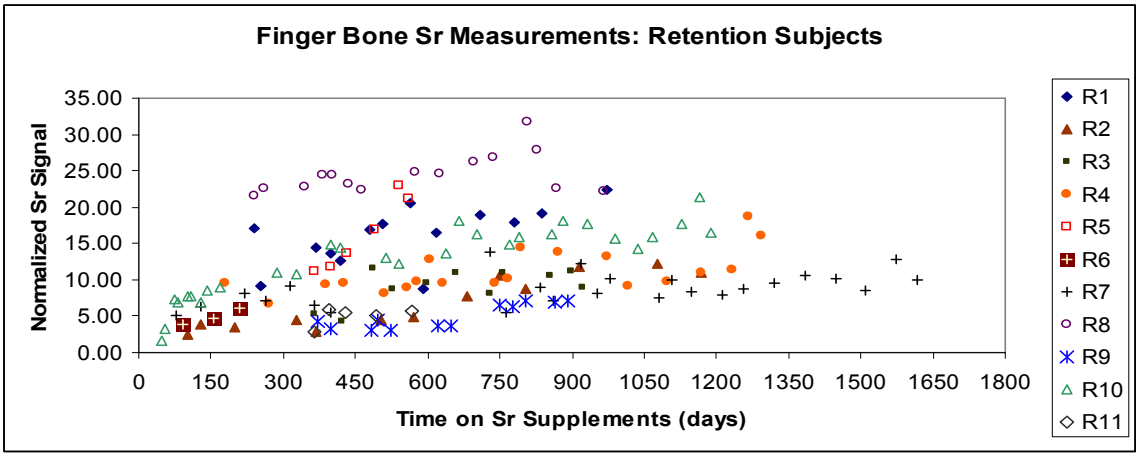

Figure 7.2: Finger bone measurements for non-baseline subjects.

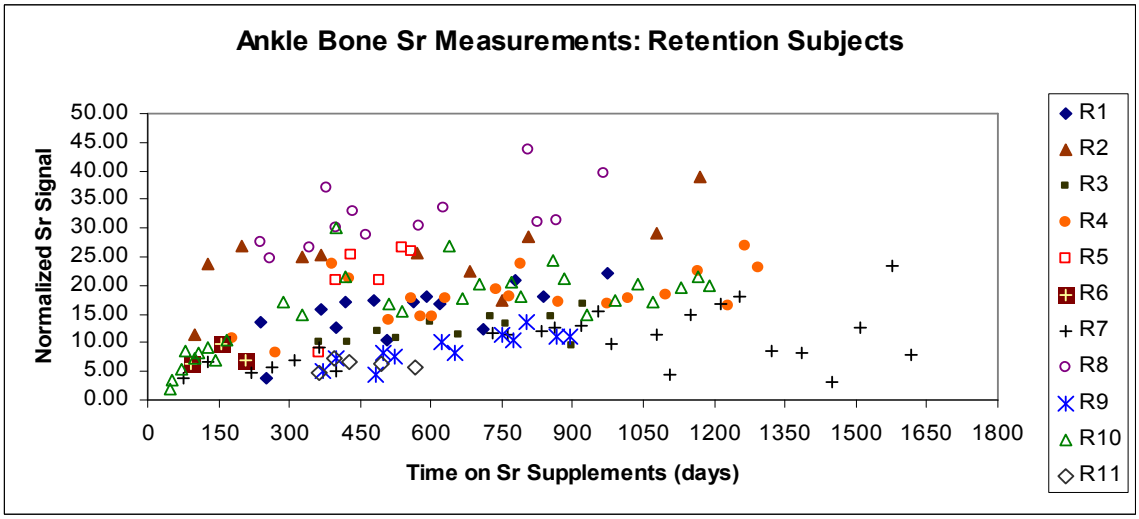

Figure 7.3: Ankle bone measurements for non-baseline subjects.

Based on the figures 7.2 and 7.3, the highest normalized strontium signal is observed for subject R8 for both the finger and ankle bone measurements. This subject's highest

normalized strontium signal was 31.68 ± 1.35 for the finger and 43.65 ± 1.61 for the ankle after an estimated strontium intake of ~2.5 years. However, this subject also had clinically diagnosed elevated alkaline phosphatase levels which may contribute to the higher than average signal. Among the retention subjects whose strontium supplementation was at least three years (N=8, the average normalized strontium signal (± SD) was 13.93±5.72 and 20.29± 9.91, for the finger and ankle, respectively. The high SD is associated with the wide variation between subjects. Comparison of the retention subjects above to the baseline subjects show similar pattern of retention in addition to the wide variation observed in the strontium signal between subjects. Of interest to note here is that the male subjects did not show any significant differences in the normalized strontium signal. However, the number of males (3) in this study was very limited and future work could look at this topic in further detail. Especially, if it is considered that females have been shown to have higher bone mass fractions of strontium compared to males (Zaichick, 2013) and the female rats show higher absorption of NSAIDs compared to male rats (personal communication, Dr. Gregory Wohl). The strontium signal as observed for subject R10 also does not seem to be affected by the strontium salt, given that this subject switched from strontium citrate supplements to strontium carbonate supplements. However, it is possible that other forms of strontium salts, such as strontium lactate or strontium gluconate may show different strontium uptake due to the different type of carrier molecule and bio-solubility of the salt. However, since subject R10 was the only subject taking strontium carbonate, whether this seems to be the case is of question.

7.4 Strontium and Cultural Heritage

With regards to genetic make-up of an individual affecting strontium absorption, an interesting observation is the difference in strontium levels observed among individuals of different cultural heritage or regional backgrounds. This observation was initially reported by Zamburlini and colleagues (2007a) who observed in their 2006 pilot study of twenty two healthy individuals that non-Continental Asians have higher strontium levels compared to Caucasian individuals. Compared to the Caucasian individuals, the Asian individuals had higher bone strontium levels by a factor of 2.4 and 2.7 for the finger and ankle respectively. While no further work was performed by Zamburlini and colleagues (2007a) to investigate this observation, a similar high bone strontium measurement was observed for a male individual from Kenya. The opportunity to measure this individual arose on his visit to McMaster University during June of 2010. His finger and ankle bone strontium measurements showed a normalized bone strontium signal of 1.93 ± 0.28 and 2.15 ± 0.53, respectively, which is slightly higher than that observed by Zamburlini and colleagues (2007a) for the Asian individuals measured in the 2006 pilot study. Interestingly, while no further measurements in African individuals were performed, further opportunities to measure bone strontium levels in Indian and Persian graduate students at McMaster University arose. Their measurements in comparison to the Asians, Caucasians, and Osteoporotic individuals are summarized in Table 7.2.

Group the individual identified with	Finger	Ankle
Caucasian (Healthy)*	0.43 ± 0.08	0.40 ± 0.13
Caucasian (Osteoporotic/osteopenic)	0.42 ± 0.13	0.39 ± 0.07
Asian *	1.03 ± 0.40	1.09 ± 0.30
South American (Female)	0.45 ± 0.09	0.28 ± 0.05
Indian (Female) Indian (Male)	0.98 ± 0.07 0.78 ± 0.05	0.87 ± 0.08 0.26 ± 0.03
Persian (Female)	1.10 ± 0.05	0.75 ± 0.04
African (Male)	1.93 ± 0.28	2.15 ± 0.53

Table 7.2: Normalized bone strontium levels observed in different groups of individuals. *Measured by Zamburlini and colleagues (2007a).

Of interest to note here is that while the question of geological differences and strontium levels has been studied in the literature (Schoeninger and Peebles, 1981, Zaichick, 2013), the basis of higher strontium levels in certain groups have been attributed to the type of diet consumed (i.e non-western diet versus western diet), such that vegetarians would show higher bone strontium levels than meat eaters. However, Table 7.1 includes measurements performed in non-Caucasian individuals who are not vegetarians, follow the western diet and still show higher strontium levels than their Caucasian counterparts. Therefore, future work could look at individuals from different ethnic backgrounds who share similar diets and country origins.

7.5 Conclusion

In conclusion, while the modeling of strontium for the eight baseline data was inconclusive due to the scattering of data points, this work points to the importance of

monitoring individuals taking strontium supplements, especially as the results show that strontium levels do not plateau even after three years of daily intake. This raises the question of strontium toxicity and also raises the question of correcting for BMD values in individuals taking strontium supplements, as strontium will artificially increase BMD test scores due to the higher atomic number of strontium (Z=38) compared to calcium (Z=20) and the attenuation of X-rays by strontium atoms. Future work could also consider incorporating BMD measurements alongside IVXRF bone strontium measurements in order to assess the degree of strontium influence on DEXA measurements. Hence, the IVXRF system emerges as a promising tool.

REFERENCES

Apostoaei, A. I. (2002). Absorption of strontium from the gastrointestinal tract into plasma in healthy human adults. *Health physics*, *83*(1), 56-65.

Atpages, JP. I-125 decay scheme. Radiochemistry: images/materials. Retrieved on June 29, 2014 from: http://www5.atpages.jp/~rad/image/materials/wikimaterial/

ATSDR. Public Health Statement for Strontium, CAS#: 7440-24-6. (April 2004). Toxic Substances Portal-Strontium. Agency for Toxic Substances and Disease Registry (ATSDR). Retrived June 2, 2014 from: http://www.atsdr.cdc.gov/phs/phs.asp?id=654&tid=120

Bain, S. D., Jerome, C., Shen, V., Dupin-Roger, I., & Ammann, P. (2009). Strontium ranelate improves bone strength in ovariectomized rat by positively influencing bone resistance determinants. *Osteoporosis international*, *20*(8), 1417-1428.

Bärenholdt, O., Kolthoff, N., & Nielsen, S. P. (2009). Effect of long-term treatment with strontium ranelate on bone strontium content. *Bone*, *45*(2), 200-206.

Bauer, G. C. H., Malmö, M.D. & Ray, R.D. (1958). Kinetics of Strontium Metabolism in Man. *The Journal of Bone and Joint Surgery,40A* (1), 171-186.

Bayhan, I., Uygur, D., Ugurlu, N., & Ozaksit, G. (2009). Strontium ranelate decreases plasma homocysteine levels in postmenopausal osteoporotic women. *Rheumatology international*, *29*(3), 263-266.

Bellis, D. J., Li, D., Chen, Z., Gibson, W. M., & Parsons, P. J. (2009). Measurement of the microdistribution of strontium and lead in bone via benchtop monochromatic microbeam X-ray fluorescence with a low power source. *Journal of analytical atomic spectrometry*, *24*(5), 622-626.

Blake, G. M., & Fogelman, I. (2005). Long-term effect of strontium ranelate treatment for post-menopausal osteoporosis: a review of safety and efficacy. *Clinical interventions in aging*, *1*(4), 367-375.

Blake, G. M., & Fogelman, I. (2006). Strontium Ranelate: a novel treatment. *Journal of bone and mineral research*, *20*(11), 1901-1904.

Blake, G. M., & Fogelman, I. (2007). Effect of bone strontium on BMD measurements. *Journal of Clinical Densitometry*, *10*(1), 34-38.

Boivin, G., Deloffre, P., Perrat, B., Panczer, G., Boudeulle, M., Mauras, Y., ... & Meunier, P. J. (1996). Strontium distribution and interactions with bone mineral in monkey iliac bone after strontium salt (S 12911) administration. *Journal of Bone and Mineral Research*, *11*(9), 1302-1311.

Boivin, G., Farlay, D., Khebbab, M. T., Jaurand, X., Delmas, P. D., & Meunier, P. J. (2010). In osteoporotic women treated with strontium ranelate, strontium is located in bone formed during treatment with a maintained degree of mineralization. *Osteoporosis international*, *21*(4), 667-677.

Börjesson, J., & Mattsson, S. (2008). X-ray fluorescence in medicine. *Spectroscopy Europe*, *20*(03), 13-17.

Brown, T. J., Bide, T., Hannis, S. D., Idoine, N. E., Hetherington, L. E., Shaw, R. A., ... & Kendall, R. (2010). *World mineral production 2004-2008*. British Geological Survey.

Busse. "Lecture 12: X-Ray Interactions" [lecture notes].Wenatchee High School, Wenatchee, WA. Retrieved on July 16, 2014 from: http://whs.wsd.wednet.edu/faculty/busse/mathhomepage/busseclasses/radiationphysics/lecturenotes/chapter12/chapter12.html

Campbell, J. L., & Jorch, H. H. (1979). On the analytic fitting of full energy peaks from Ge (Li) and Si (Li) photon detectors. II. *Nuclear Instruments and Methods*, *159*(1), 163-170.

Carleton University. IsoAid Advantage ,IA1-I125: source description. Department of Physics, Carleton University, Canada. Retrieved on June 29, 2014 from: http://www.physics.carleton.ca/clrp/seed_database/I125/Advantage_IA1-125A

Cattani-Lorente, M., Rizzoli, R., & Ammann, P. (2013). In vitro bone exposure to strontium improves bone material level properties. *Acta biomaterialia*, *9*(6), 7005-7013.

ChemicalBook. Strontium Ranelate. (2010). Retrieved June 26, 2014 from: http://www.chemicalbook.com/ChemicalProductProperty_EN_CB1838150.htm

Chettle, D. R. (2011). In vivo applications of X-ray fluorescence in human subjects. *Pramana*, *76*(2), 249-259.

Clarke, B. (2008). Normal bone anatomy and physiology. *Clinical journal of the American Society of Nephrology*, *3*(Supplement 3), S131-S139.

Cohen-Solal, M. (2002). Strontium overload and toxicity: impact on renal osteodystrophy. *Nephrology Dialysis Transplantation*, *17*(suppl 2), 30-34.

Cohn, S. H., Spencer, H., Samachson, J., & Robertson, J. S. (1962). The turnover of strontium-85 in man as determined by whole-body counting. *Radiation research*, *17*(2), 173-185.

Cooper, D. M. L., Chapman, L. D., Carter, Y., Wu, Y., Panahifar, A., Britz, H. M., ... & Doschak, M. (2012). Three dimensional mapping of strontium in bone by dual energy K-edge subtraction imaging. *Physics in medicine and biology*, *57*(18), 5777.

Cortet, B. (2009). Effects of bone anabolic agents on bone ultrastructure. *Osteoporosis international*, *20*(6), 1097-1100.

Cowan, F., Farabee, L., & Love, R. (1952). Health physics and medical aspects of a strontium 90 inhalation incident. *The American journal of roentgenology, radium therapy, and nuclear medicine*, *67*(5), 805-809.

Curzon, M. E. J., & Spector, P. C. (1977). Enamel mottling in a high strontium area of the USA. *Community dentistry and oral epidemiology*, *5*(5), 243-247.

Da Silva, E., Kirkham, B., Heyd, D. V., & Pejovic-Milic, A. (2013). Pure hydroxyapatite phantoms for the calibration of in vivo X-ray fluorescence systems of bone lead and strontium quantification. *Analytical chemistry*, *85*(19), 9189-9195.

Dahl, S. G., Allain, P., Marie, P. J., Mauras, Y., Boivin, G., Ammann, P., ... & Christiansen, C. (2001). Incorporation and distribution of strontium in bone. *Bone*, *28*(4), 446-453.

Degteva, M. O., & Kozheurov, V. P. (1994). Age-dependent model for strontium retention in human bone. *Radiation protection dosimetry*, *53*(1-4), 229-233.

Dolphin, G. W., & Eve, I. S. (1963). The metabolism of strontium in adult humans. *Physics in medicine and biology*, *8*(2), 193.

Doublier, A., Farlay, D., Khebbab, M. T., Jaurand, X., Meunier, P. J., & Boivin, G. (2011). Distribution of strontium and mineralization in iliac bone biopsies from osteoporotic women treated long-term with strontium ranelate. *European Journal of Endocrinology*, *165*(3), 469-476.

European Medicines Agency. Assessment Report for Protelos and Osseor-EMA/CHMP/261595/2012. (25 May 2012). UK. European Medicines Agency, 2012.

Frankær, C. G., Raffalt, A. C., & Stahl, K. (2014). Strontium Localization in Bone Tissue Studied by X-Ray Absorption Spectroscopy. *Calcified tissue international*, *94*(2), 248-257.

Han, Hyon, et al.(2005) "Internal circulating irradiation capsule for iodine-125 and method of producing iodine-125 using same." U.S. Patent Application 11/133,131.

Heirwegh,C. (2008). *In vivo* quantification of bone strontium using x-ray fluorescence. M.Sc. Thesis. McMaster University.

Helmenstine, AM. What are the Elements in the Human Body? AboutEducation, USA. Retrieved: June 6, 2014 from : http://chemistry.about.com/cs/howthingswork/f/blbodyelements.htm

Hodgson, S, Clark, B., Wermers, R., Hefferan, T. & Yaszemski, M. (2007). Bone Histology and Histopathology for Clinicians: A Primer. The American Society for Bone and Mineral Research, USA. Retrieved from: http://www.asbmr.org/EducationalResources/BoneHistology.aspx

Hollister, L. (2014). "Introduction to Biosolid Mechanics" [BME 332 lecture notes]. University of Michigan, USA. Retrieved from: http://www.umich.edu/~bme332/ch9bone/bme332bone.htm

Hwang, J. S., Chen, J. F., Yang, T. S., Wu, D. J., Tsai, K. S., Ho, C., ... & Tu, S. T. (2008). The effects of strontium ranelate in Asian women with postmenopausal osteoporosis. *Calcified tissue international*, *83*(5), 308-314.

IAEA (2006). Final Report of a Coordinated Research Project 2001-2006 .International Atomic Energy Agency's Advisory Group Meeting "Production Techniques and Quality Control of Sealed Radioactive Sources of Palladium-103, Iodine-125, Irridium-192 and Ytterbium-169". *International Atomic Energy Agency, June 2006.*

International Commission on Radiological Protection (1982). *General Principles of Monitoring for Radiation Protection of Workers.* Publication 35. Ann. ICRP 9(4) (Oxford: Pergamon Press)

International Commission on Radiological Protection. (1994). *Age-dependent doses to members of the public from intake of radionuclides: part 2 ingestion dose coefficients: a report of a Task group of Committee 2 the International commission on radiological protection* (Vol. 2). Elsevier Health Sciences.

IsoAid. Radiactive seeds: superior needs for the treatment of multiple types of cancer. Advantage I-125 seed. Retrieved on June 29, 2014 from: http://isoaid.com/products/radioactive-seeds.html

Johnson, A. R., Armstrong, W. D., & Singer, L. (1968). The incorporation and removal of large amounts of strontium by physiologic mechanisms in mineralized tissues of the rat. *Calcified tissue research*, *2*(1), 242-252.

Karjalainen, J., Riekkinen, O., Toyras, J., Kroger, H., & Jurvelin, J. (2008). Ultrasonic assessment of cortical bone thickness in vitro and in vivo. *Ultrasonics, Ferroelectrics and Frequency Control, IEEE Transactions on*, *55*(10), 2191-2197.

Keaveny, T. M., Morgan, E. F., & Yeh, O. C. (2004). Bone mechanics. *Standard handbook of biomedical engineering and design*, 1-24.

Kendler, D. L., Adachi, J. D., Josse, R. G., & Slosman, D. O. (2009). Monitoring strontium ranelate therapy in patients with osteoporosis. *Osteoporosis international*, *20*(7), 1101-1106.

Khan, F. (1994). *Physics of radiation therapy*. Second Edition. Lippincott Williams&Wilkins.

Kieranmaher. Photoelectric Effect. Wikibooks-Public Domain. Retrieved on July 12, 2014 from: http://en.wikibooks.org/wiki/Basic_Physics_of_Digital_Radiography/The_Patient#mediaviewer/File:PhotoelectricEffect.jpg

Knoll, G. F. (2000). *Radiation detection and measurement*. Third Edition. John Wiley & Sons.

Krane, S. M., Brownell, G. L., Stanbury, J. B., & Corrigan, H. (1956). The effect of thyroid disease on calcium metabolism in man. *Journal of Clinical Investigation*, *35*(8), 874.

Laya, M. Common Questions: What is a T-score? What is a Z-score. Osteoporosis Education (2014). University of Washington, USA. Retreived August 25, 2014 from: http://depts.washington.edu/osteoed/faqs.php?faqID=31

Leggett, R. W. (1992). A generic age-specific biokinetic model for calcium-like elements. *Radiation Protection Dosimetry*, *41*(2-4), 183-198.

Lehnerdt, F. (1910). Zur frage der substitution des calciums im knochensystem durch strontium. *Beitr Path Anat*, *47*, 215-245.

Leininger, J. R., & Riley, M. G. I. (1990). Bones, joints, and synovia. *Pathology of the Fischer Rat. GA Boorman, SL Eustis, MR Elwell, C Montgomery Jr., and WF Mackenzie (eds). Academic press, San diego*, 209-226.

Lenntech B.V: Water treatment solutions. Strontium-Sr. Retrieved June 8, 2014 from: http://www.lenntech.com/periodic/elements/sr.htm

Li, Z., Peng, S., Pan, H., Tang, B., Lam, R. W., & Lu, W. W. (2012). Microarchitecture and nanomechanical properties of trabecular bone after strontium administration in osteoporotic goats. *Biological trace element research*, *145*(1), 39-46.

Marcus, A. H., & Becker, A. (1977). Power laws in compartmental analysis—II. numerical evaluation of semi-Markov models. *Mathematical Biosciences*, *35*(1), 27-45.

MacDonald, N. S., Nusbaum, R. E., Alexander, G. V., Ezmirlian, F., Spain, P., & Rounds, D. E. (1952). The skeletal desposition of yttrium. *Journal of Biological Chemistry*, *195*(2), 837-841.

Marcus, A. H., & Becker, A. (1977). Power laws in compartmental analysis—II. numerical evaluation of semi-Markov models. *Mathematical Biosciences*, *35*(1), 27-45.

Marcus, A. H. (1979). The body burden of lead: comparison of mathematical models for accumulation. *Environmental research*, *19*(1), 79-90.

Marie, P. J., & Hott, M. (1986). Short-term effects of fluoride and strontium on bone formation and resorption in the mouse. *Metabolism*, *35*(6), 547-551.

Marie, P. J., Ammann, P., Boivin, G., & Rey, C. (2001). Mechanisms of action and therapeutic potential of strontium in bone. *Calcified tissue international*, *69*(3), 121-129.

Marie, P. J. (2006). Strontium ranelate: a physiological approach for optimizing bone formation and resorption. *Bone*, *38*(2), 10-14.

Marie, P. J. (2010). The calcium-sensing receptor in bone cells: a potential therapeutic target in osteoporosis. *Bone*, *46*(3), 571-576.

Marshall, J. H., Lloyd, E. L., Rundo, J., Liniecki, J., Marotti, G., Mays, C. W., ... & Snyder, W. S. (1973). ICRP Publication 20: Alkaline Earth Metabolism in Adult Man. *Health Physics*, *24*(2), 125-221.

McCloskey C & Furnival T. (2013). Structure and Composition of Bone. University of Cambridge, UK. Retrived June 8, 2014 from: http://www.doitpoms.ac.uk/tlplib/bones/structure.php.

Mertz, W. (1981). The essential trace elements. *Science*, *213*(4514), 1332-1338.

Meunier, P. J., & Reginster, J. Y. (2003). Design and methodology of the phase 3 trials for the clinical development of strontium ranelate in the treatment of women with postmenopausal osteoporosis. *Osteoporosis international*, *14*(3), 66-76.

Moise H. (2010). *In vivo* measurement of strontium incorporation and retention in human bone using an x-ray fluorescence system. M.Sc Thesis. Ryerson University.

Moise, H., Adachi, J. D., Chettle, D. R., & Pejović-Milić, A. (2012). Monitoring bone strontium levels of an osteoporotic subject due to self-administration of strontium citrate with a novel diagnostic tool, *in vivo* XRF: A case study. *Bone*, *51*(1), 93-97.

Moise, H., Chettle, D. R., & Pejović-Milić, A. (2014). Monitoring bone strontium intake in osteoporotic females self-supplementing with strontium citrate with a novel *in-vivo* X-ray fluorescence based diagnostic tool. *Bone*, *61*, 48-54.

Nielsen, S. P., Slosman, D., Sorensen, O.H., Basse-Cathalinat, B.C., De Cassin, P., Roux, C., and Meunier, P.J. (1999). Influence of strontium on bone mineral density and bone mineral content measurements by dual x-ray absorptiometry. *Journal of Clinical Densitometry, 2*(4), 371-379.

Nielsen, S. P., Bärenholdt, O., Bärenholdt-Schiøler, C., Mauras, Y., & Allain, P. (2004). Noninvasive measurement of bone strontium. *Journal of Clinical Densitometry*, *7*(3), 262-268.

Neuprez, A., Hiligsmann, M., Scholtissen, S., Bruyere, O., & Reginster, J. Y. (2008). Strontium ranelate: the first agent of a new therapeutic class in osteoporosis. *Advances in therapy*, *25*(12), 1235-1256.

Newton D, Rundo J, Harrison GE. (1977) The retention of alkaline earth elements in man, with special reference to barium.*Health Phys.* **33** (1): 45-53.

NRCan. Operators of Portable Flourescence Analyzers (XRF): Certification Information and Examination Preparation Booklet. Version 4 (September 4, 2013). National Resources Canada (NRCan), Government of Canada.

Oliveira, J. P., Querido, W., Caldas, R. J., Campos, A. P., Abraçado, L. G., & Farina, M. (2012). Strontium is incorporated in different levels into bones and teeth of rats treated with strontium ranelate. *Calcified tissue international*, *91*(3), 186-195.

Ozgür, S., Sümer, H., & Koçoğlu, G. (1996). Rickets and soil strontium. *Archives of disease in childhood*, *75*(6), 524-526.

Pejović-Milić, A. (2001). *In vivo* measurements of aluminum and strontium in human bone. Ph.D dissertation. McMaster University.

Pejović-Milić, A., Brito, J. A., Gyorffy, J., & Chettle, D. R. (2002). Ultrasound measurements of overlying soft tissue thickness at four skeletal sites suitable for in vivo x-ray fluorescence. *Medical physics*, *29*(11), 2687-2691.

Pejović-Milić, A., Stronach, I. M., Gyorffy, J., Webber, C. E., & Chettle, D. R. (2004). Quantification of bone strontium levels in humans by in vivo x-ray fluorescence. *Medical physics*, *31*(3), 528-538.

Peel, N. (2009). Bone remodelling and disorders of bone metabolism. *Surgery (Oxford)*, *27*(2), 70-74.

Pertinez, H., Chenel, M., & Aarons, L. (2013). A physiologically based pharmacokinetic model for strontium exposure in rat. *Pharmaceutical research*, *30*(6), 1536-1552.

Pors Nielsen, S. (2004). The biological role of strontium. *Bone*, *35*(3), 583-588.

Reeve, J.,Green, J. R., Maletskos, C. J., & Neer, R. M. (1983). Skeletal retention of 45-Ca and 85-Sr compared: Further studies on intravenously injected85Sr as a tracer for skeletal calcium. *Calcified tissue international*, *35*(1), 9-15.

Reilly, C. (2008). *The nutritional trace metals*. John Wiley & Sons.

Reinholt, F. P., Hjerpe, A., Jansson, K., & Engfeldt, B. (1984). Stereological studies on the epiphyseal growth plate in low phosphate, vitamin D-deficiency rickets with special reference to the distribution of matrix vesicles. *Calcified Tissue International*, *36*(1), 95-101.

Reginster, J. Y., Seeman, E., De Vernejoul, M. C., Adami, S., Compston, J., Phenekos, C., ... & Meunier, P. J. (2005). Strontium ranelate reduces the risk of nonvertebral fractures in postmenopausal women with osteoporosis: Treatment of Peripheral Osteoporosis (TROPOS) study. *The journal of clinical endocrinology & metabolism*, *90*(5), 2816-2822.

Reginster, J. Y., Beaudart, C., Neuprez, A., & Bruyère, O. (2013). Strontium ranelate in the treatment of knee osteoarthritis: new insights and emerging clinical evidence. *Therapeutic advances in musculoskeletal disease*, 1759720X13500862.

Rizzoli, R., Chapurlat, R. D., Laroche, J. M., Krieg, M. A., Thomas, T., Frieling, I., ... & Felsenberg, D. (2012). Effects of strontium ranelate and alendronate on bone microstructure in women with osteoporosis. *Osteoporosis International*, *23*(1), 305-315.

Schoeninger, M. J., & Peebles, C. S. (1981). Effect of mollusc eating on human bone strontium levels. *Journal of Archaeological Science*, *8*(4), 391-397.

Science Encyclopedia. Trace Elements. Retrieved on August 21, 2014 from: http://science.jrank.org/pages/6890/Trace-Elements.html

Schrooten, I., Cabrera, W., Goodman, W. G., Dauwe, S., Lamberts, L. V., Marynissen, R., ... & D'Haese, P. C. (1998). Strontium causes osteomalacia in chronic renal failure rats. *Kidney international*, *54*(2), 448-456.

Schoeninger, M. J., & Peebles, C. S. (1981). Effect of mollusc eating on human bone strontium levels. *Journal of Archaeological Science*, *8*(4), 391-397.
Shackley, M. S. (2011). *X-ray fluorescence spectrometry (XRF) in geoarchaeology*. New York: Springer.

Shagina, N. B., Tolstykh, E. I., & Degteva, M. O. (2003). Improvements in the biokinetic model for strontium with allowance for age and gender differences in bone mineral metabolism. *Radiation protection dosimetry*, *105*(1-4), 619-622.

Shorr, E., & Carter, A. C. (1947). Studies on the effect of estrogens, androgens, and vitamin D2 on the calcium and the strontium metabolism. In *Transactions. Conference on Metabolic Aspects of Convalescence* (Vol. 60, p. 99).

Smith DA, Speirs CF, Shimmins J. (1967) The long-term skeletal retention and recirculation of 85Sr in man. *Calcif. Tissue Res.* **1** (2): 144-152.

Somervaille, L. J., Chettle, D. R., & Scott, M. C. (1985). In vivo measurement of lead in bone using x-ray fluorescence. *Physics in medicine and biology*, *30*(9), 929.

Staub, J. F., Foos, E., Courtin, B., Jochemsen, R., & Perault-Staub, A. M. (2003a). A nonlinear compartmental model of Sr metabolism. I. Non-steady-state kinetics and model building. *American Journal of Physiology-Regulatory, Integrative and Comparative Physiology*, *284*(3), R819-R834.

Staub, J. F., Foos, E., Courtin, B., Jochemsen, R., & Perault-Staub, A. M. (2003b). A nonlinear compartmental model of Sr metabolism. II. Its physiological relevance for Ca metabolism. *American Journal of Physiology-Regulatory, Integrative and Comparative Physiology*, *284*(3), R835-R852.

Storey, E. (1962). Intermittent bone changes and multiple cartilage defects in chronic strontium rickets in rats. *Journal of Bone & Joint Surgery, British Volume*, *44*(1), 194-208.

Tamarkin, D. (January 2011). "Bone Development and Growth" [Biol 132 lecture notes]. Springfield Technical Community College. Springfield, Massachusetts. Retrieved August 5, 2015 from:
http://faculty.stcc.edu/AandP/AP/AP1pages/Units5to9/bone/bonedev.htm

Treece, G. M., Gee, A. H., Mayhew, P. M., & Poole, K. E. S. (2010). High resolution cortical bone thickness measurement from clinical CT data. *Medical image analysis*, *14*(3), 276-290.

Turekian, K. K., & Wedepohl, K. H. (1961). Distribution of the elements in some major units of the earth's crust. *Geological Society of America Bulletin*, *72*(2), 175-192.

Underwood, E. (2012). *Trace Elements in Human and Animal Nutrition 4e*. Elsevier.
Wielopolski, L., Rosen, J. F., Slatkin, D. N., Vartsky, D., Ellis, K. J., & Cohn, S. H. (1983). Feasibility of noninvasive analysis of lead in the human tibia by soft x-ray fluorescence. *Medical physics*, *10*(2), 248-251.

Wohl, G. R., Chettle, D. R., Pejović-Milić, A., Druchok, C., Webber, C. E., Adachi, J. D., & Beattie, K. A. (2013). Accumulation of bone strontium measured by *in vivo* XRF in rats supplemented with strontium citrate and strontium ranelate. *Bone*, *52*(1), 63-69.
World Health Organization. (2004, May). WHO scientific group on the assessment of osteoporosis at primary health care level. In *Summary Meeting Report* (pp. 5-7).

Zaichick, V., Ovchjarenko, N., & Zaichick, S. (1999). *In vivo* energy dispersive X-ray fluorescence for measuring the content of essential and toxic trace elements in teeth. *Applied radiation and isotopes*, *50*(2), 283-293.

Zaichick, V. (2013). Data for the Reference Man: skeleton content of chemical elements. *Radiation and environmental biophysics*, *52*(1), 65-85.

Zamburlini, M., Pejović-Milić, A., & Chettle, D. R. (2006). Evaluation of geometries appropriate for 125 I in vivo bone strontium X-ray fluorescence measurement. *Journal of radioanalytical and nuclear chemistry*, *269*(3), 625-629.

Zamburlini, M., Pejović-Milić, A., Chettle, D. R., Webber, C. E., & Gyorffy, J. (2007a). In vivo study of an x-ray fluorescence system to detect bone strontium non-invasively. *Physics in medicine and biology*, *52*(8), 2107.

Zamburlini, M., Byun, S. H., Pejović-Milić, A., Prestwich, W. V., & Chettle, D. R. (2007b). Evaluation of MCNP5 and EGS4 for the simulation of in vivo strontium XRF measurements. *X-Ray Spectrometry*, *36*(2), 76-81.

Zamburlini, M., Pejović-Milić, A., & Chettle, D. R. (2008a). Coherent normalization of finger strontium XRF measurements: feasibility and limitations. *Physics in medicine and biology*, *53*(15), N307.

Zamburlini, M., Pejović-Milić, A., & Chettle, D. R. (2008b). Spectrometry methods for in vivo bone strontium measurements. *X-Ray Spectrometry*, *37*(1), 42-50.

Zamburlini M. (2008c). *In vivo* measurement of bone strontium with x-ray fluorescence. Ph.D. Dissertation. McMaster University.

Zanzonico, P. (2011). *Basic sciences of nuclear medicine*. Heidelberg: Springer.

Ziegler, J., Müller, C., Mann, G., & Hess, A. (2002). *U.S. Patent No. 6,485,406*. Washington, DC: U.S. Patent and Trademark Office. Available at: http://www.google.com/patents/US6485406

APPENDIX

In chapter six, modeling of the strontium baseline data in eight subjects was presented. Examples of three subject's data were given in this chapter. Although, all subject's data was presented in chapter six, as a continuation, this appendix includes the remaining graphs for the remainder five subjects based on the application of the one and two compartmental models as discussed.

A1.1 One compartmental model

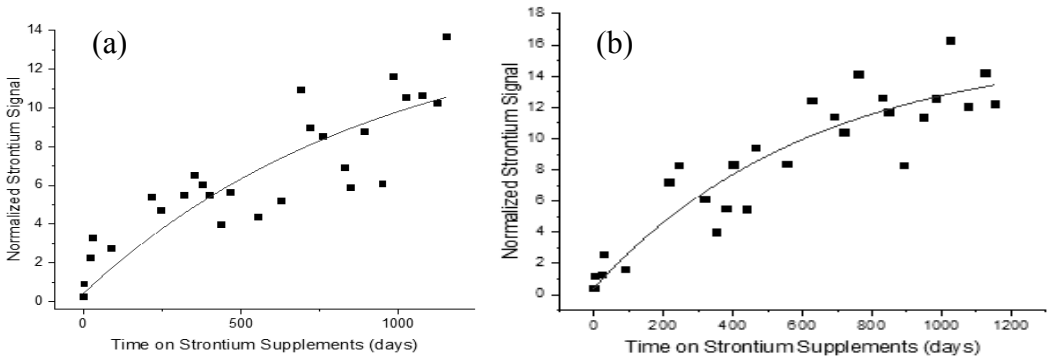

Figure A1.1(a) finger and (b) ankle; Graphical representation of one compartmental model for subject #1.

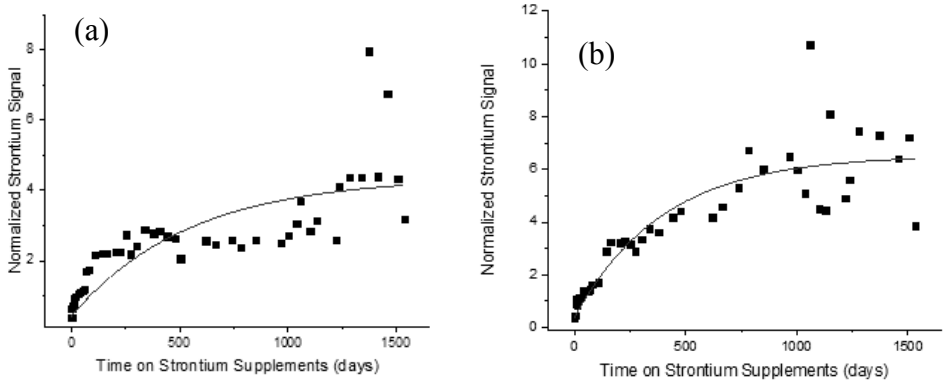

Figure A1.2(a) finger and (b) ankle; Graphical representation of one compartmental model for subject #4.

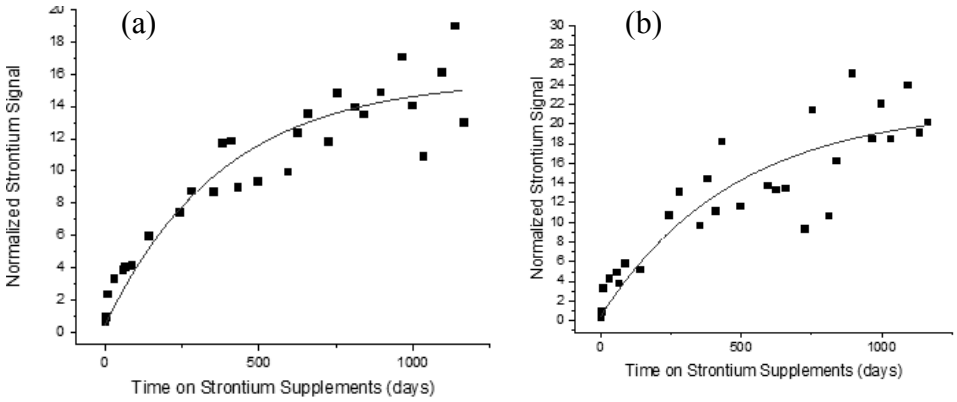

Figure A1.3(a) finger and (b) ankle; Graphical representation of one compartmental model for subject #5.

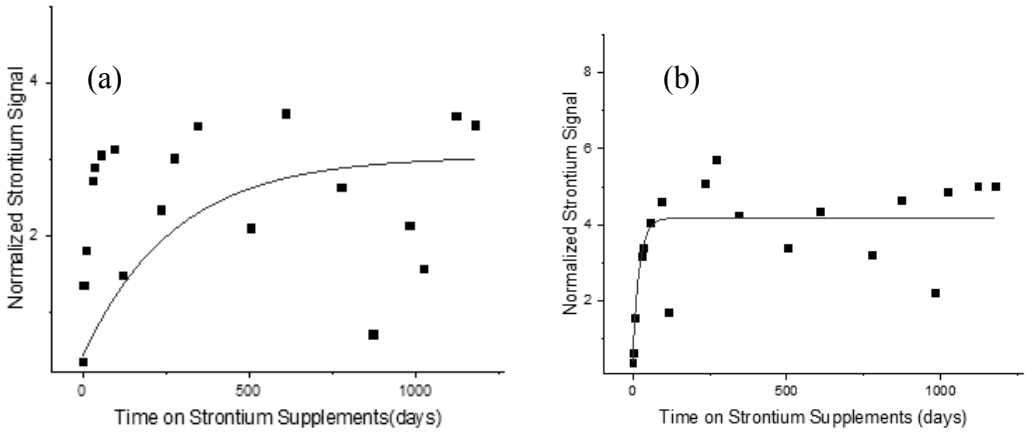

Figure A1.4 (a) finger and (b) ankle; Graphical representation of one compartmental model for subject #7.

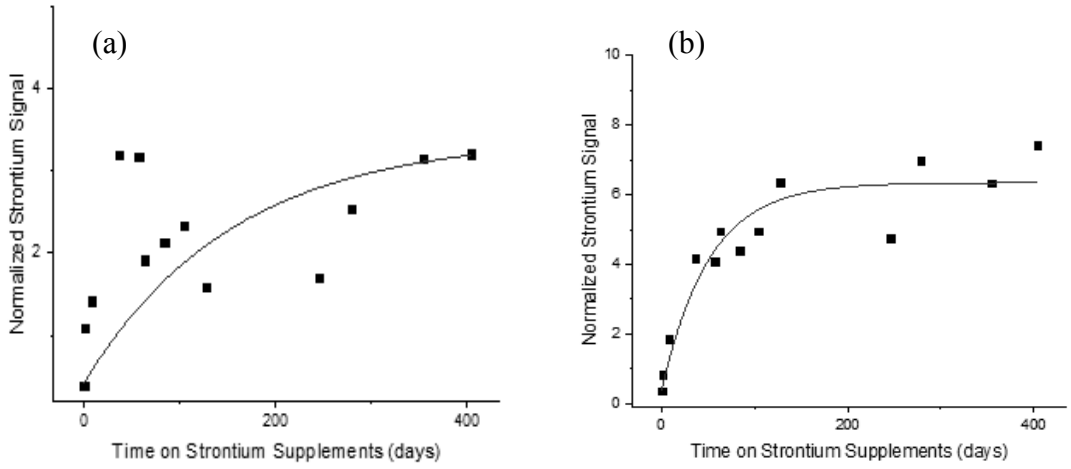

Figure A1.5: (a) finger and (b) ankle; Graphical representation of one compartmental model for subject #8.

A1.2 Two compartmental model

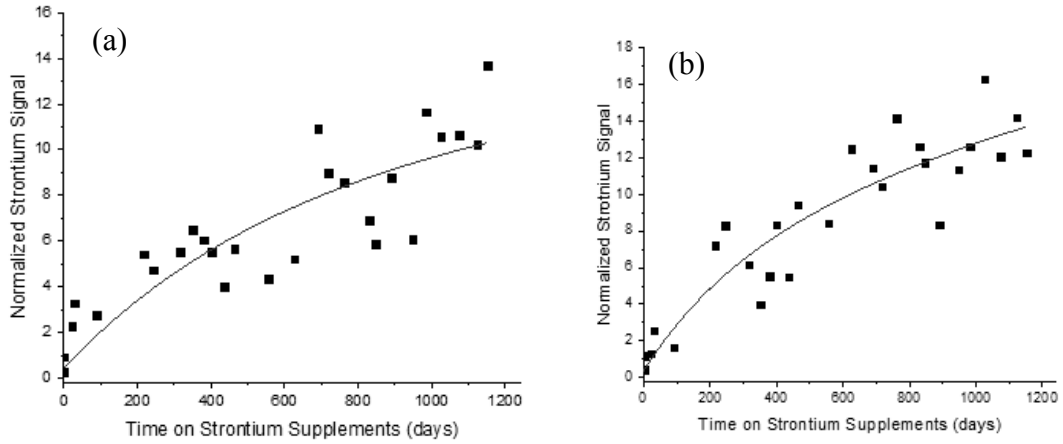

Figure A2.1: (a) finger and (b) ankle; Graphical representation of two compartmental model for subject #1.

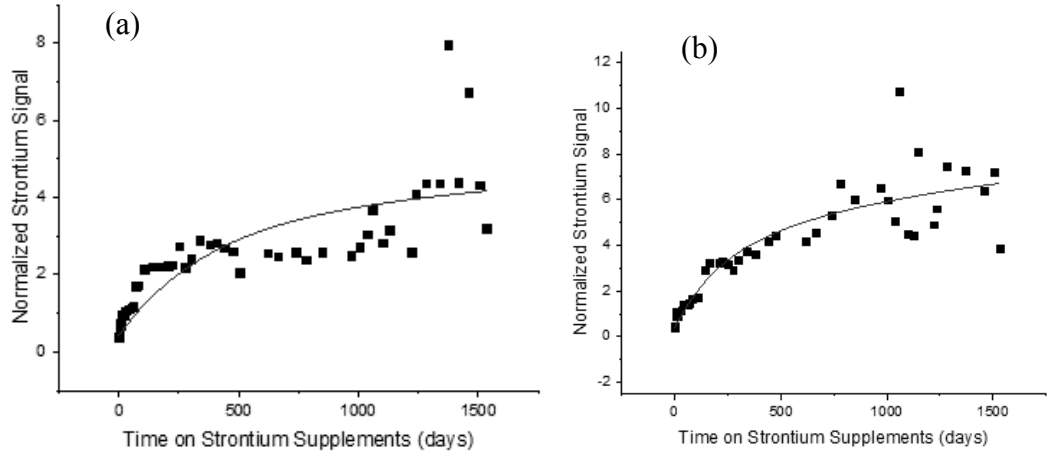

Figure A2.2: (a) finger and (b) ankle; Graphical representation of two compartmental model for subject #4.

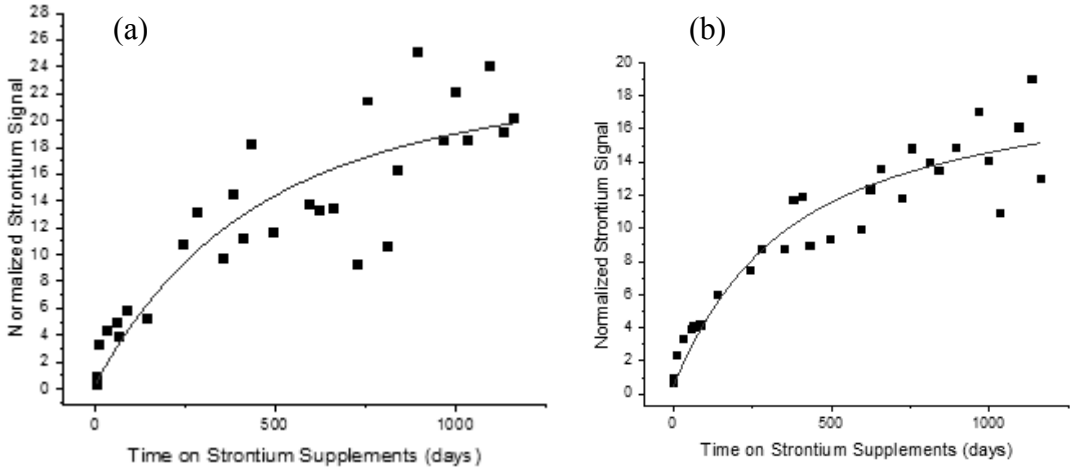

Figure A2.3: (a) finger and (b) ankle; Graphical representation of two compartmental model for subject #5.

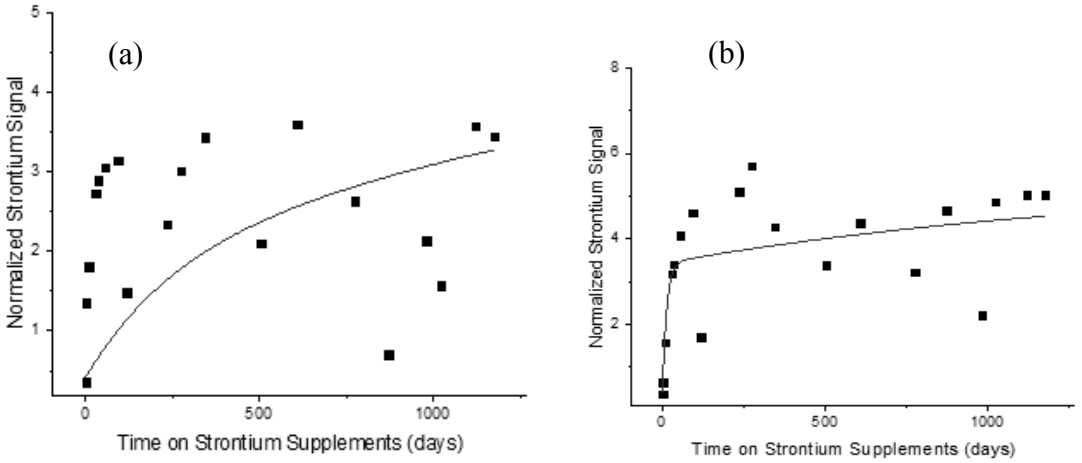

Figure A2.4: (a) finger and (b) ankle; Graphical representation of two compartmental model for subject #7.

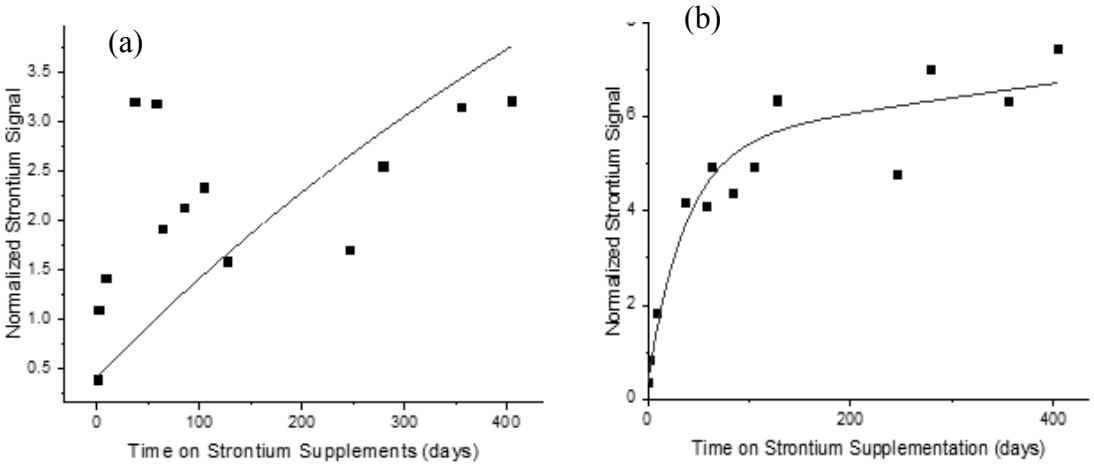

Figure A2.5: (a) finger and (b) ankle; Graphical representation of two compartmental model for subject #8.